1998

Development and saw device implementation of a new weighted stepped chirp code signal for direct sequence spread spectrum communications systems

Scott Edward Carter
scarter99@cfl.rr.com

DEVELOPMENT AND SAW DEVICE IMPLEMENTATION OF A NEW WEIGHTED STEPPED CHIRP CODE SIGNAL FOR DIRECT SEQUENCE SPREAD SPECTRUM COMMUNICATIONS SYSTEMS

by

SCOTT EDWARD CARTER
B.S.E.E. University of Central Florida, 1993
M.S.E.E. University of Central Florida, 1995

A dissertation submitted in partial fulfillment of the requirements
for the degree of Doctor of Engineering
in the Department of Electrical and Computer Engineering
in the College of Engineering
at the University of Central Florida
Orlando, Florida

Summer Term
1998

Major Professor: Dr. Donald C. Malocha

ABSTRACT

This work introduces the new weighted stepped chirp code signal for direct sequence spread spectrum (DS/SS) communications systems. This code signal uses the truncated cosine series functions as the chip functions. This code signal is the result of discretizing a continuous wave (CW) chirp which results in enhanced performance versus a pseudonoise (PN) code and equivalent performance and easier implementation than a CW chirp. This code signal will be shown to possess improved compression ratio (CR), peak sidelobe level (PSL), integrated sidelobe level (ISL), and bit error rate (BER) when compared to a PN code of identical code length and chip length. It also will be shown to have a similar CR, PSL, ISL, and loss in processing gain (LPG) when compared to a CW chirp with identical pulse length and frequency deviation.

The code signal is implemented on surface acoustic wave (SAW) devices which can be used as the code signal generator at the transmitter and the correlator at the receiver in a DS/SS communications system. SAW design considerations for the weighted stepped chirp signal are discussed. Experimental data is presented and compared to the predicted CR, PSL, ISL, LPG, and BER.

ACKNOWLEDGMENTS

First I would like to thank the people who directly contributed to this research. My advisor Dr. Donald Malocha has provided tremendous technical assistance and guidance in both my studies and my career. Dr. Madjid Belkerdid has provided technical assistance in the field of communications. Mr. Kevin Casey of the Consortium for Applied Acoustoelectronic Technology at the University of Central Florida fabricated the experimental SAW devices. Drs. Jackie Hines and Scott Knapp of Sawtek Inc. expedited the dicing and packaging of the experimental SAW devices. The Advanced Research Projects Agency of the Department of Defense funded my Ph.D. research for three years.

Next I'd like to thank all of my colleagues at the Consortium for Applied Acoustoelectronic Technology at the University of Central Florida. Their friendship and support have been greatly appreciated.

Finally, a special thanks to my family for all of their support through my many years of studies. Especially my parents who have provided guidance and support to me throughout my life.

TABLE OF CONTENTS

LIST OF FIGURES

LIST OF TABLES

CHAPTER 1

INTRODUCTION

This research introduces the weighted stepped chirp code signal for use in direct sequence spread spectrum (DS/SS) communications systems. The use of a frequency stepped pulse train for pulse compression radar has been previously evaluated in [1][2]. The optimal choice of center frequency and frequency step were not investigated. Also, DS/SS communications systems require the correlation of a stream of pulses with phase reversal between pulses.

Chapter 2 provides a discussion of spread spectrum systems and code signals. The three basic types of spread spectrum systems: DS/SS, frequency hopped spread spectrum (FH/SS), and pulse compression radar are covered. Figures of merit for spread spectrum systems are introduced. Examples of pseudonoise (PN) code and continuous wave (CW) chirp PSD and correlation functions are shown.

Chapter 3 defines the time and frequency responses of the weighted stepped chirp code signal. This includes optimization of the center frequency and frequency step for optimal correlation results.

Chapters 4 and 5 present the theoretical results for the weighted stepped chirp code signal. Chapter 4 shows the effects of code length and weighting on the correlation

function. Chapter 5 compares the bit error rate (BER) of the weighted stepped chirp code signal to that of a PN code of equal code length.

Chapter 6 provides a discussion of the use of surface acoustic wave (SAW) devices as code signal generators and correlators in DS/SS communications systems. The advantages of using SAW devices are presented. The system implementation is discussed.

Chapter 7 discusses the design of the experimental weighted stepped chirp code signal SAW devices. The design specifications are presented. Design considerations such as intersymbol interference (ISI), weighting of the second transducer, RF feed-through, and waveguiding are discussed. The fabrication process for the experimental weighted stepped chirp code signal SAW devices is also presented.

Chapters 8 and 9 present the results from the experimental weighted stepped chirp code signal SAW devices. Chapter 8 compares the PSD and correlation functions for the different designs and discusses the effects of code length, weighting, and sampling on the correlation function. These results are compared to the theoretical results from Chapter 4. Chapter 9 presents the BER for the experimental weighted stepped chirp code signal SAW devices and compares them to the theoretical BER results from Chapter 5.

Chapter 10 summarizes the performance of the weighted stepped chirp code signal versus PN codes. It also compares the theoretical results to the experimental results.

CHAPTER 2

SPREAD SPECTRUM SYSTEMS AND CODE SIGNALS

Spread spectrum communications systems [3]-[5] have been in use since their development in the 1940's. A system is spread spectrum if it meets the following criteria defined as [3]

1. The signal occupies a bandwidth much in excess of the minimum bandwidth necessary to send the information.
2. Spreading is accomplished by means of a spreading signal, often called a code signal, which is independent of the data.
3. At the receiver, despreading (recovering the original data) is accomplished by the correlation of the received spread signal with a synchronized replica of the spreading signal used to spread the information.

There are several advantages in the use of a spread spectrum system. They are defined as [6]

1. Anti-jamming
2. Anti-interference
3. Low probability of intercept

4. Multiple user random access communications with selective addressing capability
5. High resolution ranging
6. Accurate universal timing

The anti-jamming and anti-interference qualities arise from the despreading of the spread spectrum signal at the receiver. Despreading the spread spectrum signal at the receiver spreads the interference power I and the jammer power J over the spread bandwidth B_{ss}. When bandpass filtered over the original data bandwidth B, the resulting I' and J' will be reduced. This results in a processing gain in the signal-to-jammer ratio (SJR) and the signal-to-interference ratio (SIR) equal to the ratio of B_{ss}/B. The spreading/despreading has no effect on the signal-to-noise ratio (SNR) because white gaussian noise has infinite power spread uniformly over all frequencies. When the noise is spread, the noise power in B remains the same as before spreading. Thus, no improvement in the SNR is realized.

The low probability of intercept results from the fact that the data signal power can be spread such that the signal power is hidden in the background noise and is thus undetectable. Even assuming detection, the correct code signal is required in order to despread and recover the data signal.

Code division multiple access (CDMA) is realized using orthogonal or near orthogonal code signals for multiple users. The cross-correlation between such codes is near zero. This enables the receiver to select the correct user's code with little interference from other users' transmissions.

High resolution ranging results from the use of spread spectrum techniques in pulse compression radar [7]-[10]. Spreading the signal bandwidth of the transmitted radar pulse and then correlating it with its matched filter when it returns results in a correlation pulse which has a much narrower pulse width then the pulse which was originally transmitted. The compressed pulse width results in less ambiguity about the distance to the detected object.

The universal timing accuracy is another benefit of pulse compression. The narrower pulse width also results in less ambiguity about where the peak pulse correlation occurs. This results in better synchronization and tracking of the received spread spectrum signal at the receiver

The three basic spread spectrum systems are FH/SS, DS/SS, and pulse compression radar. Each meets the three criteria defined previously to qualify as a spread spectrum system.

2.1 Frequency Hopped Spread Spectrum

The spreading in a FH/SS communications system is achieved by pseudorandomly changing the carrier frequency of the system with a code signal. Therefore the spread data spectrum is the same as the data spectrum at any instant in time, but can be located within a bandwidth equal to 2^N times the data bandwidth where N is the number of chips in the code signal. Currently, realizable FH/SS bandwidths are an order of magnitude larger than realizable DS/SS bandwidths due to limits in current technology [11].

The most widely used FH/SS communications system is M-ary frequency shift keying (MFSK)/FH/SS [3]. Figure 1 shows the general diagram of a MFSK/FH/SS communications system. The data d(t) is first converted to MFSK by the MFSK modulator. It is then modulated to a carrier frequency which is pseudorandomly changed by the code signal c(t). The signal is sent over the channel and the carrier frequency is demodulated by the code signal at the receiver. The resulting MFSK signal is then demodulated to recover the data signal d′(t).

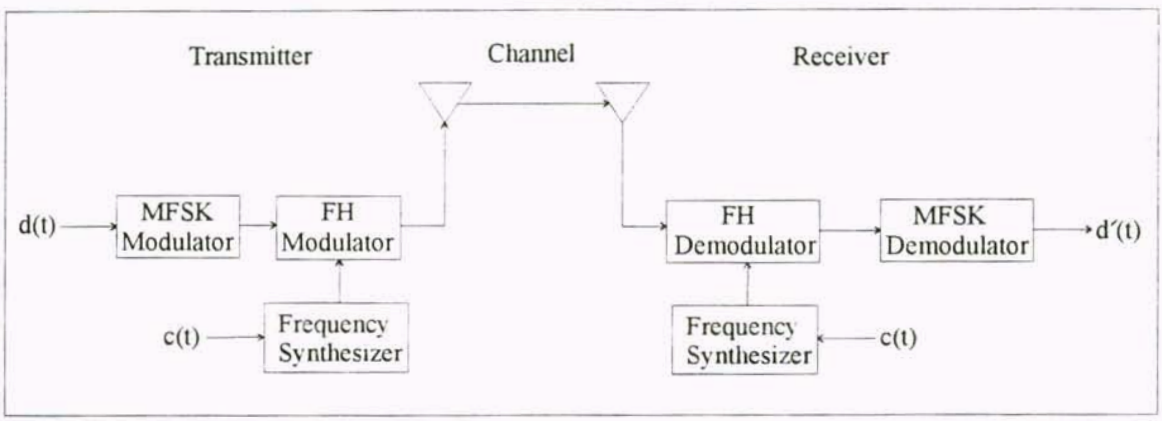

Figure 1. General diagram of a MFSK/FH/SS communications system.

2.2 Spread Spectrum Using Correlation

DS/SS and pulse compression radar are similar since both use a code signal to spread the data bandwidth and a correlator to recover the information. The figures of merit for pulse compression radar systems and DS/SS communications systems are the pulse compression ratio (CR), the peak sidelobe level (PSL), the integrated sidelobe level (ISL), and the loss in processing gain (LPG). These are defined as [9]

$$CR = \frac{T}{\tau} \tag{1}$$

$$PSL = 10\log\left(\frac{\text{maximum sidelobe power}}{\text{peak response power}}\right) \tag{2}$$

$$ISL = 10\log\left(\frac{\text{total power in the sidelobes}}{\text{peak response power}}\right) \tag{3}$$

$$LPG = 20\log\left(\frac{CR}{\text{peak response voltage}}\right) \tag{4}$$

where T is the uncompressed pulse length and τ is the compressed pulse length. The CR is a measure of the compression of the compressed pulse versus an uncompressed pulse. The PSL and ISL measure the peak sidelobe level and the average power in the sidelobes which together measure the code signal's immunity to false alarms due to noise and interference. The LPG measures the loss in SNR due to mismatched filtering which is a technique used to lower the PSL and ISL to acceptable levels. The ideal spread spectrum system would have an infinite CR, infinitely negative PSL and ISL in dB, and 0 dB LPG.

2.21 Direct Sequence Spread Spectrum

The spreading in a DS/SS communications system is realized by multiplying each data bit of length T_b with a code signal composed of chips of length T_c such that $T_c \ll T_b$. This results in a spreading of the signal bandwidth by a factor of T_b/T_c. Multiplying by the same code signal at the receiver despreads the data for recovery. When the received

signal is despread, finite power signals such as from jammers or interference are spread thus resulting in a processing gain in the SJR and SIR equal to T_b/T_c. As mentioned earlier this has no effect on the SNR because white gaussian noise has infinite power spread uniformly over all frequencies.

Figure 2 shows the data signal frequency spectrum (solid line) and the spread data frequency spectrum (dashed line) where T_b/T_c equals 5. The DS/SS has spread the signal power over a new bandwidth which is 5 times greater than the original data bandwidth.

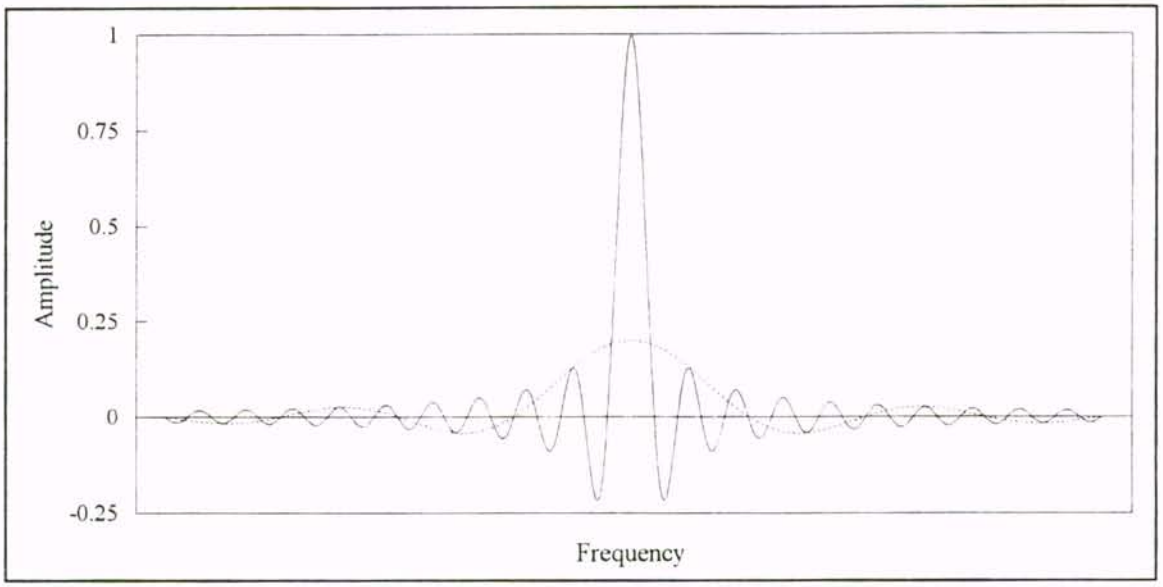

Figure 2. Effects of spreading in a DS/SS communications system where the solid line is the data frequency spectrum before spreading and the dashed line is the data frequency spectrum after spreading.

Figure 3 shows the general diagram of a DS/SS communications system. At the transmitter, the data signal d(t) with bit length T_b is mixed with a code signal c(t) with chip length T_c which spreads the frequency bandwidth of d(t). It is then mixed with a carrier

frequency ω_o and transmitted over the channel. At the receiver, the modulated spread signal is received and demodulated. The signal is then low pass filtered to obtain the base-band signal. The correlator despreads the signal by mixing it with the matched filter $c(T_b-t)$ to the code signal c(t) at the transmitter. The despread signal is then integrated over T_b and output to a threshold detector which determines whether the received signal $d'(t)$ is a +1, -1, or indeterminate.

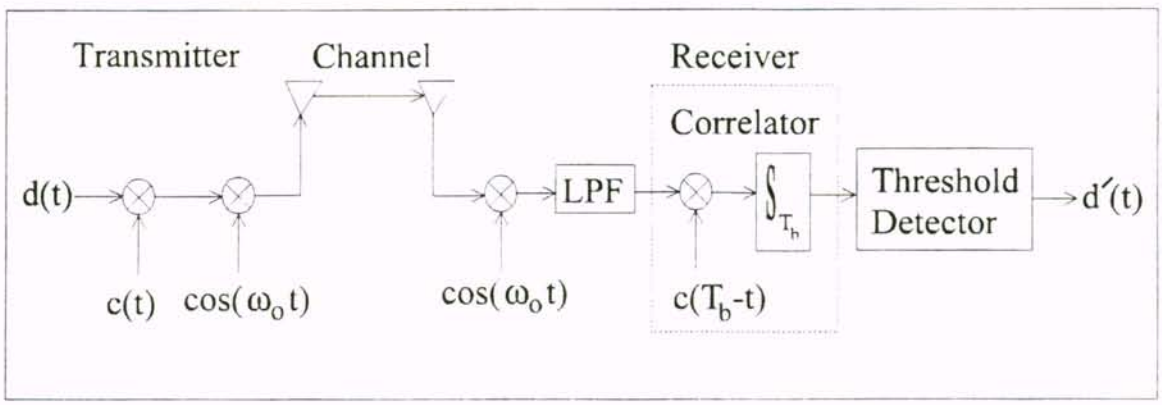

Figure 3. General diagram of a DS/SS communications system.

DS/SS uses a PN code to spread the data signal. These are binary codes which are called pseudonoise because they have the statistical properties of sampled white noise. They meet the three criteria for randomness in a binary signal [4]

1. The number of 1's and 0's differs by at most one.
2. The lengths of the runs of 1's or 0's are about one-half length 1, one-fourth length 2, one-eighth length 3, etc.

3. Comparing the sequence to a shifted sequence results in at most a difference of one between the number of agreements with the number of disagreements.

When implemented the binary 0's are replaced by -1's. The CR and PSL for a PN code using a matched filter are [3]

$$CR = N \tag{5}$$

$$PSL = 20\log(\tfrac{1}{N}) \tag{6}$$

where N is the number of chips in the code. The ISL depends on the PN code being used but is bounded by

$$ISL \leq 10\log(\tfrac{1}{N^2}) \tag{7}$$

Figure 4 shows the normalized correlation of the 13 chip Barker code [3] (+1,+1,+1,+1,+1,-1,-1,+1,+1,-1,+1, -1,+1) over 3 input bits (+1,+1,-1) where the correlator was initialized with zero input at t = 0 usec, T_c = 1 usec, and f_o = 100.5 MHz. Figure 5 shows the normalized correlation peak at the second +1 bit seen at t = 26 usec in Figure 4. The correlation peak is $2T_c$ wide and triangular in shape which is to be expected when correlating two pulses each T_c wide. The CR = 13 and PSL = -22.3 dB which are in agreement with Equations 5 and 6. The ISL = -24 dB which obeys the bound set by Equation 7 and the LPG = 0 dB since no mismatched filtering technique was employed.

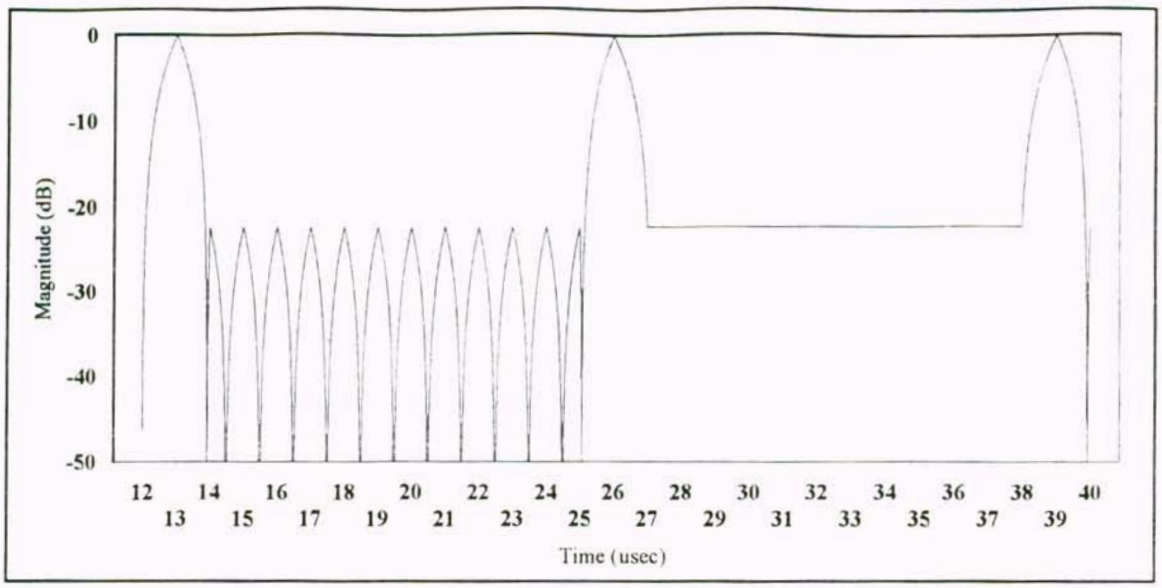

Figure 4. Normalized correlation of the 13 chip Barker code over three bits (+1,+1,-1) where the correlator was initialized with zero input at t = 0 usec, T_c = 1 usec, and f_o = 100.5 MHz.

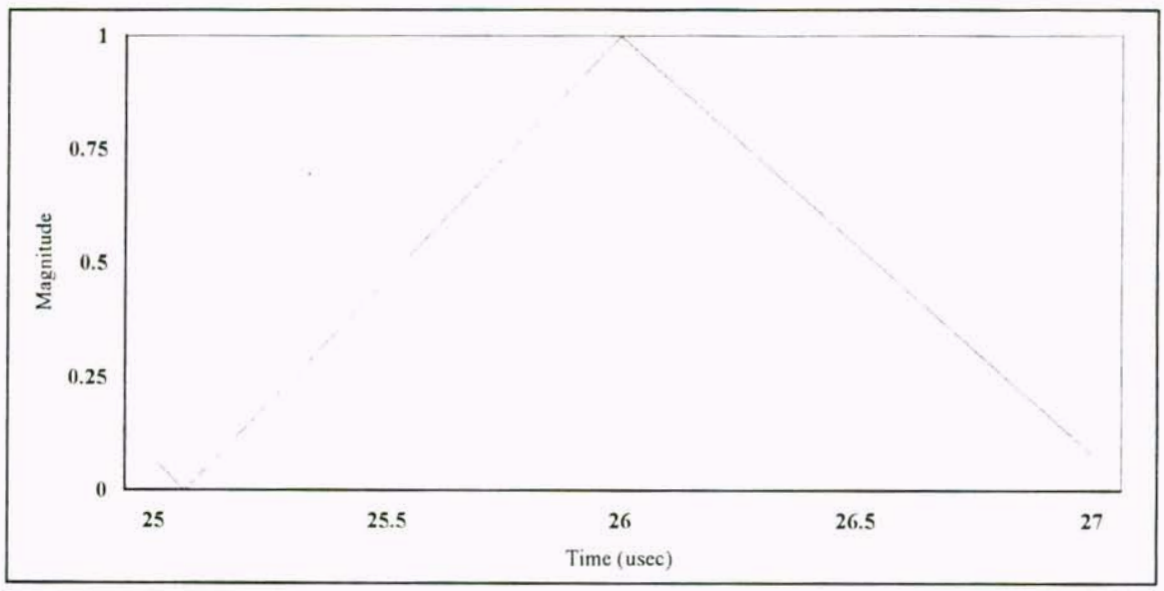

Figure 5. Normalized correlation of the 13 chip Barker code at the second +1 bit correlation peak where the correlator was initialized with zero input at t = 0 usec, T_c = 1 usec, and f_o = 100.5 MHz.

2.22 Pulse Compression Radar

In pulse compression radar the range resolution is defined as [9]

$$\delta_r = \frac{c}{2B} \tag{8}$$

where c is the speed of light (3×10^8 m/s) and B is the bandwidth of the transmitted signal. If an uncompressed pulse of length T is transmitted, Equation 8 becomes

$$\delta_r = \frac{cT}{2} \tag{9}$$

In pulse compressed radar, the transmitted signal is spread in order to achieve a reduction in the range resolution. If the system's effective pulse length τ is chosen such that $\tau \ll T$, then Equation 9 becomes

$$\delta_r = \frac{c\tau}{2} \tag{10}$$

which results in a narrower range resolution.

Pulse compression radar uses a CW frequency chirp to spread the frequency of the pulse. The CW chirp with a carrier ω_o is

$$c(t) = \cos(\omega_o t + \pi k t^2) rect(\tfrac{t}{T}) \tag{11}$$

where T is the pulse length, ω_o is the carrier frequency, and k^2 defines the rate of the frequency chirp over the pulse. The frequency deviation Δf over the pulse is determined by

$$\Delta f = |k|T \tag{12}$$

The frequency response of the chirp using the example in [1] to evaluate the Fourier transform integrals is

$$H(f) = \frac{1}{2\sqrt{2|k|}}[\{C(z_1) + C(z_2) \mp j[S(z_1) + S(z_2)]\}e^{\frac{j\pi(f-f_o)^2}{k}} + \{C(z_3) + C(z_4) \pm j[S(z_3) + S(z_4)]\}e^{-\frac{j\pi(f-f_o)^2}{k}}] \tag{13}$$

where the imaginary components are the top sign for $k > 0$ and the bottom sign for $k < 0$. C(z) and S(z) are the tabulated Fresnel integrals. The z_1, z_2, z_3, and z_4 terms are

$$z_1 = \sqrt{2|k|}\,(\frac{T}{2} + \frac{f+f_o}{k}) \tag{14}$$

$$z_2 = \sqrt{2|k|}\,(\frac{T}{2} - \frac{f+f_o}{k}) \tag{15}$$

$$z_3 = \sqrt{2|k|}\,(\frac{T}{2} - \frac{f-f_o}{k}) \tag{16}$$

$$z_4 = \sqrt{2|k|}\left(\frac{T}{2} + \frac{f - f_o}{k}\right) \tag{17}$$

The power spectral density (PSD) function is found by

$$S(f) = |H(f)|^2 \tag{18}$$

The autocorrelation function of the CW chirp can then be determined from

$$R(\tau) = \Im^{-1}\{S(f)\} \tag{19}$$

Upon correlation, the CW chirp pulse compresses into a sin(x)/x waveform if $T\Delta f$ is sufficiently large (approximately greater than 100) [5]. This is because the PSD function begins to closely approximate a rect function at this point which inverse Fourier transfoms to a sin(x)/x autocorrelation function.

The CR and PSL for a sufficiently large $T\Delta f$ with using matched filtering are [9]

$$CR = T\Delta f \tag{20}$$

$$PSL = -13.3\ dB \tag{21}$$

Figure 6 shows the normalized PSD function for a CW chirp where f_o = 100.5 MHz, Δf = 13 MHz, and T = 1 usec. It shows that a $T\Delta f$ = 13 is insufficient to realize a rect PSD function. Figure 7 shows the normalized compressed pulse for the same CW chirp. The shape only loosely resembles a sin(x)/x with a CR = 12.8, a PSL = -14.4 dB, and an ISL = -25 dB.

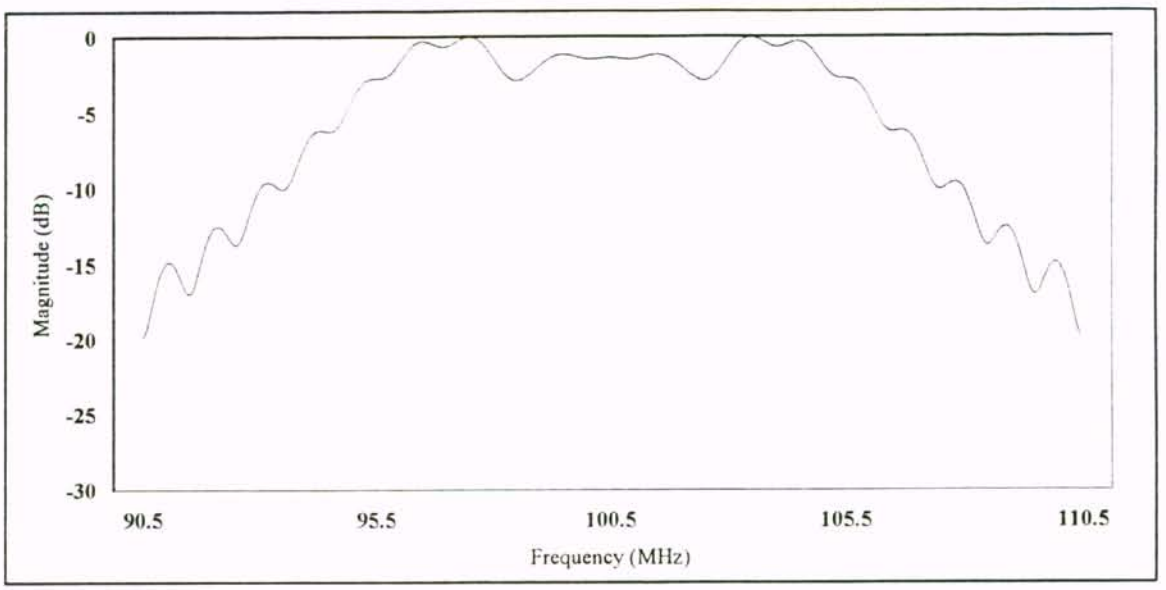

Figure 6. Normalized PSD function of a CW chirp where f_o = 100.5 MHz, Δf = 13 MHz, and T = 1 usec.

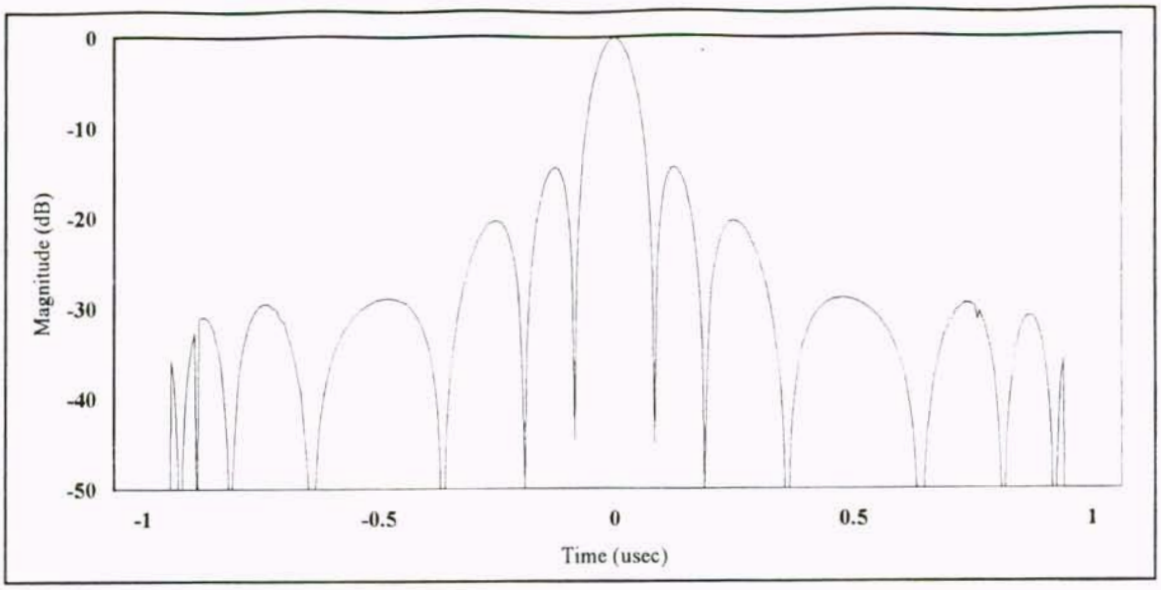

Figure 7. Normalized compressed pulse for a CW chirp where f_o = 100.5 MHz, Δf = 13 MHz, and T = 1 usec.

Figure 8 shows the normalized PSD function for a CW chirp where f_o = 100.5 MHz, Δf = 13 MHz, and T = 13 usec. This results in a $T\Delta f$ = 169 which is sufficient to realize a close approximation to a rect PSD function. The normalized compressed pulse for this CW chirp is found in Figure 9. The shape is virtually identical to a sin(x)/x and has a CR = 169 and a PSL = -13.3 dB which are in good agreement with Equations 20 and 21. The ISL has improved versus the first CW chirp to -35.4 dB.

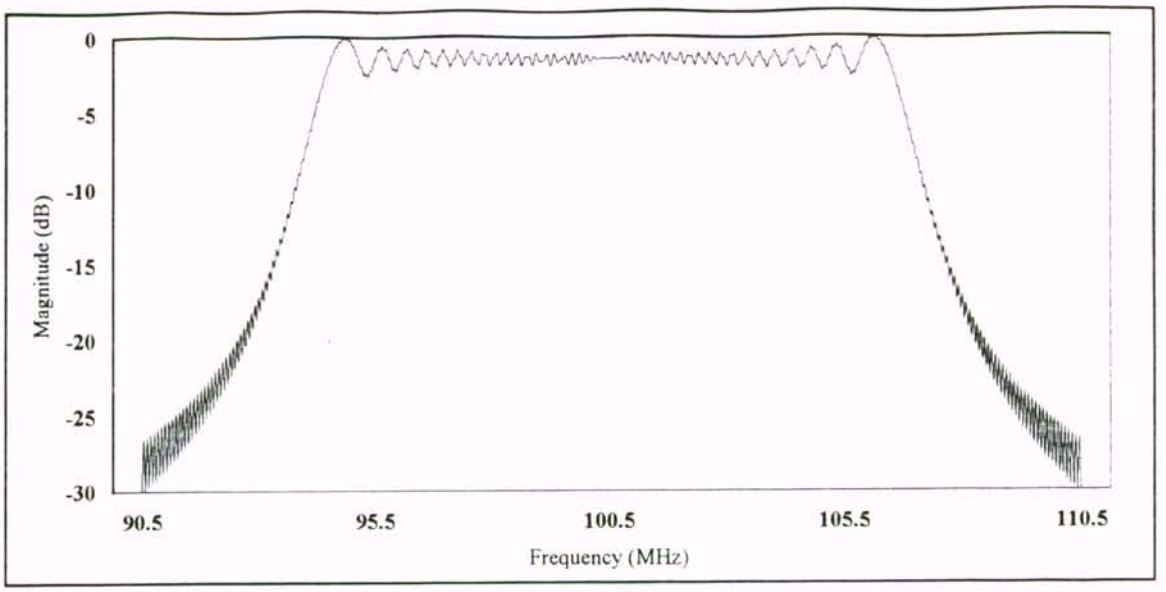

Figure 8. Normalized PSD function of a CW chirp where f_o = 100.5 MHz, Δf = 13 MHz, and T = 13 usec.

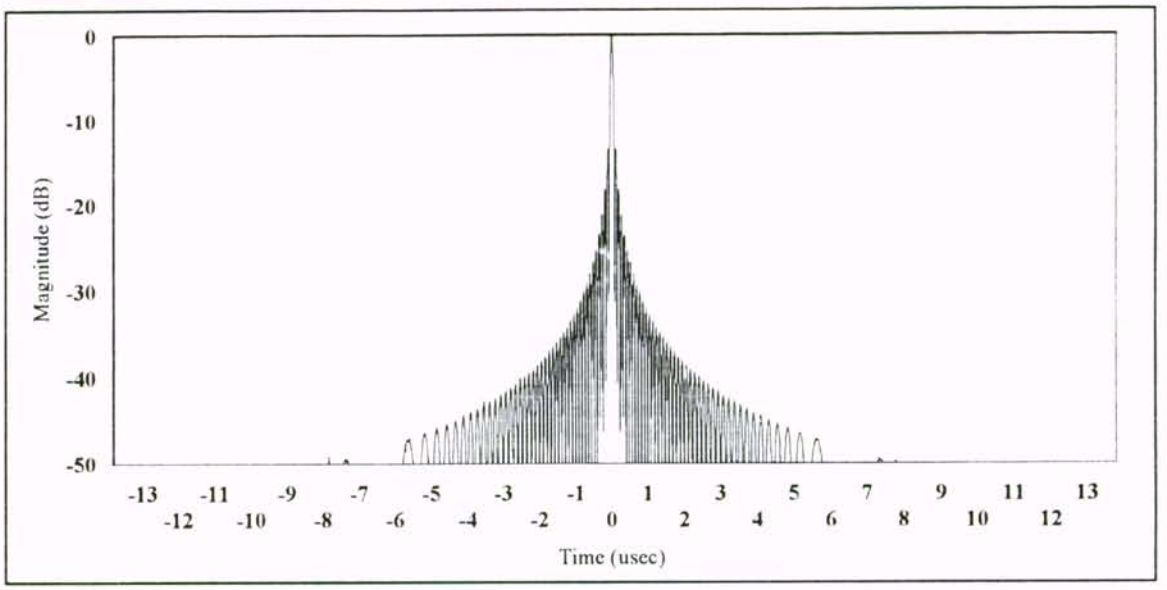

Figure 9. Normalized compressed pulse for a CW chirp where f_o = 100.5 MHz, Δf = 13 MHz, and T = 13 usec.

CHAPTER 3

THE WEIGHTED STEPPED CHIRP CODE SIGNAL

The weighted stepped chirp code signal is a combination of the chips in a PN code and the frequency dispersion of a CW chirp. The frequency dispersion is realized using the truncated cosine series functions defined and modified for asymmetry in [12] as the chip functions. These functions are further modified with a time delay on each function as

$$c(t) = \sum_{n=-\frac{(N-1)}{2}}^{\frac{(N-1)}{2}} a_n \cos((\omega_o + \frac{2\pi n}{T_c})(t - nT_c))rect(\frac{t-nT_c}{T_c}) \qquad (22)$$

where a_n is the weighting coefficient, ω_o is the carrier frequency, T_c is the chip length, N is the number of chips in the code, and n is the chip number ranging from -(N-1)/2 to (N-1)/2 incremented by one. The index n is an integer for the odd series (N odd) and an integer plus one-half for the even series (N even). Figure 10 shows a sample weighted stepped chirp code signal with uniform weighting, N = 5, and $f_0 = 3.5/T_c$. The X's mark the chip transitions. This illustrates the discretization of a CW chirp by the weighted stepped chirp. The frequency step can be seen from Equation 22 to be $1/T_c$.

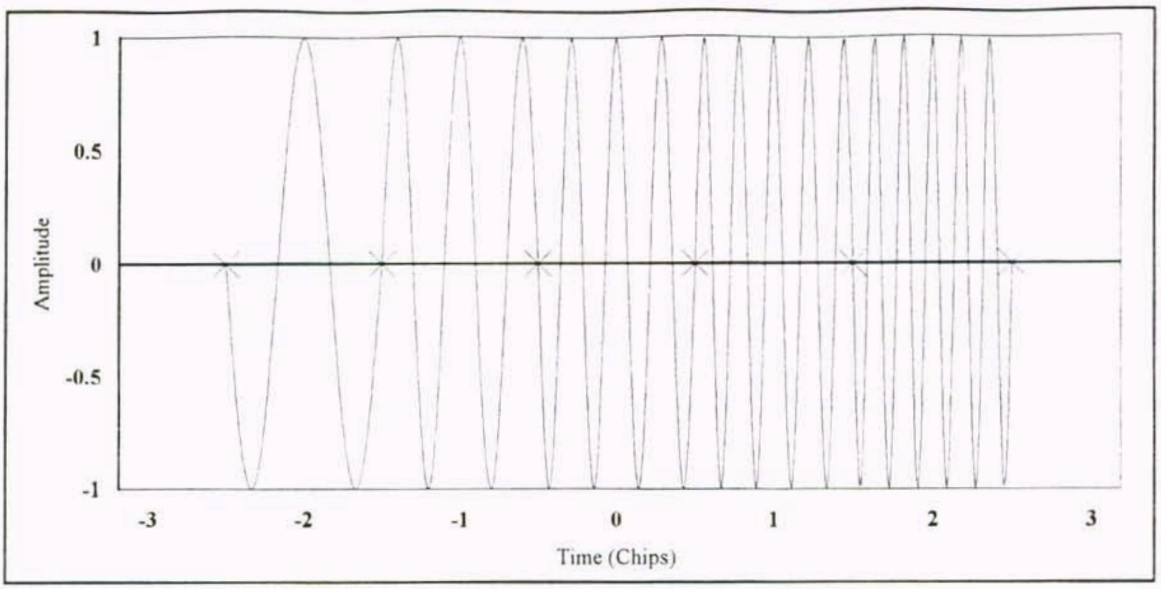

Figure 10. Sample weighted stepped chirp code signal with uniform weighting, N = 5, and $f_o = 3.5/T_c$. The X's mark the chip transitions.

These functions were chosen because they form a basis set of sin(x)/x functions in the frequency domain which minimizes the number of functions necessary to approximate a CW chirp and also because they have relatively small cross-correlation between functions. The frequency response of the weighted stepped chirp code signal is

$$H(f) = \frac{\tau}{2} \sum_{n=-\frac{(N-1)}{2}}^{\frac{(N-1)}{2}} a_n \{ Sa[\pi(f+f_o+\tfrac{n}{T_c})\tau] + Sa[\pi(f-f_o-\tfrac{n}{T_c})\tau] \} e^{-j2\pi fnT_c} \qquad (23)$$

3.1 Chip to Chip Correlation

The chip to chip correlation has been solved analytically in Equations 24a and 24b for chips with the same frequency $\omega_n = \omega_o + \frac{2\pi n}{T_c}$ and in Equations 25a and 25b for chips with different frequencies $\omega_n = \omega_o + \frac{2\pi n}{T_c}$ and $\omega_m = \omega_o + \frac{2\pi m}{T_c}$. The correlation of the

weighted stepped chirp code signal can be calculated by the summation of the chip to chip correlations in Equations 24a, 24b, 25a, and 25b thus eliminating the need to compute the correlation integral.

$$R(\tau) = \frac{\omega_n(T_c+\tau)\cos(\omega_n\tau)+\sin(\omega_n(T_c+\tau))}{2\omega_n} \quad \text{for } -T_c \le \tau \le 0 \tag{24a}$$

$$R(\tau) = \frac{\omega_n(T_c-\tau)\cos(\omega_n\tau)+\sin(\omega_n(T_c-\tau))}{2\omega_n} \quad \text{for } 0 < \tau \le T_c \tag{24b}$$

$$R(\tau) = T_c\left[\frac{\sin\left(\frac{2\pi n\tau+\omega_o\tau T_c+\omega_o T_c^2+\pi m T_c+\pi n T_c}{T_c}\right)+\sin\left(\frac{2\pi m\tau+\omega_o\tau T_c+\omega_o T_c^2+\pi m T_c+\pi n T_c}{T_c}\right)}{4(\omega_o T_c+\pi m+\pi n)} + \right.$$

$$\left.\frac{\sin\left(\frac{2\pi n\tau+\omega_o\tau T_c-\pi m T_c+\pi n T_c}{T_c}\right)-\sin\left(\frac{2\pi m\tau+\omega_o\tau T_c+\pi m T_c-\pi n T_c}{T_c}\right)}{4\pi(n-m)}\right] \quad \text{for } -T_c \le \tau \le 0 \tag{25a}$$

$$R(\tau) = T_c\left[\frac{\sin\left(\frac{-2\pi m\tau-\omega_o\tau T_c+\omega_o T_c^2+\pi m T_c+\pi n T_c}{T_c}\right)+\sin\left(\frac{-2\pi n\tau-\omega_o\tau T_c+\omega_o T_c^2+\pi m T_c+\pi n T_c}{T_c}\right)}{4(\omega_o T_c+\pi m+\pi n)} + \right.$$

$$\left.\frac{\sin\left(\frac{2\pi m\tau+\omega_o\tau T_c-\pi m T_c+\pi n T_c}{T_c}\right)-\sin\left(\frac{2\pi n\tau+\omega_o\tau T_c+\pi m T_c-\pi n T_c}{T_c}\right)}{4\pi(n-m)}\right] \quad \text{for } 0 < \tau \le T_c \tag{25b}$$

3.2 Optimal Center Frequency

It has been determined empirically that the optimal choice for a center frequency is one such that the chip functions are continuous. This is accomplished by setting f_o such that

$$f_o T_c = I + 0.5 \quad \text{for N odd} \tag{26}$$

$$f_o T_c = I \quad \text{for N even} \tag{27}$$

where I is an integer. In the sample weighted stepped chirp code signal in Figure 10, $f_o = 3.5/T_c$ and N = 5 which satisfies Equation 26 for continuity between chips. The chips can be seen to be continuous at the transitions marked by the X's.

CHAPTER 4

THEORETICAL CORRELATION RESULTS

The theoretical results for a 9 chip uniformly weighted, a 9 chip cosine-squared weighted, a 13 chip uniformly weighted, and a 13 chip Hamming weighted stepped chirp code signal are presented where the correlator was initialized with zero input at t = 0 usec, T_c = 1 usec, and f_o = 100.5 MHz. T_c and f_o satisfy the continuity requirements from Equation 26 in Chapter 3. The correlation functions were calculated using the chip to chip correlations in Equations 24a, 24b, 25a, and 25b from Chapter 3. Appendix A shows the MathCAD file used to compute the theoretical correlation functions.

The PSD function is determined by

$$S(f) = |H_T(f)||H_R(f)| \tag{28}$$

where $H_T(f)$ is the transmitted code signal's frequency response and $H_R(f)$ is the matched filter code signal's frequency response. Both can be determined using Equation 23 in Chapter 3.

4.1 The 9 Chip Weighted Stepped Chirp Code Signal

The theoretical PSD and correlation functions for both a 9 chip uniformly weighted stepped chirp code signal and a 9 chip cosine-squared weighted stepped chirp code signal are presented. Their performances are compared to each other and to PN codes.

4.11 Uniformly Weighted

Figure 11 shows the normalized PSD function for the 9 chip uniformly weighted stepped chirp code signal. It closely resembles the PSD function expected for a similar CW chirp except for some minor differences in the shape of the sidelobes and a less smooth response over Δf.

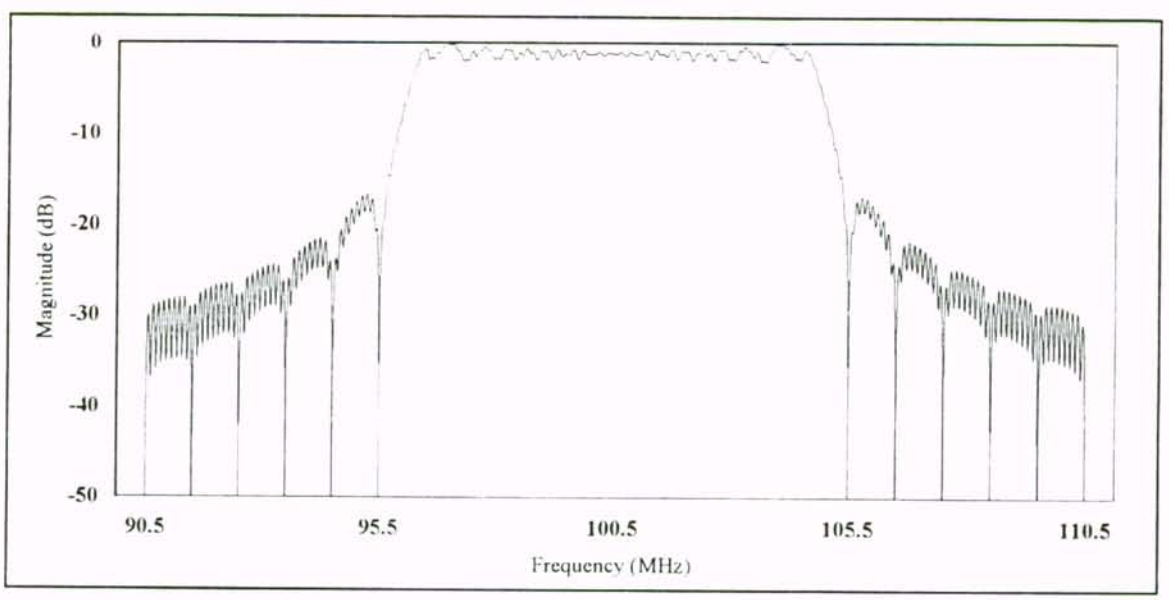

Figure 11. Normalized PSD function of an uniformly weighted stepped chirp code signal where N = 9, T_c = 1 usec, and f_o = 100.5 MHz.

Figure 12 shows the normalized correlation of the 9 chip uniformly weighted stepped chirp code signal over three bits (+1,+1,-1). The correlation function possesses equally good time sidelobes in both the in-phase (+1,+1) and phase reversal (+1,-1) regions. The correlation function also displays sin(x)/x correlation peaks as shown in Figure 13. This sin(x)/x response occurs because the correlation of the chips with their matched filter counterparts is approximated by the correlation of a CW chirp where $T = T_c$ and $\Delta f = N/T_c$, and the uniformly weighted stepped chirp code signal results in a flat PSD function over Δf regardless of the value of $T\Delta f$. This results in a CR = 9 and a PSL = -13.3 dB in the peak correlation regions even though $T\Delta f << 100$. This means that the peak correlation region is predictably a sin(x)/x for any $T\Delta f$. Outside of the peak correlation region, the CR = 9 due to the use of 9 chips and the PSL = -28.2 dB from the cross-correlation of the chip functions. This results in an overall CR = 81 and a PSL = -13.3 dB due to the sin(x)/x correlation peaks. The ISL = -29.4 dB with no LPG.

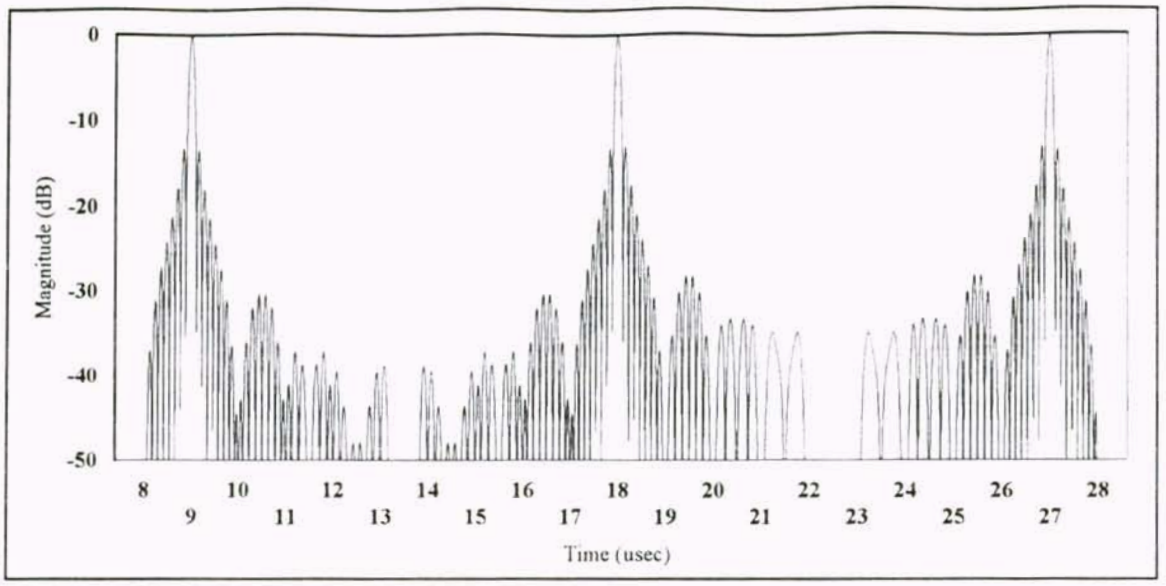

Figure 12. Normalized correlation of an uniformly weighted stepped chirp over three bits (+1,+1,-1) where the correlator was initialized with zero input at t = 0 usec, N = 9, T_c = 1 usec, and f_o = 100.5 MHz.

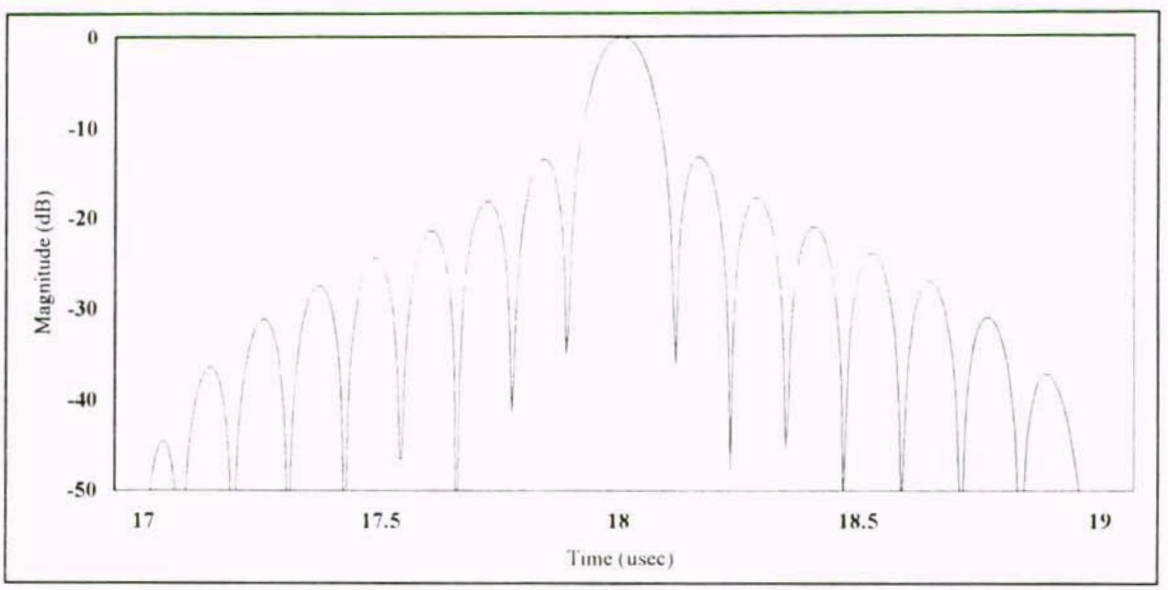

Figure 13. Normalized correlation of an uniformly weighted stepped chirp at the second +1 correlation peak where the correlator was initialized with zero input at t = 0 usec, N = 9, T_c = 1 usec, and f_o = 100.5 MHz.

4.12 Cosine-squared Weighted

The 9 chip uniformly weighted stepped chirp code signal has the CR of an 81 chip PN code, but the PSL of a 4 chip PN code and the ISL of a 24 chip PN code using Equations 5 and 6 from Chapter 2 to evaluate the equivalent PN code length for the CR and PSL and Equation 29 to evaluate the equivalent PN code length for the ISL assuming a PN code with half the sidelobes being triangular and half the sidelobes being rectangular.

$$N = \sqrt{\frac{2}{3\log^{-1}(\frac{ISL}{10})}} \tag{29}$$

The time sidelobes of the peak correlation region must be reduced in order to make the weighted stepped chirp code signal useful. In [6] the time sidelobes of a CW chirp in pulse compression radar were shown to be reduced by weighting the frequency response. The tradeoff is that the CR decreases as the PSL and ISL decrease.

From [9], the PSL of a CW chirp can be reduced to -32.2 dB with a pulse widening of 1.62 using the cosine-squared window function to weight the PSD function of the stepped chirp code signal. The weighting is done only at the correlator so that the power from the transmitter is maximized for all frequencies. The cost of mismatching the filter is a reduction in the SNR which results in a LPG = 1.76 dB for the cosine-squared window function.

For the weighted stepped chirp code signal, the window function is placed over the code signal's time response with a time length equal to that of the code signal. Each chip

is assigned a weight a_n by sampling the window function at the center of chip n as shown in Figure 14 where the dashed line is the cosine-squared window function and the solid line is the cosine-squared weighted stepped chirp code signal's chips.

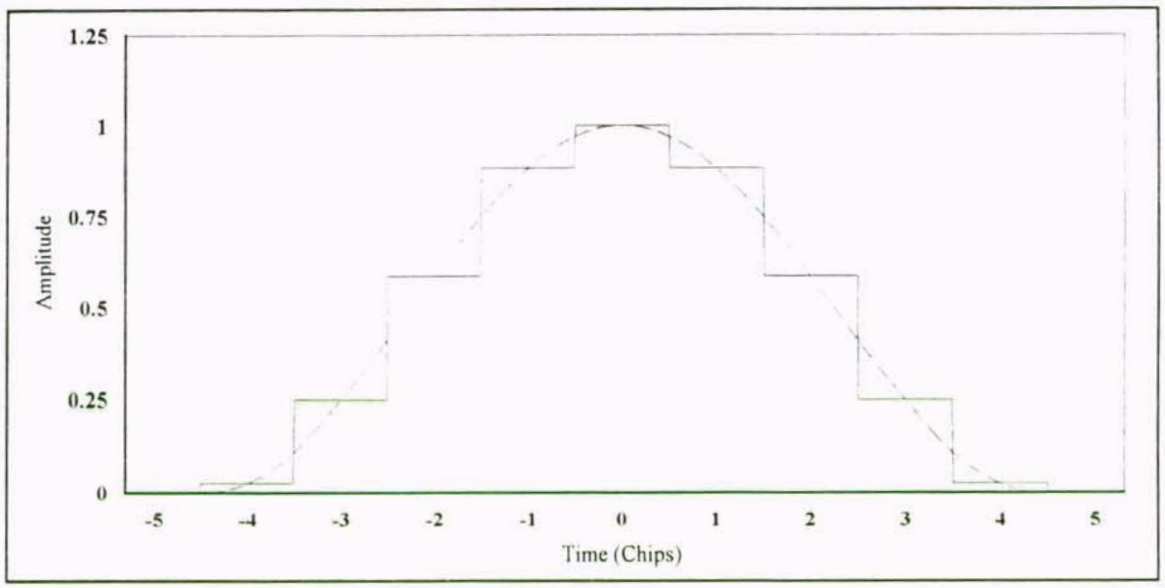

Figure 14. Selection of chip weights for a cosine-squared weighted stepped chirp code signal where N = 9. The dashed line is the cosine-squared window function and the solid line is the cosine-squared weighted stepped chirp code signal's chips.

The weighting coefficients can be found using

$$a_n = \cos^2\left(\frac{\pi n}{N}\right) \tag{30}$$

The weighting coefficients for the 9 chip cosine-squared weighted stepped chirp code signal are found in Table 1.

Chip n	a_n
-4	0.030
-3	0.250
-2	0.587
-1	0.883
0	1
1	0.883
2	0.587
3	0.250
4	0.030

Table 1. Weighting coefficients for the 9 chip cosine-squared weighted stepped chirp code signal.

These weighting coefficients result in the PSD function being weighted by the cosine-squared window function as seen in Figure 15. The PSD function shows some minor differences in the shape of the sidelobes and a less smooth response over Δf than would be expected for a similarly weighted CW chirp.

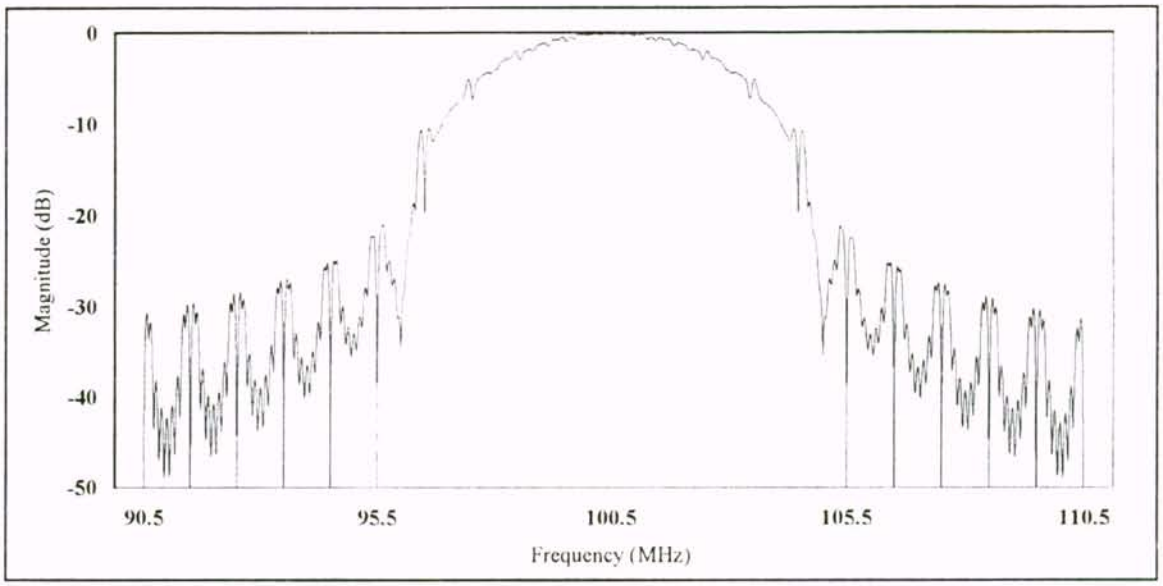

Figure 15. Normalized PSD function of a cosine-squared weighted stepped chirp code signal where N = 9, T_c = 1 usec, and f_o = 100.5 MHz.

Figure 16 shows the normalized correlation of the 9 chip cosine-squared weighted stepped chirp code signal over three bits (+1,+1,-1). The correlation function still possesses equally good time sidelobes in both the in-phase (+1,+1) and phase reversal (+1,-1) regions. The peak correlation region in Figure 17 now corresponds to a cosine-squared weighted CW chirp where $T = T_c$ and $\Delta f = N/T_c$ with a PSL = -32.2 dB and a CR = 5.56. Outside of the peak correlation region, the CR = 9 due to the use of 9 chips and the PSL = -32.4 dB from the cross-correlation of the chip functions. The cosine-squared weighting has not only reduced the sidelobes in the peak correlation region as predicted, but has also reduced the sidelobes in the cross-correlation region from -28.2 dB to -32.4 dB. This results in an overall CR = 50 and a PSL = -32.2 dB due to the peak correlation region. The ISL = -43.3 dB which is a 13.9 dB improvement over the 9 chip uniformly weighted stepped chirp code signal with a LPG = 1.76 dB. The CR corresponds to that of a 50 chip PN code, the PSL corresponds to that of a 40 chip PN code, and the ISL is corresponds to that of a 119 chip PN code. Thus, a 9 chip cosine-squared weighted stepped chirp code signal's performance equals or exceeds that of a 40 chip PN code.

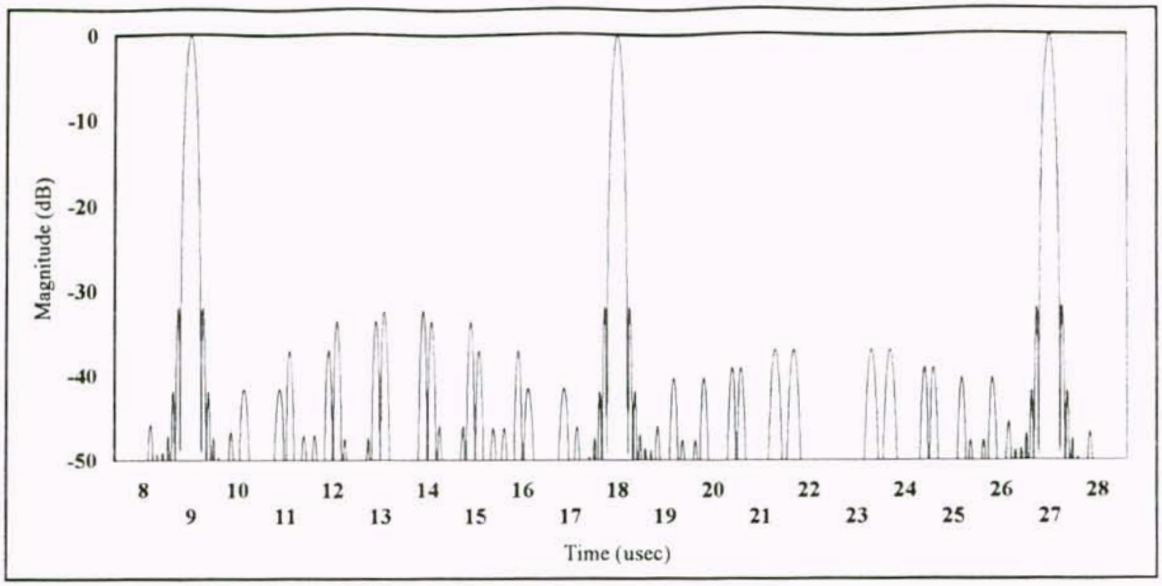

Figure 16. Normalized correlation of a cosine-squared weighted stepped chirp over three bits (+1,+1,-1) where the correlator was initialized with zero input at t = 0 usec, N = 9, T_c = 1 usec, and f_o = 100.5 MHz.

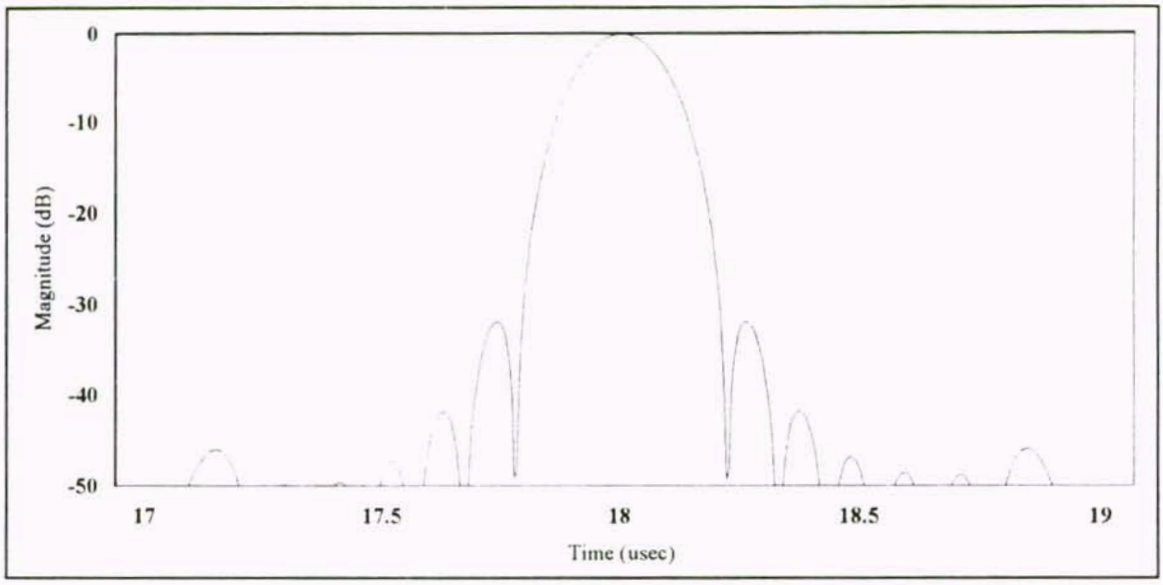

Figure 17. Normalized correlation of a cosine-squared weighted stepped chirp at the second +1 correlation peak where the correlator was initialized with zero input at t = 0 usec, N = 9, T_c = 1 usec, and f_o = 100.5 MHz.

4.2 The 13 Chip Weighted Stepped Chirp Code Signal

The theoretical PSD and correlation functions for both a 13 chip uniformly weighted stepped chirp code signal and a 13 chip Hamming weighted stepped chirp code signal are presented. Their performances are compared to each other and to PN codes.

4.21 Uniformly Weighted

Figure 18 shows the normalized PSD function for the 13 chip uniformly weighted stepped chirp code signal. It closely resembles the PSD function expected for a similar CW chirp except for some minor differences in the shape of the sidelobes and a less smooth response over Δf.

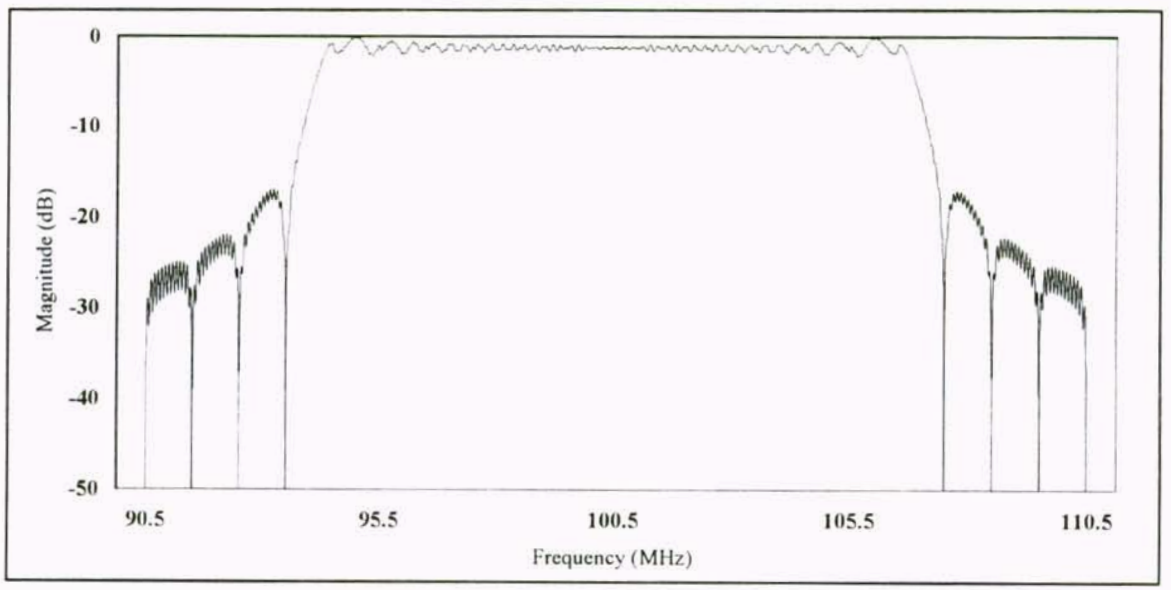

Figure 18. Normalized PSD function of an uniformly weighted stepped chirp code signal where N = 13, T_c = 1 usec, and f_o = 100.5 MHz.

Figure 19 shows the normalized correlation of the uniformly weighted stepped chirp code signal over three bits (+1,+1,-1). The correlation function possesses equally good time sidelobes in both the in-phase (+1,+1) and phase reversal (+1,-1) regions. The correlation function also displays the expected sin(x)/x correlation peaks as shown in Figure 20. This results in a CR = 13 and a PSL = -13.3 dB in the peak correlation regions. Outside of the peak correlation region, the CR = 13 due to the use of 13 chips and the PSL = -33.1 dB from the cross-correlation of the chip functions. This results in an overall CR = 169 and a PSL = -13.3 dB due to the sin(x)/x correlation peaks. The ISL = -32.5 dB with no LPG.

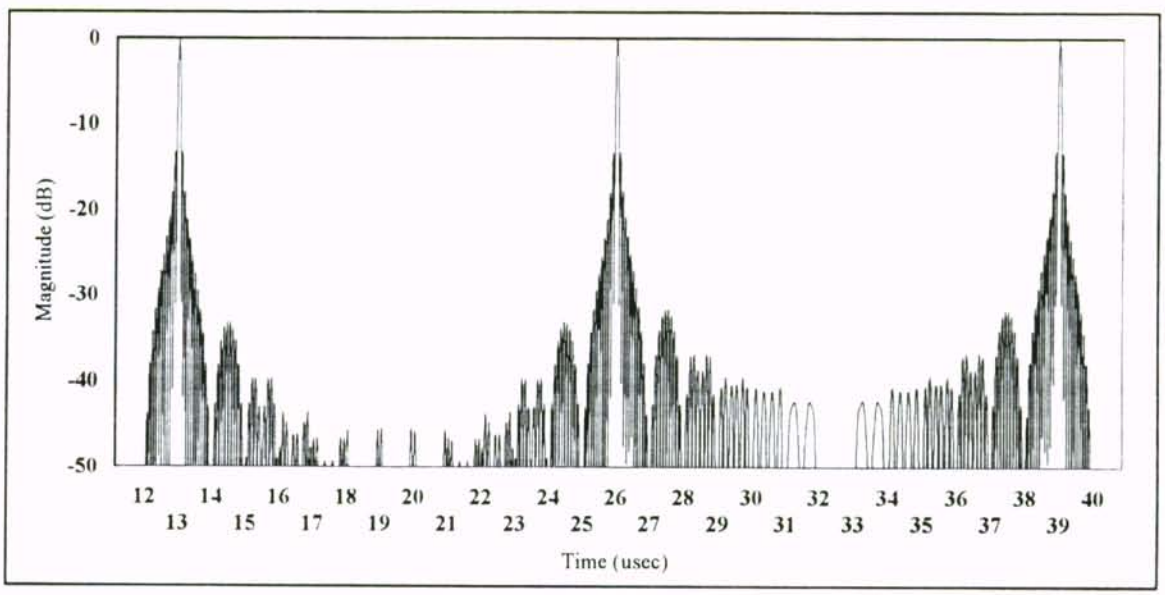

Figure 19. Normalized correlation of an uniformly weighted stepped chirp over three bits (+1,+1,-1) where the correlator was initialized with zero input at t = 0 usec, N = 13, T_c = 1 usec, and f_o = 100.5 MHz.

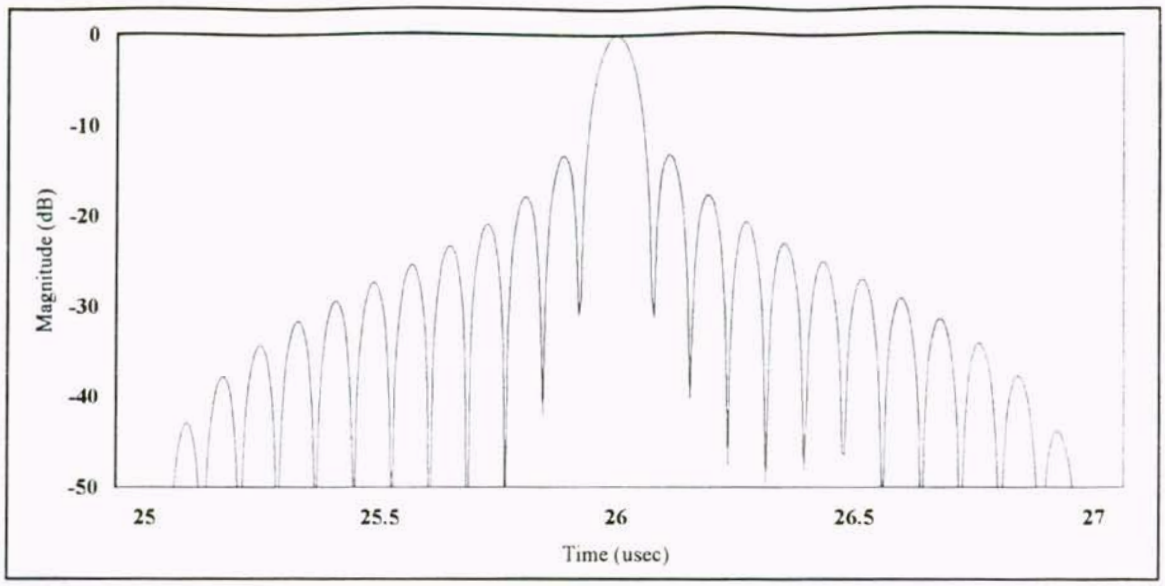

Figure 20. Normalized correlation of an uniformly weighted stepped chirp at the second +1 correlation peak where the correlator was initialized with zero input at t = 0 usec, N = 13, T_c = 1 usec, and f_o = 100.5 MHz.

4.22 Hamming Weighted

The 13 chip uniformly weighted stepped chirp code signal has the CR of a 169 chip PN code, but the PSL of a 4 chip PN code and an ISL of a 34 chip PN code. As with the 9 chip uniformly weighted stepped chirp code signal, the time sidelobes of the peak correlation region must be reduced in order to make the stepped chirp code signal useful.

From [9], the PSL of a CW chirp can be reduced to -42.8 dB with a pulse widening of 1.47 using the Hamming window function to weight the PSD function of the weighted stepped chirp code signal. Again the weighting is done only at the correlator so that the power from the transmitter is maximized for all frequencies. The cost of mismatching the filter is a LPG = 1.34 dB for the Hamming window function.

Each chip is assigned a weight a_n by sampling the Hamming window function at the center of chip n as shown in Figure 21 where the dashed line is the Hamming window function and the solid line is the Hamming weighted stepped chirp code signal's chips.

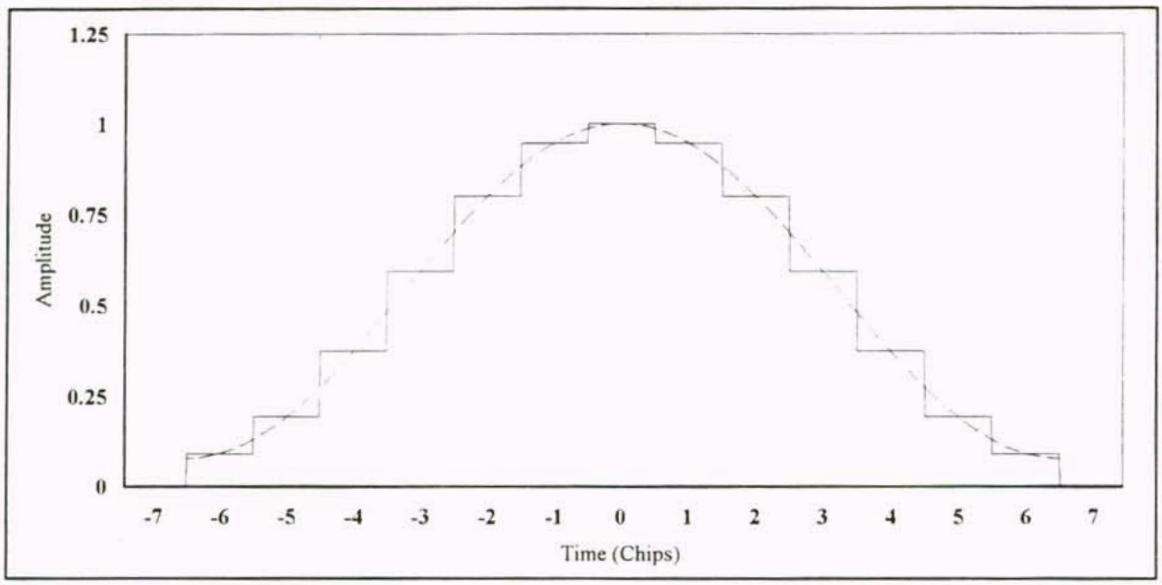

Figure 21. Selection of chip weights for a Hamming weighted stepped chirp code signal where N = 13. The dashed line is the Hamming window function and the solid line is the Hamming weighted stepped chirp code signal's chips.

The weighting coefficients can be found using

$$a_n = 0.08 + 0.92\cos^2(\tfrac{\pi n}{N}) \tag{31}$$

The weighting coefficients for the 13 chip Hamming weighted stepped chirp code signal are found in Table 2.

Chip n	a_n
-6	0.093
-5	0.196
-4	0.377
-3	0.595
-2	0.801
-1	0.947
0	1
1	0.947
2	0.801
3	0.595
4	0.377
5	0.196
6	0.093

Table 2. Weighting coefficients for the 13 chip Hamming weighted stepped chirp code signal.

This results in the PSD function being weighted by the Hamming window function as shown in Figure 22. The PSD function shows some minor differences in the shape of the sidelobes and a less smooth response over Δf than for a similarly weighted CW chirp.

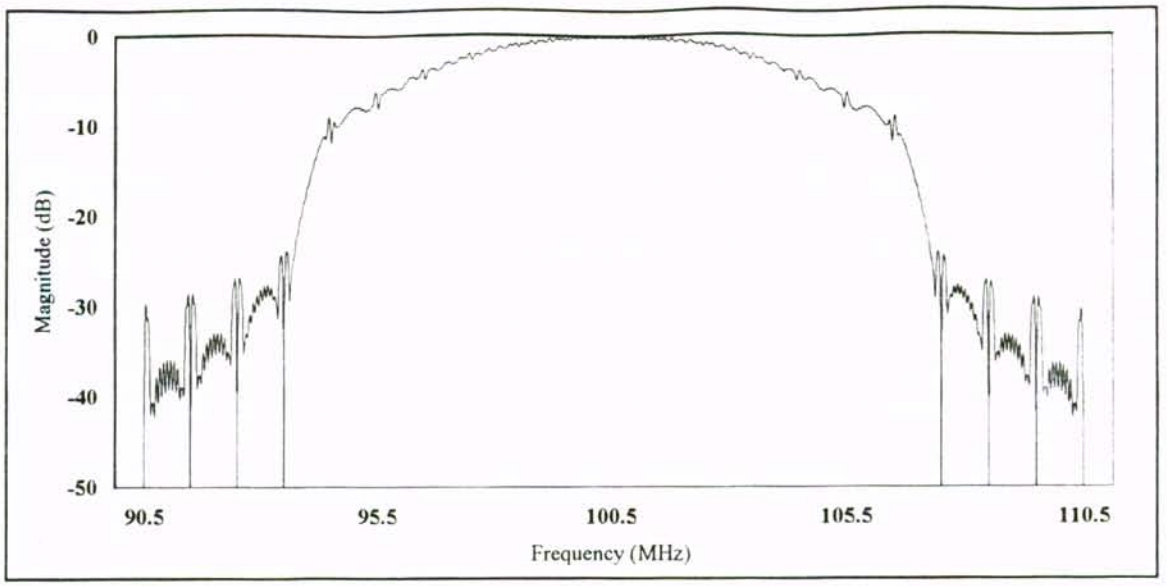

Figure 22. Normalized PSD function of a Hamming weighted stepped chirp code signal where N = 13, T_c = 1 usec, and f_o = 100.5 MHz.

Figure 23 shows the normalized correlation of the Hamming weighted stepped chirp code signal over three bits (+1,+1,-1). The correlation function still possesses equally good time sidelobes in both the in-phase (+1,+1) and phase reversal (+1,-1) regions. The peak correlation region in Figure 24 now corresponds to a Hamming weighted CW chirp where $T = T_c$ and $\Delta f = N/T_c$ with a PSL = -42.8 dB and a CR = 8.84. Outside of the peak correlation region, the CR = 13 due to the use of 13 chips and the PSL = -39.4 dB from the cross-correlation of the chip functions. The Hamming weighting has not only reduced the sidelobes in the peak correlation region as predicted, but has also reduced the sidelobes in the cross-correlation region from -33.1 dB to -39.4 dB. This results in an overall CR = 115 and a PSL = -39.4 dB due to the cross-correlation region. The ISL = -49.7 dB which is a 17.2 dB improvement versus the 13 chip uniformly

weighted stepped chirp code signal with a LPG = 1.34 dB. The CR corresponds to that of a 115 chip PN code, the PSL corresponds to that of a 93 chip PN code, and the ISL corresponds to that of a 249 chip PN code. Thus, a 13 chip Hamming weighted stepped chirp code signal's performance equals or exceeds that of a 93 chip PN code.

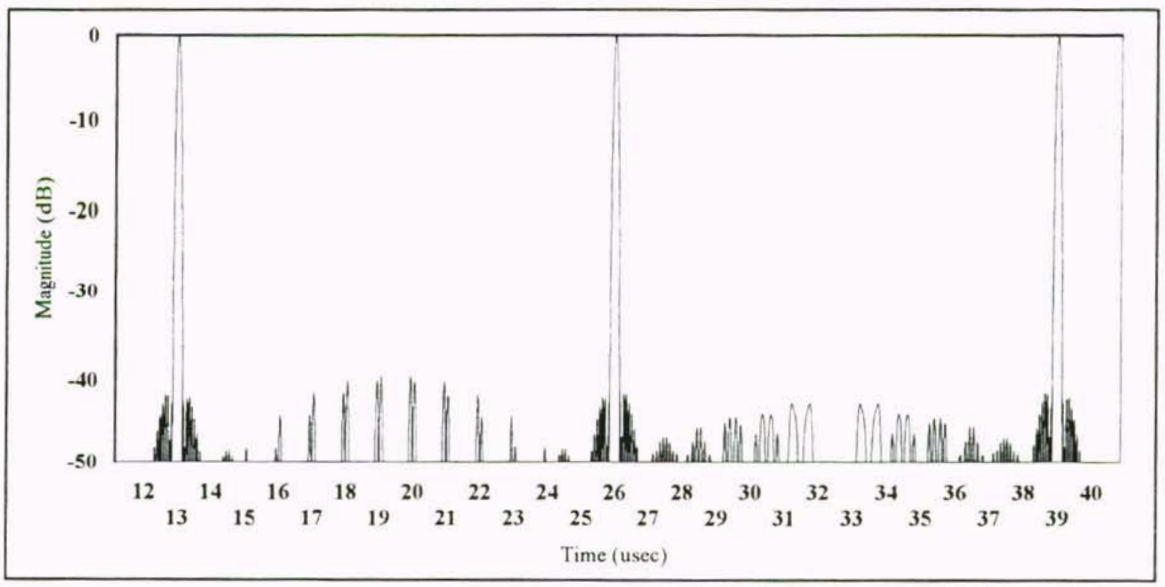

Figure 23. Normalized correlation of a Hamming weighted stepped chirp over three bits (+1,+1,-1) where the correlator was initialized with zero input at t = 0 usec, N = 13, T_c = 1 usec, and f_o = 100.5 MHz.

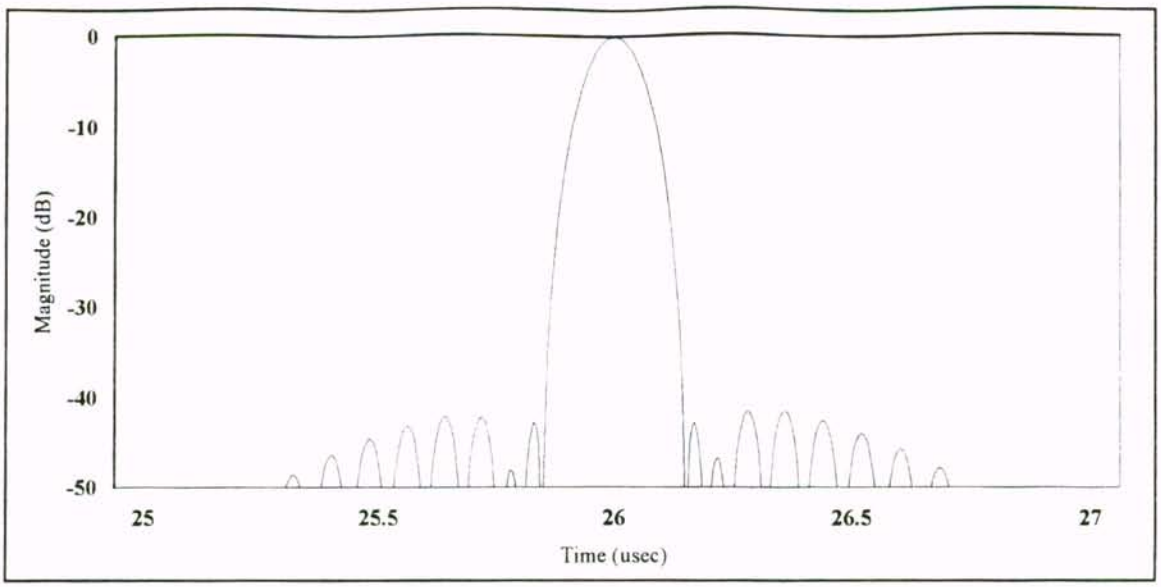

Figure 24. Normalized correlation of a Hamming weighted stepped chirp at the second +1 correlation peak where the correlator was initialized with zero input at t = 0 usec, N = 13, T_c = 1 usec, and f_o = 100.5 MHz.

CHAPTER 5

THEORETICAL PROBABILITY OF ERROR

The most important measure of a digital communications system is its BER. For DS/SS communications systems, the BER is a function of the SJR and the processing gain G_p. The SNR is not significant in calculating the BER because the jammer power is much greater than the thermal background noise power. Equation 32 shows the BER for a DS/SS communications system transmitting a binary phase shift keying (BPSK) data stream with received power S with a single tone CW jammer with power J [13]

$$BER = Q(\sqrt{4(SJR)G_p}) \tag{32}$$

where Q is the complimentary error function

$$Q(x) = \int_x^\infty \frac{1}{\sqrt{2\pi}} e^{-\frac{u^2}{2}} du \tag{33}$$

The G_p for a matched filter DS/SS code signal is

$$G_p = CR \tag{34}$$

For a mismatched filter configuration the LPG must be taken into account

$$G_p = 20\log(CR) - LPG \tag{35}$$

where G_p is in dB.

Figure 25 compares the BER for the 9 chip uniformly and cosine-squared weighted stepped chirp code signals to that of a 9 chip PN code. This graph shows that both 9 chip weighted stepped chirp code signals result in significantly better BER when compared to the 9 chip PN code. Using a BER of 10^{-5} as the delineation between unacceptable and acceptable BER, the 9 chip PN code has an acceptable BER down to a SJR = -11.4 dB. The 9 chip uniformly weighted stepped chirp code signal operates effectively down to a SJR = -30.5 dB while the 9 chip cosine-squared weighted stepped chirp code signal is useful to a SJR = -24.5 dB. The 6 dB difference between acceptable SJR's for the weighted stepped chirp code signals is attributable to the LPG = 1.76 dB due to mismatching and the difference in CR's between the two code signals which both effect G_p. The uniformly weighted stepped chirp code signal has a better BER compared to the cosine-squared weighted stepped chirp code signal, but the reduced sidelobes of the correlation function reduce the probability of false alarms due to jamming or interference.

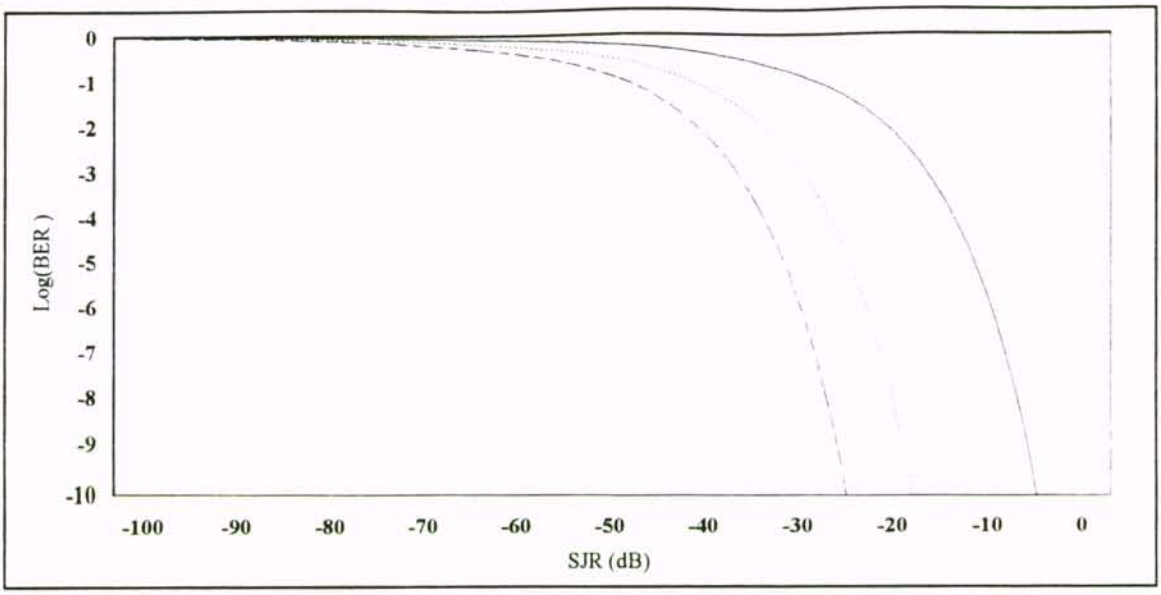

Figure 25. BER for a BPSK data stream as a function of the SJR for the 9 chip uniformly (dashed line) and cosine-squared (dotted line) weighted stepped chirp code signals, and a 9 chip PN code (solid line).

Figure 26 compares the BER for the 13 chip uniformly and Hamming weighted stepped chirp code signals to that of a 13 chip PN code. This graph shows that both 13 chip weighted stepped chirp code signals result in significantly better BER when compared to the 13 chip PN code. The 13 chip PN code has an acceptable BER down to a SJR = -14.6 dB. The 13 chip uniformly weighted stepped chirp code signal operates effectively down to a SJR = -36.9 dB while the 13 chip Hamming weighted stepped chirp code signal is useful to a SJR = -32.2 dB. The 4.7 dB difference between acceptable SJR's for the weighted stepped chirp code signals is once again attributable to the LPG = 1.34 dB due to mismatching and the difference in CR's between the two code signals.

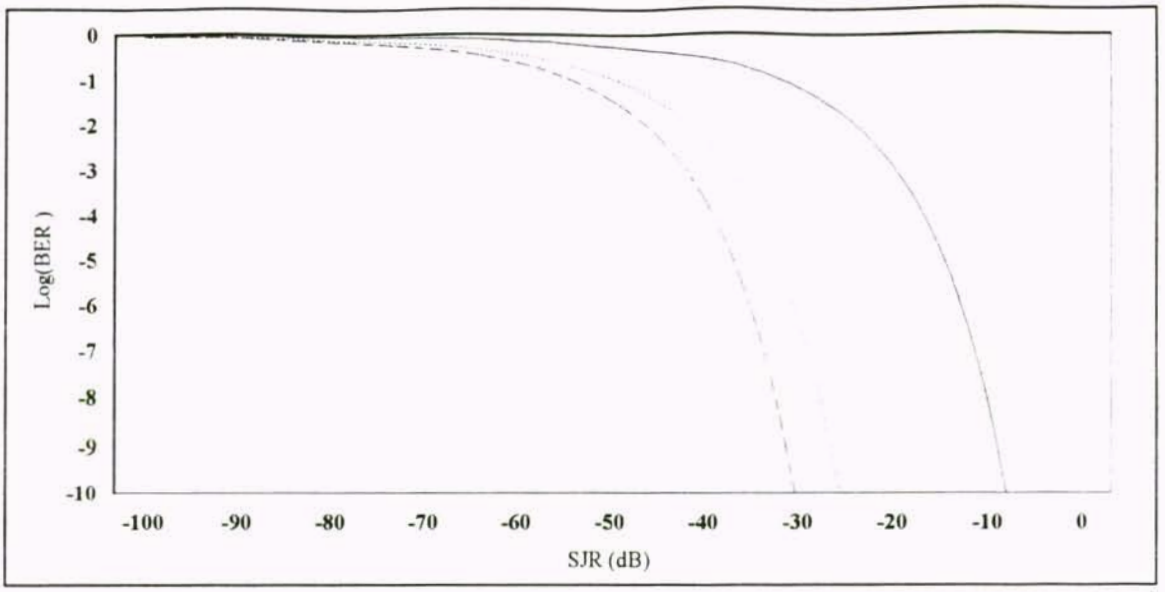

Figure 26. BER for a BPSK data stream as a function of the SJR for the 13 chip uniformly (dashed line) and Hamming (dotted line) weighted stepped chirp code signals, and a 13 chip PN code (solid line).

CHAPTER 6

SAW DEVICES IN DS/SS COMMUNICATIONS SYSTEMS

The use of SAW devices as code signal generators and correlators for spread spectrum systems has been well documented [14]-[16]. SAW devices are desirable because they eliminate many of the components in a DS/SS communications system resulting in a smaller, less expensive, more power efficient receiver. Correlation using a SAW device eliminates the need to synchronize the code signal at the receiver with the incoming code signal because the SAW device acts as a sliding correlator. This eliminates the need for acquisition and tracking loops which greatly reduces the number of components and also enhances performance by eliminating start up time for code signal alignment. The biggest disadvantages for SAW devices are the restriction on code length due to wafer size, the possibility of waveguiding effects, and the frequency limitations due to limits in current fabrication techniques.

In the case of the weighted stepped chirp code signal, SAW devices are even more desirable. Since the code signal requires different frequencies for each chip, multiple frequencies must be generated. A frequency synthesizer, a voltage controlled oscillator with great frequency range, or multiple oscillators would be required to generate the code signal at both the transmitter and the receiver. All of these would necessitate acquisition

and tracking loops which increase cost, increase size, and result in a loss in performance. Performance loss also arises from the changes in frequency between chips. These frequency changes result in degradation due to switching noise and also due to the discontinuities created by phase shifts introduced between chips.

Figure 27 shows the general diagram of a DS/SS communications system using SAW devices as the code signal generator at the transmitter and the correlator at the receiver. The data is converted to impulses which are used to generate the code signal from the SAW device at the transmitter. At the receiver, another SAW device is used as a correlator to generate the correlation of the transmitted code signal with the code signal at the receiver. The output of the correlator is then mixed with the carrier frequency and low pass filtered in order to obtain the base-band correlation function. This is then input to a threshold detector in order to determine whether the received data was a +1, -1, or indeterminate.

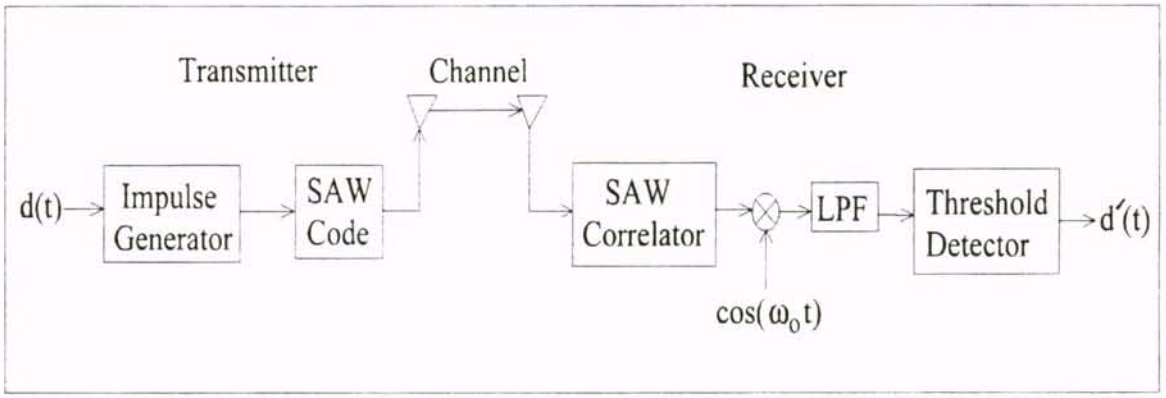

Figure 27. General diagram of a DS/SS communications system using SAW devices as the code signal generator at the transmitter and the correlator at the receiver.

For the weighted stepped chirp code signal, the SAW code signal generator at the transmitter will need to be weighted in order to compensate for the frequency response of the impulse generator since the chips are frequency dependent. If the impulse generator output were an ideal impulse then the frequency spectrum would be uniform and the SAW code signal would be generated without any distortion. Since an ideal impulse is impossible to generate, the impulse generator output can be modeled as an extremely short triangular pulse of length 2τ.

$$i(t) = \Lambda(\tfrac{t}{\tau}) \tag{36}$$

This results in a frequency response

$$I(f) = \tau Sa^2(\pi f \tau) \tag{37}$$

Each chip of the weighted stepped chirp code signal must be weighted in order to compensate for I(f). This is accomplished by evaluating I(f) at the center frequency of each chip, taking the inverse, normalizing, and weighting each chip accordingly.

CHAPTER 7

EXPERIMENTAL SAW DEVICE DESIGNS

The weighted stepped chirp code signal was implemented on SAW devices incorporating 8 different designs in order to evaluate the difference in performance due to code length (9 or 13 chips), weighting (uniformly weighted or window function weighted), and sampling ($4f_o$ across the code signal or $4f_n$ across each chip n). Table 3 shows the code length, weighting, and sampling for the 8 different weighted stepped chirp code signal SAW designs.

Device	Chips	Weighting	Sampling
1	13	Uniform	$4f_o$
2	13	Hamming	$4f_o$
3	9	Uniform	$4f_o$
4	9	Cosine-squared	$4f_o$
5	13	Uniform	$4f_n$
6	13	Hamming	$4f_n$
7	9	Uniform	$4f_n$
8	9	Cosine-squared	$4f_n$

Table 3. Code length, weighting, and sampling technique for the 8 experimental weighted stepped chirp code signal SAW designs.

The 9 and 13 chip devices will show how the number of chips effects the performance of the weighted stepped chirp code signal. From the theoretical results in

Chapter 4, the CR and PSL improve as the number of chips in the code increases. The cosine-squared and Hamming window functions were chosen as the weighting functions for the 9 and 13 chip weighted stepped chirp code signals, respectively, so that the PSL in the peak correlation region would match the PSL in the cross-correlation region. Tables 1 and 2 in Chapter 4 show the weighting coefficients for the 9 chip cosine-squared and 13 chip Hamming weighted stepped chirp code signals, respectively. Two different sampling methods were employed. One involved sampling across the entire weighted stepped chirp code signal at $4f_o$. The other technique sampled each chip of the code at $4f_n$ where f_n is the center frequency of chip n. Theoretically, $4f_o$ sampling results in a loss of 3 dB compared to $4f_n$ sampling due to the difference in power between the apodized samples when $4f_o$ sampling and the uniform samples when $4f_n$ sampling. This results in a 6 dB loss for a transmitter/receiver pair of SAW devices.

7.1 SAW Device Design Considerations

Several SAW second order effects must be considered when designing weighted stepped chirp code signals on SAW devices. These include ISI, output transducer weighting, waveguiding, and RF feed-through. Table 4 shows the experimental SAW device design specifications. The product of f_o and T_c satisfy the continuity requirements found in Equation 26 in Chapter 3. Figure 28 shows the device layout for the 9 chip weighted stepped chirp code signal experimental SAW devices. The layout for the 13 chip devices is identical except for a longer code signal transducer. Note that two output transducers were used in the designs. This was done so that each device could be used as

either a code signal generator or a correlator and also so that any waveguiding in the devices could be detected by shorting out the code signal transducer and looking at the response of the output transducers.

Substrate	40° rotated quartz
SAW velocity (v_{SAW})	3157 m/s
Center frequency (f_o)	85.79 MHz
Wavelength (λ_o)	36.8 um
Electrode width ($\lambda_o/8$)	4.6 um
Beam aperture (W)	$50\lambda_o$
Chip length (T_c)	$43.5\lambda_o$ (0.507 usec)
Chip to chip spacing	$0\lambda_o$
Output transducer length	$7.5\lambda_o$
Distance to output transducers	1 mm, 1.93 mm

Table 4. Experimental SAW device design specifications.

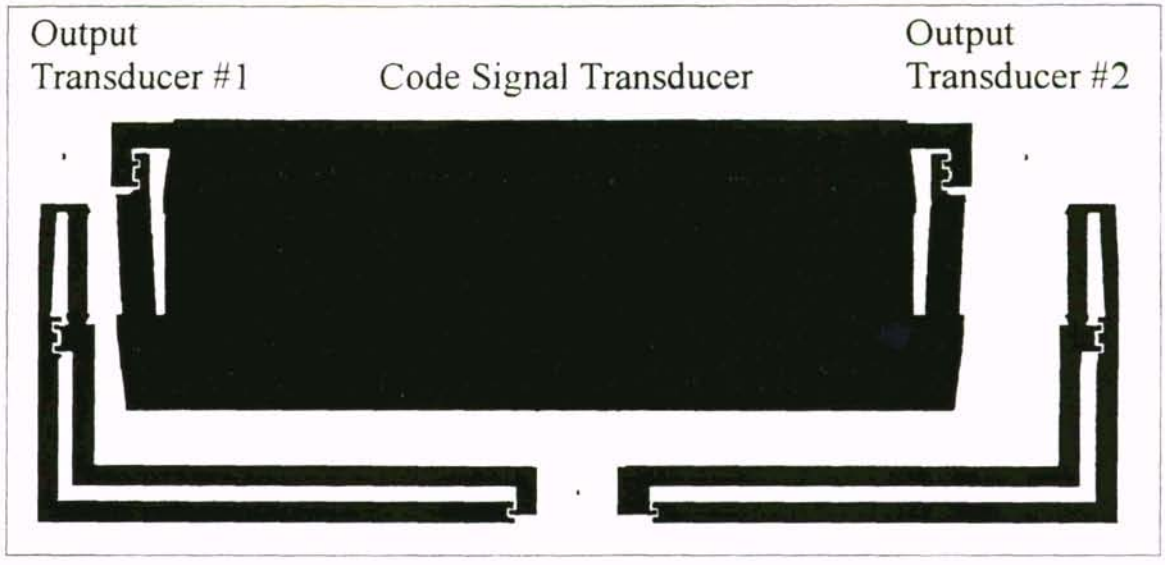

Figure 28. Layout for the 9 chip weighted stepped chirp code signal experimental SAW devices.

7.11 Intersymbol Interference

ISI occurs in a SAW device due to the convolution of the output transducer with the code signal transducer as seen in Figure 29. If the chips are placed adjacent to one another, they smear into each other as they convolve with the output transducer. The amount of overlap between adjacent chips is equal to the length of the output transducer Lo. This results in interference of a chip by its adjacent chips. The impact of ISI decreases as the chip length Lc increases versus Lo. ISI may be eliminated by spacing the chips in the code signal transducer by a distance Ls which is equal to Lo as in Figure 30.

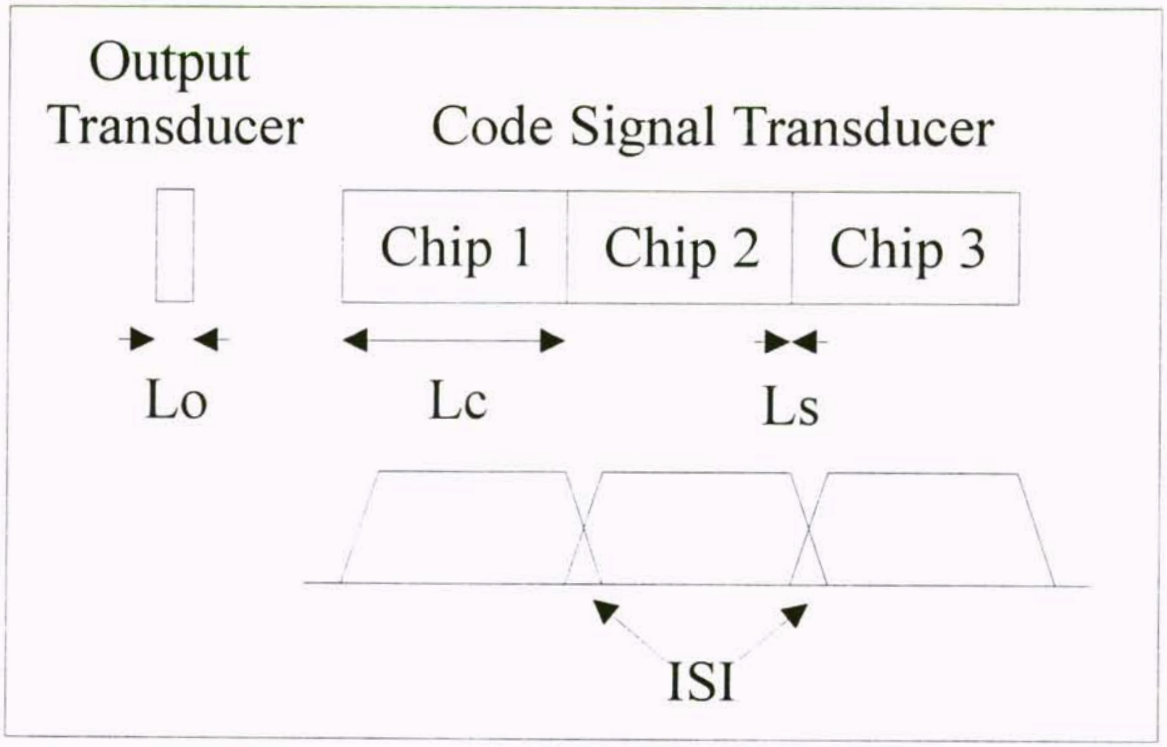

Figure 29. ISI due to an output transducer of length Lo convolving with the chips of the code signal transducer where the chips are Lc in length and the separation between chips Ls = 0.

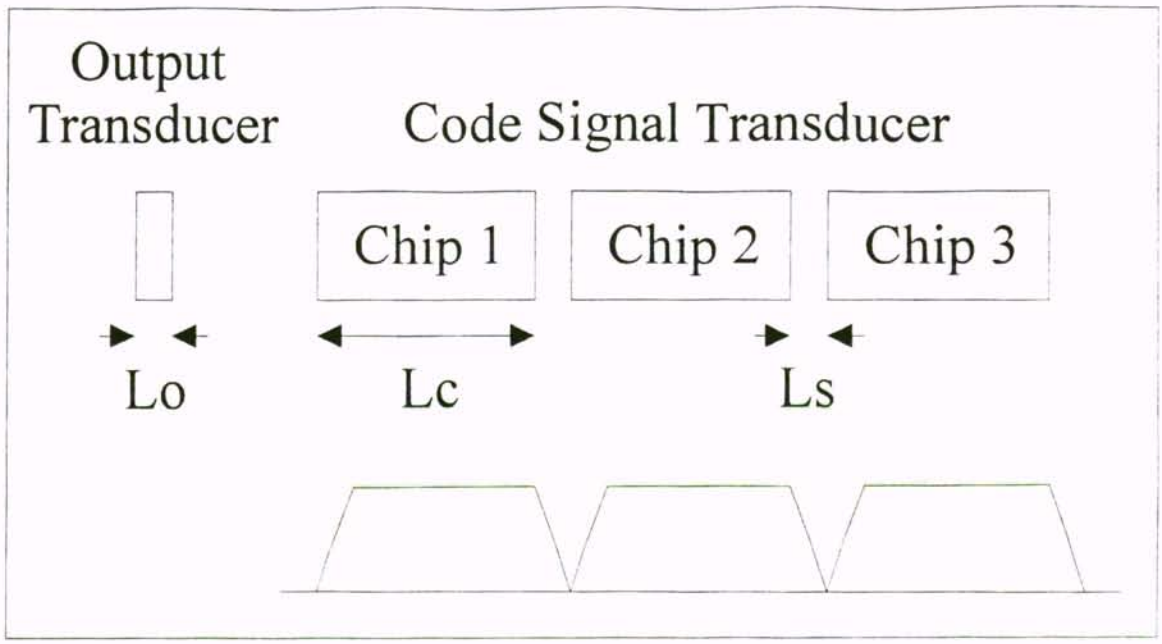

Figure 30. Elimination of ISI when an output transducer of length Lo convolves with the chips of the code signal transducer where the chips are Lc in length and the separation between chips Ls = Lo.

For the experimental weighted stepped chirp code signal SAW devices, the chips were not spaced apart. This was done for several reasons. First, the size of the device needed to be kept to a minimum due to the constraint of fitting them all onto one 3 inch wafer and also due to the increased probability of waveguiding problems as the device gets longer. Secondly, the chip length was $43.5\lambda_o$ which is almost 6 times the output transducer length of $7.5\lambda_o$ which reduces the effects of ISI. Thirdly, since the code signal definition included continuity and spacing requirements it was considered best not to space the chips. Finally, since the chips possess orthogonal frequencies the effects of ISI should be minimal.

7.12 Output Transducer Compensation

In a SAW device, the frequency response of the device is equal to the multiplication of the frequency responses of the two transducers. For DS/SS code signal generators and correlators, the SAW devices consist of a code signal transducer and an output transducer. With PN codes, the chips of the code signal are all at the same frequency so the effects of the output transducer's frequency response are minimal assuming that the output transducer has a broad enough 3 dB bandwidth to pass the main lobe and first few sidelobes of the code signal transducer's frequency response. This is generally accomplished using a uniform transducer $3\lambda_o$ to $5\lambda_o$ long.

For the weighted stepped chirp code signal, each chip is at a different frequency which means that the chips must be weighted in order to compensate for the output transducer's frequency response. Since weighting the chips to compensate for a uniform transducer's sin(x)/x response will result in a significant loss of power in the code signal, a uniform transducer with a λ_o of reversed phase electrodes at each end is used. This results in the broader and flatter frequency response shown in Figure 31 for a $7.5\lambda_o$ output transducer including array factor as modeled by SAWCAD-PC, a SAW design and analysis program developed at the University of Central Florida.

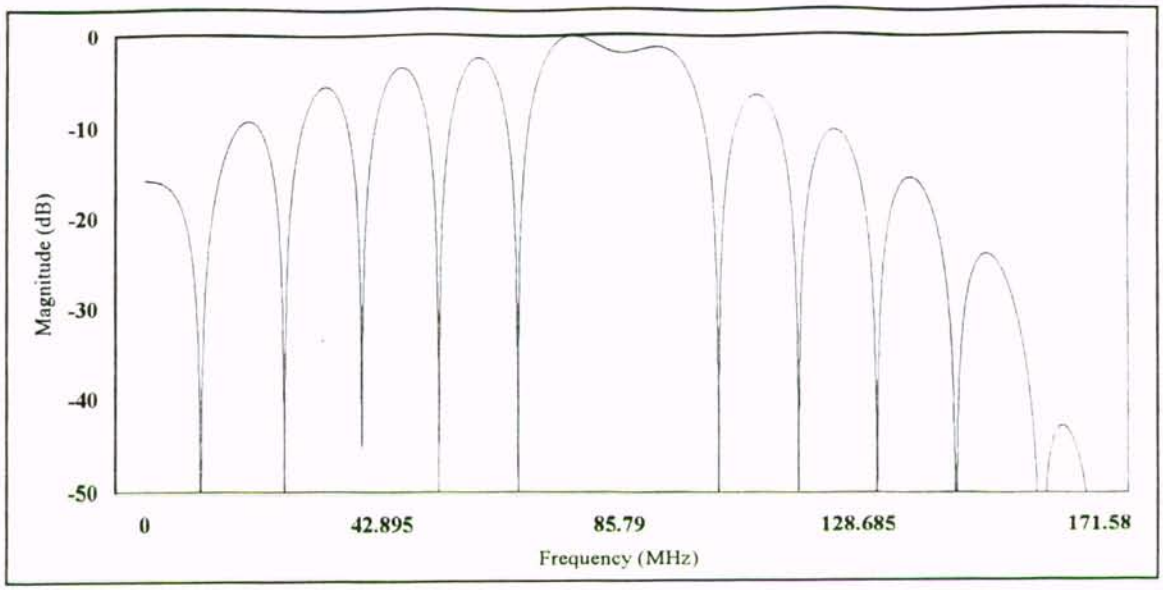

Figure 31. Frequency response of the output transducer with split electrodes with a polarity pair sequence of (++----++--++--++--++---++----++).

Table 5 shows the center frequencies for each chip in the experimental SAW device weighted stepped chirp code signal for the $4f_o$ sampled case and the weights necessary to compensate for the output transducer's frequency response from Figure 31.

Chip n	Frequency (MHz)	9 Chip Weights	13 Chip Weights
-6	73.96	NA	0.804
-5	75.93	NA	0.719
-4	77.90	0.805	0.704
-3	79.87	0.839	0.734
-2	81.84	0.898	0.786
-1	83.82	0.961	0.841
0	85.79	1	0.88
1	87.76	0.998	0.873
2	89.73	0.966	0.845
3	91.70	0.933	0.816
4	93.67	0.929	0.813
5	95.65	NA	0.863
6	97.62	NA	1

Table 5. Weights to compensate for the output transducer for the 9 and 13 chip $4f_o$ sampled weighted stepped chirp code signal transducers.

The frequencies of the chips for the $4f_n$ sampled experimental SAW devices are different from those in Table 5 because of limitations in the accuracy of the line widths of the mask that would be needed to fabricate the devices. The maximum accuracy of the mask lines was 0.1 um. By taking the frequencies from Table 5 and using

$$\lambda_n = \frac{v_{SAW}}{f_n} \tag{38}$$

the wavelength for each chip can be found. From this the corresponding electrode width for each chip is found by dividing the wavelength by 8. These results were rounded to the nearest 0.1 um and then converted back to frequency by rearranging Equation 38 as

$$f_n = \frac{v_{SAW}}{\lambda_n} \tag{39}$$

The $4f_n$ chip frequencies and their corresponding electrode widths can be found in Table 6.

Chip n	Frequency (MHz)	Electrode Width (um)
-6	74.46	5.3
-5	75.89	5.2
-4	77.38	5.1
-3	80.54	4.9
-2	82.21	4.8
-1	83.96	4.7
0	85.79	4.6
1	87.69	4.5
2	89.69	4.4
3	91.77	4.3
4	93.96	4.2
5	96.25	4.1
6	98.66	4.0

Table 6. Center frequencies and electrode widths for the $4f_n$ sampled weighted stepped chirp code signal transducers.

From these $4f_n$ chip frequencies, the weights necessary to compensate for the output transducer's frequency response from Figure 31 can be determined and found in Table 7.

Chip n	Frequency (MHz)	9 Chip Weights	13 Chip Weights
-6	74.46	NA	0.670
-5	75.89	NA	0.630
-4	77.38	0.803	0.611
-3	80.54	0.854	0.650
-2	82.21	0.909	0.692
-1	83.96	0.966	0.735
0	85.79	1	0.76
1	87.69	0.997	0.759
2	89.69	0.965	0.734
3	91.77	0.932	0.709
4	93.96	0.933	0.710
5	96.25	NA	0.780
6	98.66	NA	1

Table 7. Weights to compensate for the output transducer for the 9 and 13 chip $4f_n$ sampled weighted stepped chirp code signal transducers.

Using the cosine-squared and Hamming weights from Tables 1 and 2 in Chapter 4 and the weights necessary to compensate for the output transducer from Tables 5 and 7, the weights for the 9 chip cosine-squared and the 13 chip Hamming weighted stepped chirp code signals can be found in Table 8.

Chip n	9 Chip $4f_o$ Weights	9 Chip $4f_n$ Weights	13 Chip $4f_o$ Weights	13 Chip $4f_n$ Weights
-6	NA	NA	0.085	0.082
-5	NA	NA	0.161	0.161
-4	0.024	0.024	0.303	0.303
-3	0.210	0.214	0.499	0.508
-2	0.527	0.534	0.720	0.728
-1	0.849	0.853	0.910	0.915
0	1	1	1	1
1	0.881	0.881	0.945	0.945
2	0.567	0.566	0.774	0.773
3	0.233	0.233	0.555	0.554
4	0.028	0.028	0.350	0.352
5	NA	NA	0.193	0.197
6	NA	NA	0.106	0.122

Table 8. Weights to compensate for the output transducer and to realize the desired weighting function for the 9 chip cosine-squared and 13 chip Hamming weighted stepped chirp code signal transducers.

7.13 Waveguiding

Waveguiding can be a problem in the implementation of the weighted stepped chirp code signal in SAW devices because of their long length. The velocity in the code signal transducer is reduced from the free surface velocity due to the mass loading of the metal of the electrodes and the piezoelectric effect which is important for high coupling substrates such as lithium niobate and lithium tantalate. These effects result in waveguiding for sufficiently long transducers. This results in a separation of the modes due to the velocity difference. Assuming that the output transducers in Figure 28 are uniform and that the code signal transducer is shorted, the impulse response of the SAW device looking between the output transducers would look like that in Figure 32 if the code signal transducer were acting as a waveguide. It shows two triangular pulses instead

of the expected one due to two different modes traveling at different velocities through the code signal transducer.

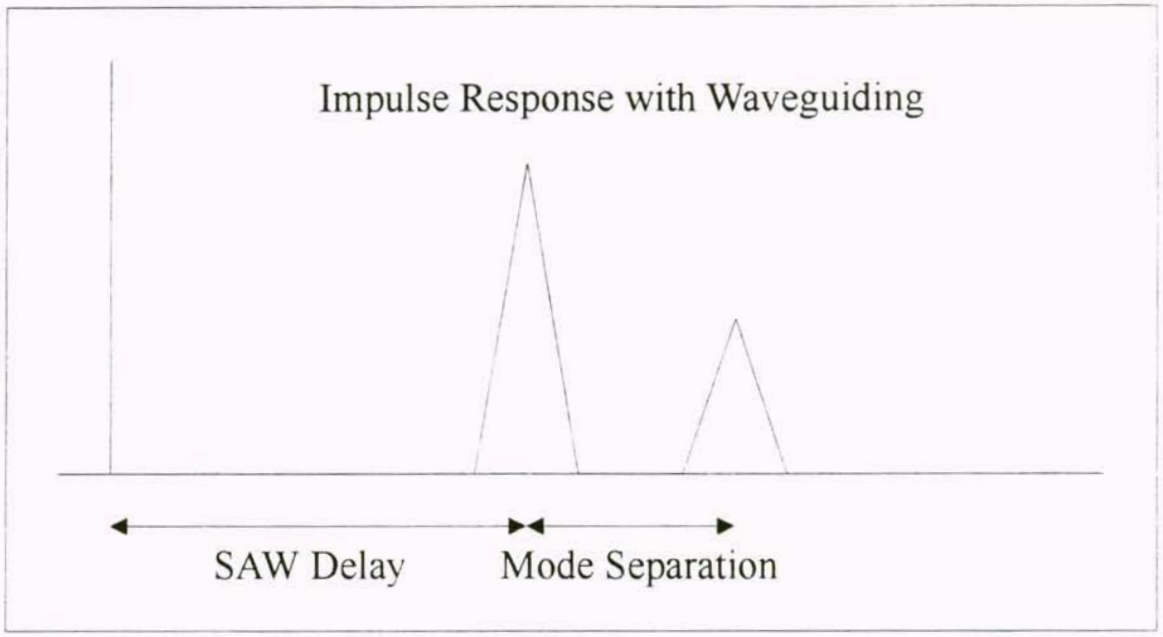

Figure 32. Possible effects of waveguiding in a SAW device impulse response with two uniform transducers separated by a long code signal transducer. The two pulses represent 2 modes of the waveguide traveling at different velocities.

Two things were done to avoid the effects of waveguiding. As discussed in the section on ISI the length of the code signal transducer was kept to a minimum by not separating the chips in the code. Also, the experimental SAW devices were fabricated on 40° rotated quartz which is a low coupling device which reduces the effects of waveguiding.

7.14 RF Feed-through

RF feed-through occurs when the RF energy input to the device couples directly to the output of the device without traveling through the crystal. This can occur due to the capacitive coupling between the transducers due to the proximity of the transducers to each other or due to energy radiated from the bond wires.

Several things can be done to reduce RF feed-through in SAW devices. Figure 33 shows the packaging and wire bonding diagram for the 9 chip weighted stepped chirp code signal experimental SAW devices. The 13 chip devices were packaged and wire bonded similarly. The transducers should be placed a minimum of 1 mm apart to keep the capacitive coupling low. The output transducers of the experimental SAW devices were placed 1 mm and 1.93 mm from the code signal transducer. The hot and ground bus bar orientation of the output transducers is opposite that of the code signal transducer. This increases the distance between the input and output of the device which reduces capacitive coupling. It also enables the bond wires to be run to opposite sides of the package since only the ground bond wire should pass over the device. The output transducers were bonded to pins that were as far from the code signals' pins as possible to isolate the connections. The ground bond wires of the output transducers were placed closest to the code signal transducer in order to keep the hot bond wires as far away as possible for maximum isolation. The ground bond wire of the code signal transducer was placed to the side of the closest output transducer to maximize the isolation of the code signal transducer's hot bond wire. The bond wires themselves were kept as short as possible and as low to the device as possible to reduce the possibility of radiating energy to the other

transducers. Ground shields were placed between the code signal transducer and the output transducers to increase RF isolation between the transducers.

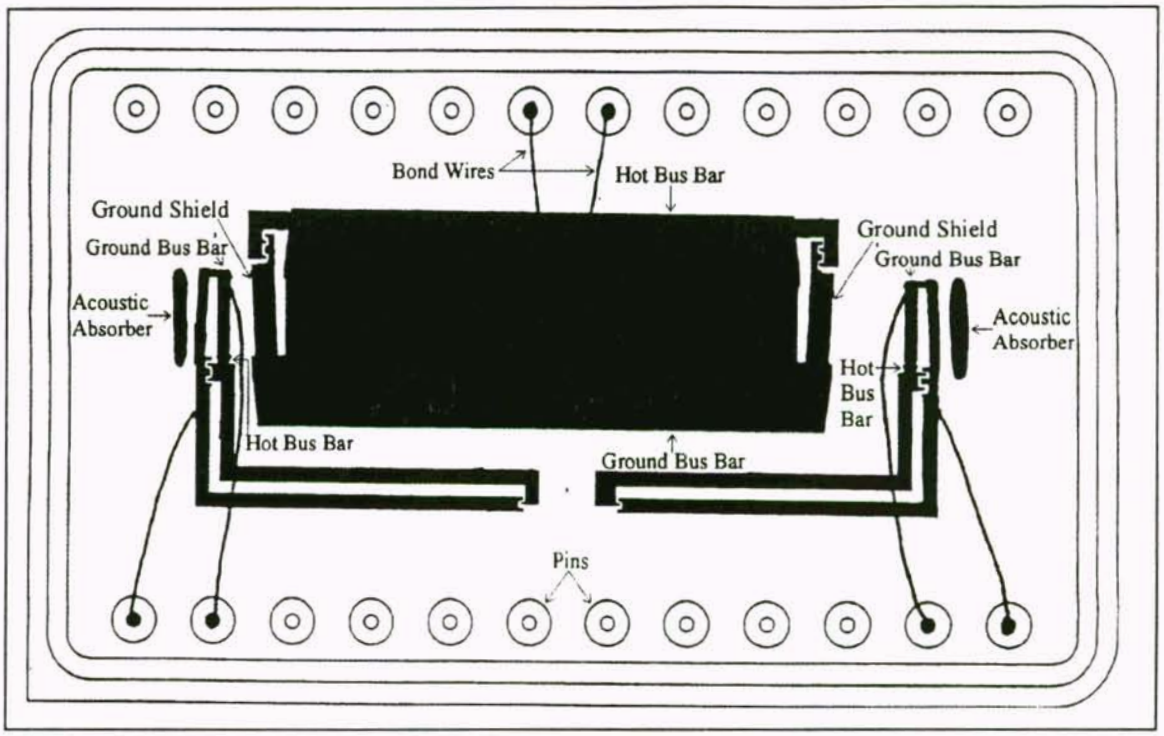

Figure 33. Packaging and wire bonding diagram for the 9 chip weighted stepped chirp code signal experimental SAW devices.

7.2 SAW Device Layout, Fabrication, and Packaging

The mask layout for the experimental SAW devices was drawn on SAWDRAW, a drawing program written at the University of Central Florida specifically for mask generation. A 4 inch by 4 inch, 1x mask was manufactured from the SAWDRAW data by Harris Corp. in Palm Bay, FL.

This mask was used in a one step photolithography process to expose a 3 inch 40° rotated quartz wafer coated with negative photo resist. The wafer was then developed to remove the resist from the areas covered by the dark field of the mask. Next, the wafer was placed in a vacuum chamber and a 2000 A° aluminum film was evaporated onto it. A lift-off process was then performed to remove the aluminum from the areas where the resist was still present (the clear field areas of the mask). The lift-off process eliminates the effects of undercutting which occurs when metal is etched. Figure 34 shows the difference in results between the lift-off and etching processes. The line width of the metal after lift-off is unchanged while the line width after etching is reduced by approximately twice the height of the metal resulting in errors between the mask and the actual devices.

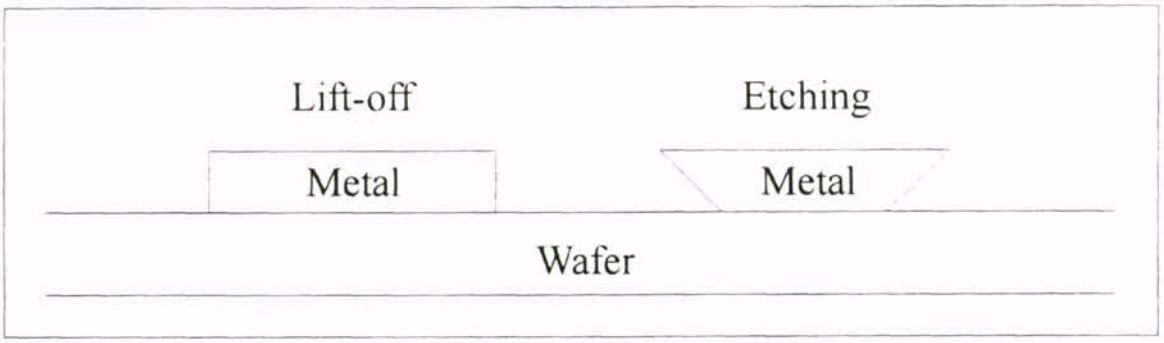

Figure 34. Difference in line widths between removing metal with a lift-off process and an etching process.

The finished wafers were diced with a diamond wafer saw at Sawtek Inc. of Apopka, FL. They were then packaged and wire bonded at Sawtek, into 2 mm x 3.5 mm 24 pin DIP packages. Acoustic absorber was placed at the ends of the devices to eliminate reflections of acoustic energy from the edges of the die as seen in Figure 33.

CHAPTER 8

EXPERIMENTAL SAW DEVICE CORRELATION RESULTS

The experimental SAW devices were to have been tested in a configuration as in Figure 35. An impulse generator was to be used to excite a SAW device acting as a code signal generator. The receiving SAW device would then correlate the transmitted code signal with its code signal. The correlation response would then be mixed and low pass filtered in order to obtain the base-band correlation function.

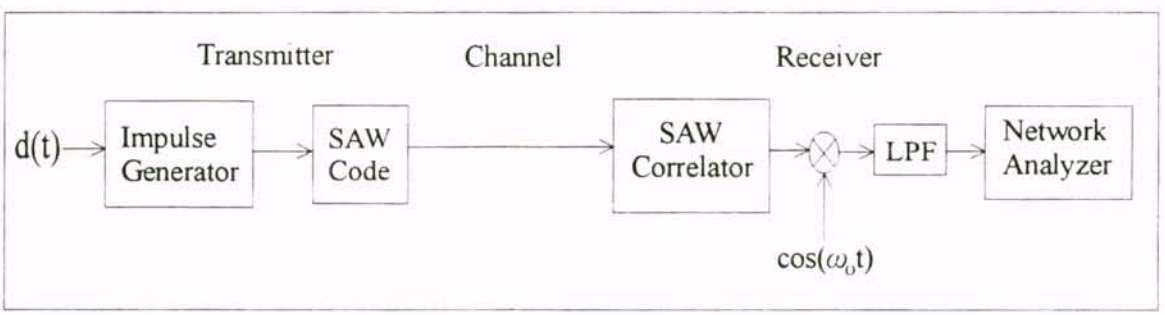

Figure 35. Test configuration for obtaining the correlation function from the experimental SAW devices.

This testing configuration had to be abandoned upon initial evaluation of the experimental SAW devices. Figure 36 shows the impulse response for a 13 chip uniformly weighted stepped chirp code signal experimental SAW device. The response at t = 0 usec is RF feed-through. It can be seen that the RF feed-through is about 25 dB

above the code signal response located from about t = 0.5 usec to t = 7 usec. Figure 37 shows the impulse response for a 13 chip Hamming weighted stepped chirp code signal experimental SAW device. Again the RF feed-through at t = 0 usec is about 25 dB above the code signal response located from about t = 1 usec to t = 8 usec. When these SAW devices are correlated in Figure 38, the combined RF feed-throughs correlate about t = 0 usec, the individual RF feed-throughs correlate with the opposite SAW device's code signal from about t = 0.5 usec to t = 7.5 usec, and the two code signals correlate from about t = 1.5 usec to t = 14.5 usec with a correlation peak at about t = 8 usec. The RF feed-through to RF feed-through correlation and the RF feed-through to code signal correlations have rendered the compressed correlation pulse useless.

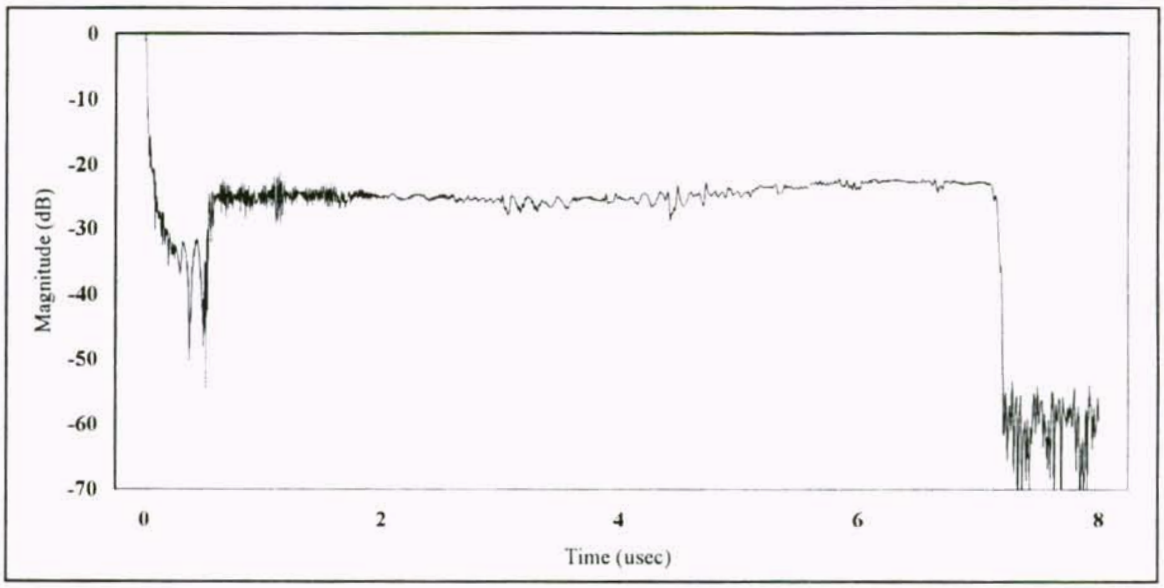

Figure 36. Normalized impulse response of a 13 chip uniformly weighted stepped chirp code signal experimental SAW device where f_o = 85.79 MHz and T_c = 0.507 usec.

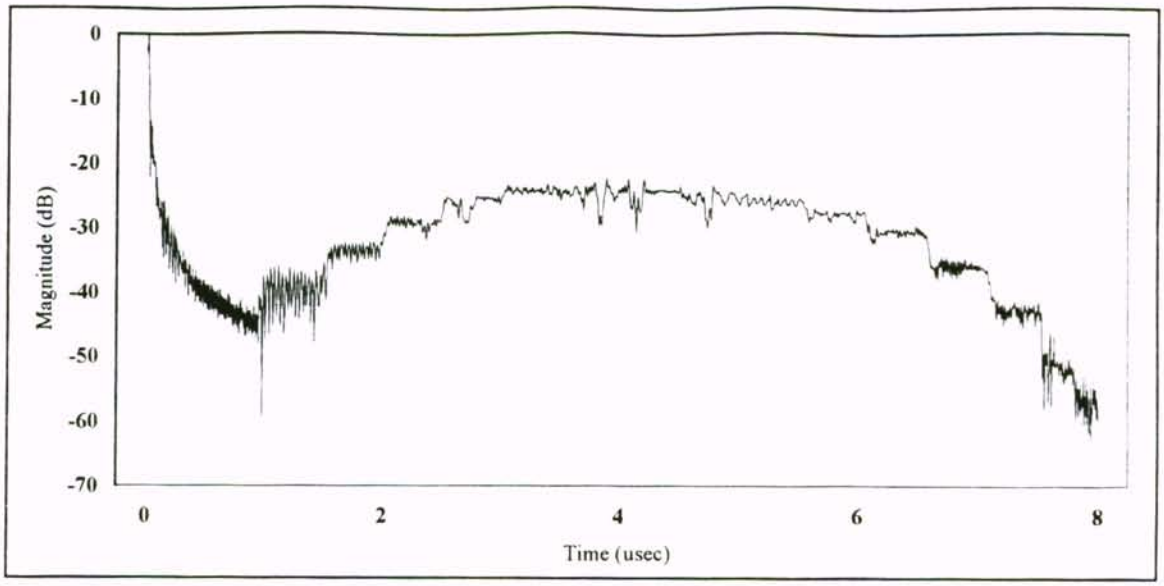

Figure 37. Normalized impulse response of a 13 chip Hamming weighted stepped chirp code signal experimental SAW device where f_o = 85.79 MHz and T_c = 0.507 usec.

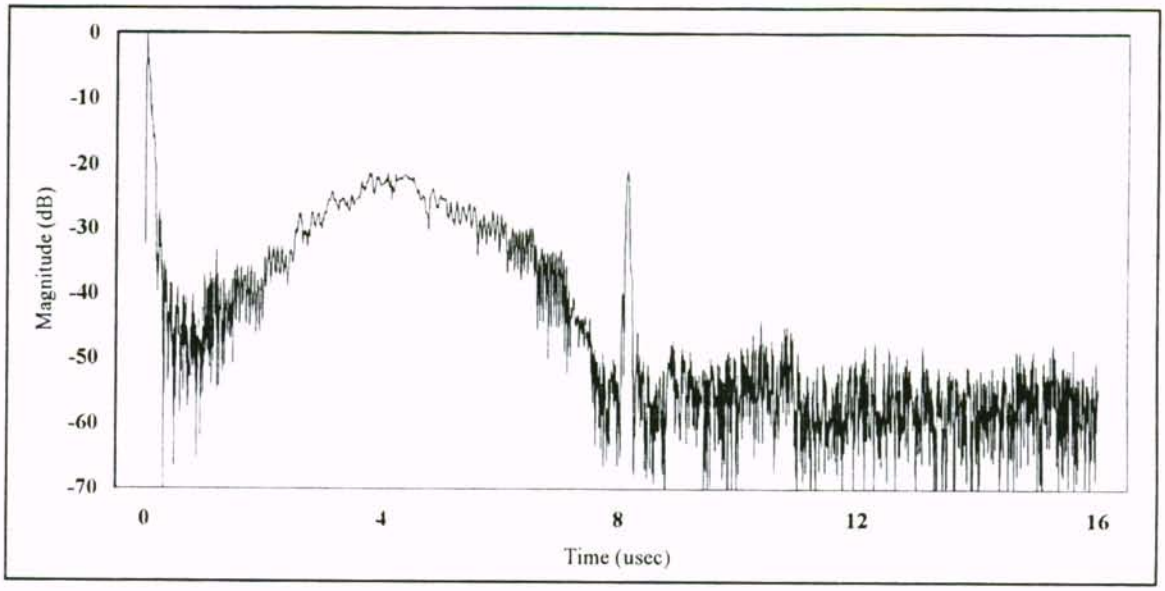

Figure 38. Normalized correlation function for a 13 chip uniformly weighted stepped chirp code signal experimental SAW device and a 13 chip Hamming weighted stepped chirp code signal experimental SAW device where f_o = 85.79 MHz and T_c = 0.507 usec.

The degradation of the correlation function due to RF feed-through is the product of a relatively high RF feed-through due to the close proximity and large size of the SAW transducers and the high insertion loss in the -60 to -70 dB range due to the spreading of the input power over a large bandwidth. In a second design pass, the RF feed-through may be reduced by altering the transducer geometry. The high insertion loss may be reduced by using a higher coupling material such as lithium niobate or lithium tantalate, however, the risk of waveguiding will increase.

8.1 Sampling at $4f_o$

The PSD functions and correlation functions for the weighted stepped chirp code signal experimental SAW devices sampled at $4f_o$ are presented and compared to the theoretical results.

8.11 The 9 Chip Weighted Stepped Chirp Code Signal

The 9 chip uniformly weighted stepped chirp code signal and the 9 chip cosine-squared weighted stepped chirp code signal experimental SAW device PSD and correlation functions are compared to the theoretical results when sampling at $4f_o$.

8.111 Uniformly Weighted

Figure 39 compares the experimental SAW device (solid line) and theoretical (dashed line) PSD functions for the $4f_o$ sampled 9 chip uniformly weighted stepped chirp code signal. The experimental PSD function can be seen to have a slight bow in its

response. The source of these weighting errors and compensation for them will be discussed in the Section 8.2. The experimental PSD function also has different sidelobe shaping due to the frequency response of the second transducer found in Figure 31 of Chapter 7. These differences from the theoretical PSD function will be seen to slightly degrade the correlation performance of the experimental SAW devices.

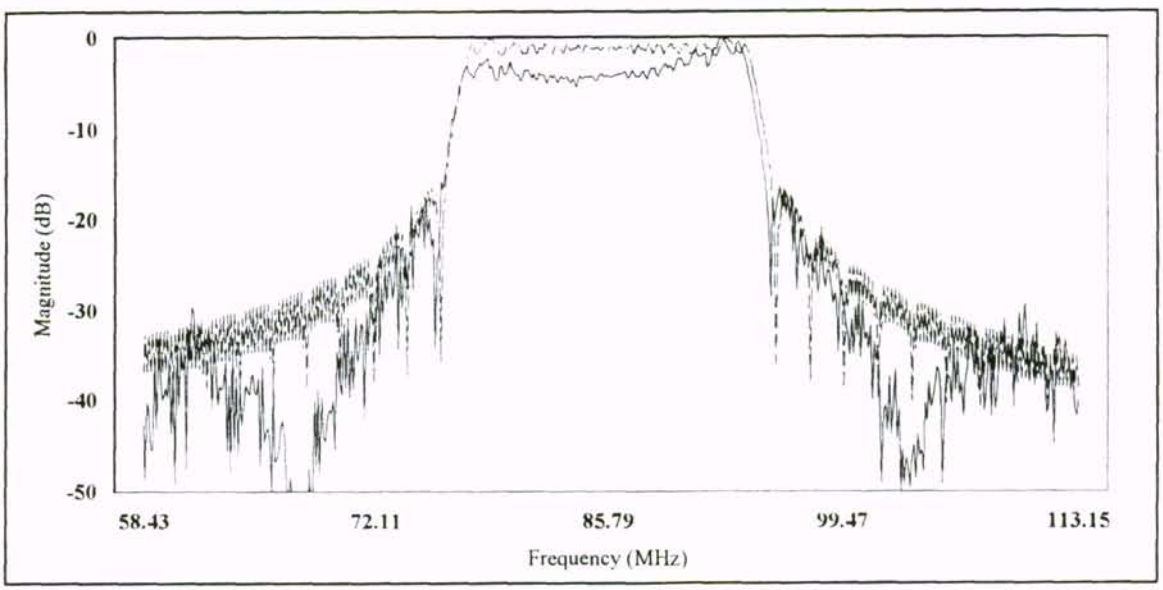

Figure 39. Normalized experimental SAW device (solid line) and theoretical (dashed line) PSD functions for a $4f_o$ sampled 9 chip uniformly weighted stepped chirp code signal where $f_o = 85.79$ MHz and $T_c = 0.507$ usec.

Figures 40 and 41 show the experimental SAW device (solid line) and theoretical (dashed line) correlation functions for the $4f_o$ sampled 9 chip uniformly weighted stepped chirp code signal. The experimental correlation function has a CR = 87, a PSL in the peak correlation region of -9.5 dB, a PSL in the cross-correlation region of -26.3 dB, and an ISL = -28.5 dB. The theoretical correlation function has a CR = 81, a PSL in the peak

correlation region of -13.3 dB, a PSL in the cross-correlation region of -28.2 dB, and an ISL = -29.4 dB. The experimental results show good agreement with the theoretical results. The differences in the results can be attributed to the errors in the experimental PSD function due to imperfections in the weighting of the code signal transducers.

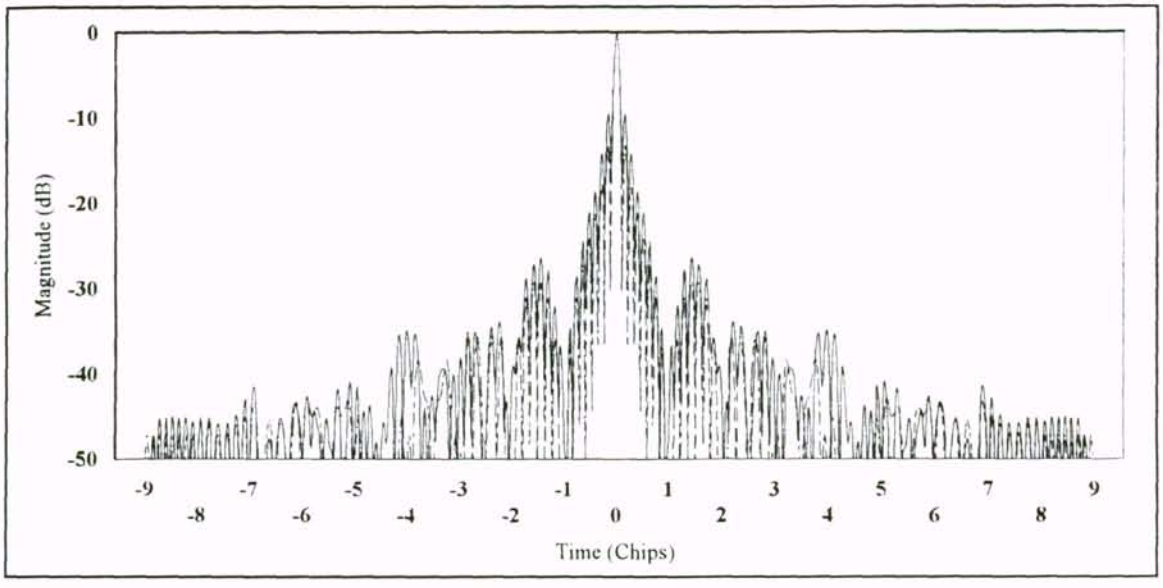

Figure 40. Normalized experimental SAW device (solid line) and theoretical (dashed line) correlation functions for a $4f_o$ sampled 9 chip uniformly weighted stepped chirp code signal where f_o = 85.79 MHz and T_c = 0.507 usec.

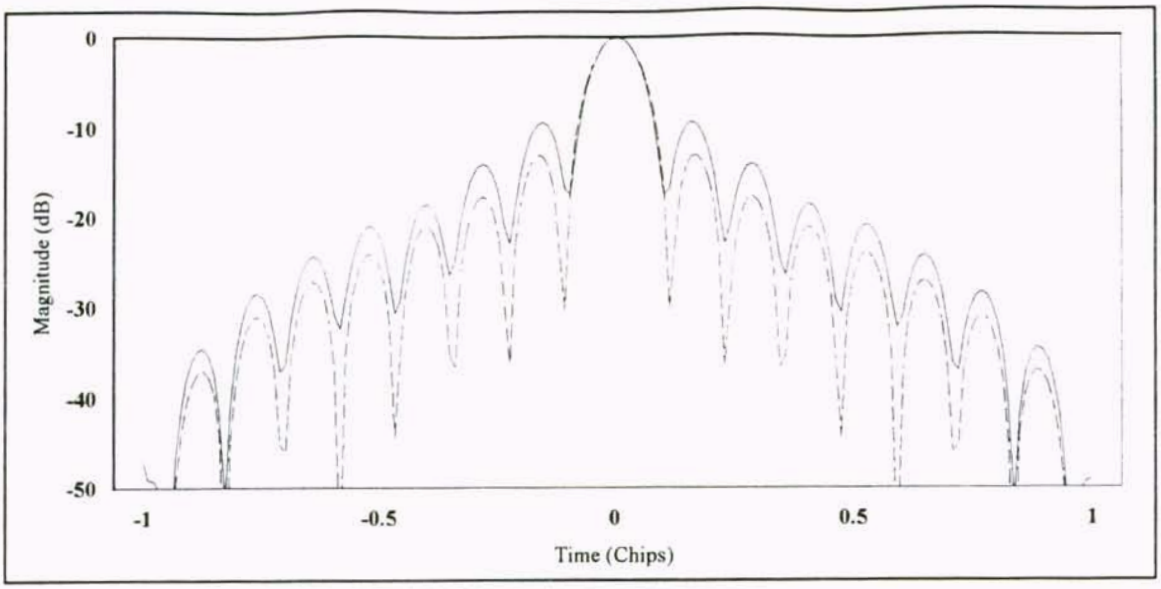

Figure 41. Normalized experimental SAW device (solid line) and theoretical (dashed line) peak correlation regions for a $4f_o$ sampled 9 chip uniformly weighted stepped chirp code signal where $f_o = 85.79$ MHz and $T_c = 0.507$ usec.

8.112 Cosine-squared Weighted

Figure 42 compares the experimental SAW device (solid line) and theoretical (dashed line) PSD functions for the $4f_o$ sampled 9 chip cosine-squared weighted stepped chirp code signal. Again, the experimental PSD function can be seen to have a lift in its response at the edges when compared to the theoretical PSD function. The sidelobes have been shaped by the output transducer's frequency response. The weighting errors in the PSD function will be seen to have a greater impact on the correlation performance of these experimental SAW devices than for the uniformly weighted experimental SAW devices in Section 8.111 because weighting errors at the edges where the chip weights are small result in a greater percent error.

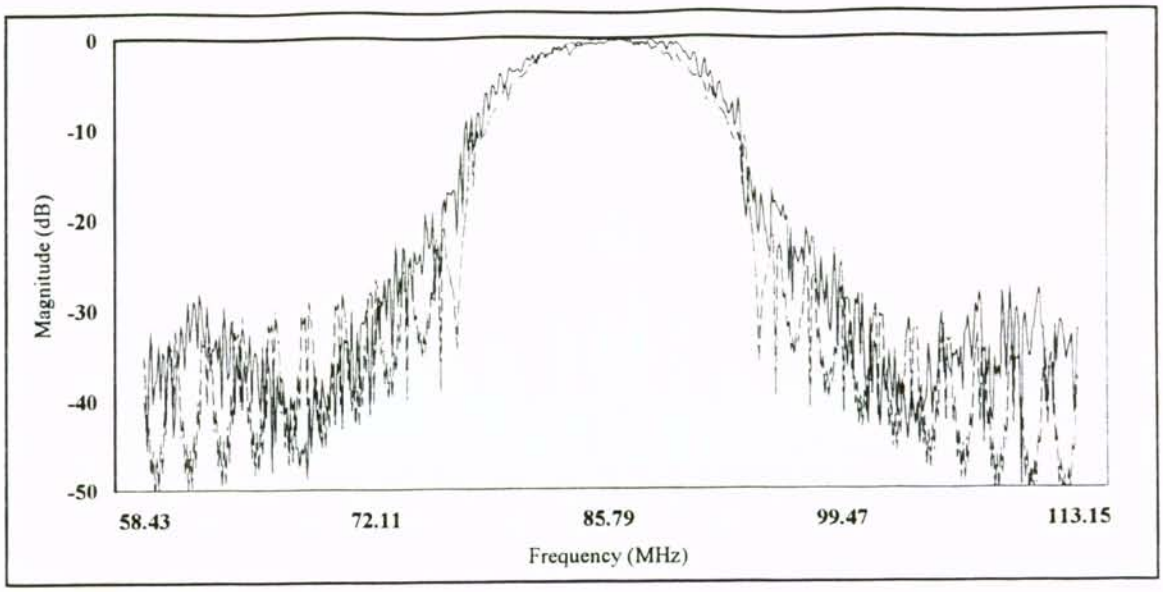

Figure 42. Normalized experimental SAW device (solid line) and theoretical (dashed line) PSD functions for a $4f_o$ sampled 9 chip cosine-squared weighted stepped chirp code signal where f_o = 85.79 MHz and T_c = 0.507 usec.

Figures 43 and 44 show the experimental SAW device (solid line) and theoretical (dashed line) correlation functions for the $4f_o$ sampled 9 chip cosine-squared weighted stepped chirp code signal. The experimental correlation function has a CR = 56, a PSL in the peak correlation region of -21.9 dB, a PSL in the cross-correlation region of -33.3 dB, and an ISL = -39.6 dB. The theoretical correlation function has a CR = 50, a PSL in the peak correlation region of -32.2 dB, a PSL in the cross-correlation region of -32.4 dB, and an ISL = -43.3 dB. The experimental correlation function shows good agreement to the theoretical correlaction function in CR but a much degraded sidelobe response due to the inaccuracies in the weighting of the code signal transducers. Due to the small weights on the chips at the ends of the code signal, the impact of the weighting errors are more pronounced than for the uniformly weighted stepped chirp code signal.

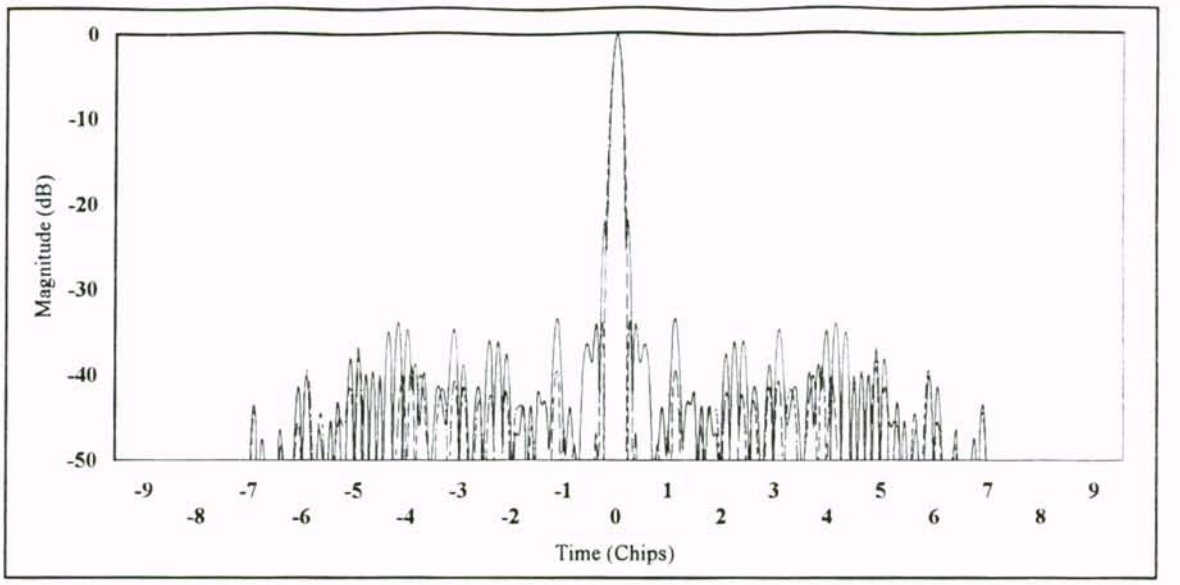

Figure 43. Normalized experimental SAW device (solid line) and theoretical (dashed line) correlation functions for a $4f_o$ sampled 9 chip cosine-squared weighted stepped chirp code signal where $f_o = 85.79$ MHz and $T_c = 0.507$ usec.

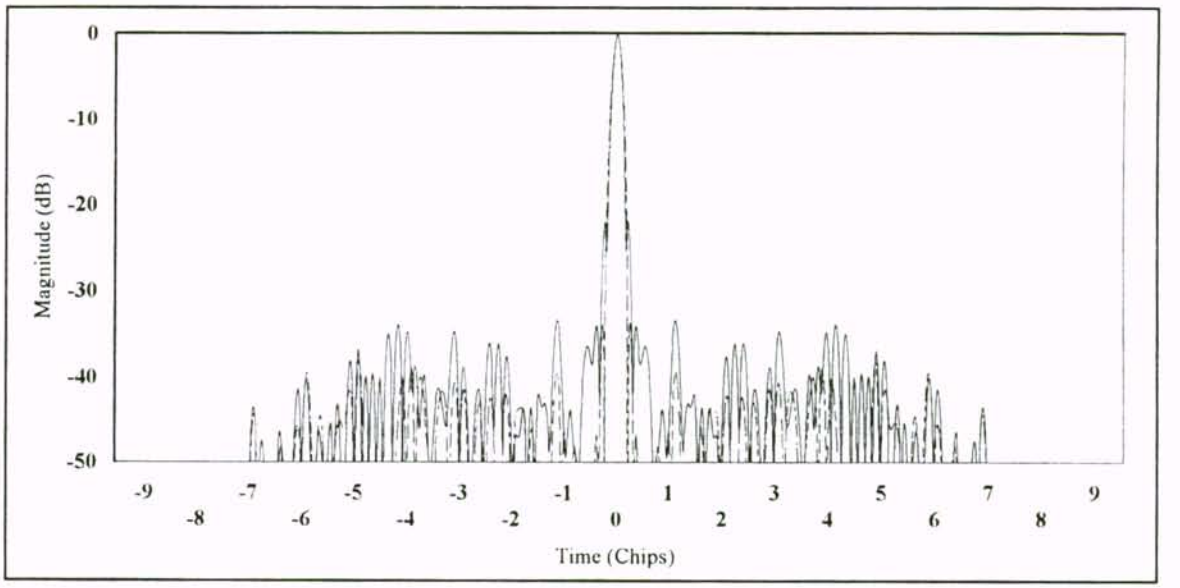

Figure 44. Normalized experimental SAW device (solid line) and theoretical (dashed line) peak correlation regions for a $4f_o$ sampled 9 chip cosine-squared weighted stepped chirp code signal where $f_o = 85.79$ MHz and $T_c = 0.507$ usec.

8.12 The 13 Chip Weighted Stepped Chirp Code Signal

The 13 chip uniformly weighted stepped chirp code signal and the 13 chip Hamming weighted stepped chirp code signal experimental SAW device PSD and correlation functions are compared to the theoretical results when sampling at $4f_o$.

8.121 Uniformly Weighted

Figure 45 compares the experimental SAW device (solid line) and theoretical (dashed line) PSD functions for the $4f_o$ sampled 13 chip uniformly weighted stepped chirp code signal. The experimental PSD function can be seen to have a more pronounced bow than for the 9 chip SAW device PSD function in Figure 39 due to the larger Δf. These weighting errors will slightly degrade the correlation performance of the experimental SAW devices.

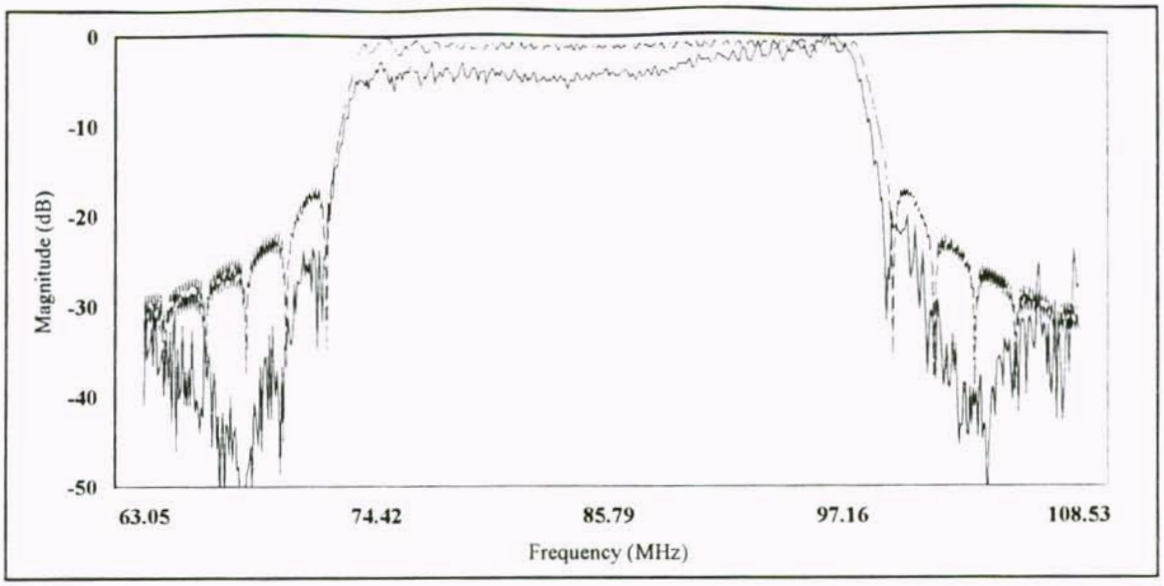

Figure 45. Normalized experimental SAW device (solid line) and theoretical (dashed line) PSD functions for a $4f_o$ sampled 13 chip uniformly weighted stepped chirp code signal where f_o = 85.79 MHz and T_c = 0.507 usec.

Figures 46 and 47 show the experimental SAW device (solid line) and theoretical (dashed line) correlation functions for the $4f_o$ sampled 13 chip uniformly weighted stepped chirp code signal. The experimental correlation function has a CR = 174, a PSL in the peak correlation region of -9.7 dB, a PSL in the cross-correlation region of -32.2 dB, and an ISL = -31.9 dB. The theoretical correlation function has a CR = 169, a PSL in the peak correlation region of -13.3 dB, a PSL in the cross-correlation region of -33.1 dB, and an ISL = -32.5 dB. The experimental results show good agreement with the theoretical results. Again the differences in the results can be attributed to the errors in the experimental PSD function due to imperfections in the weighting of the code signal transducers.

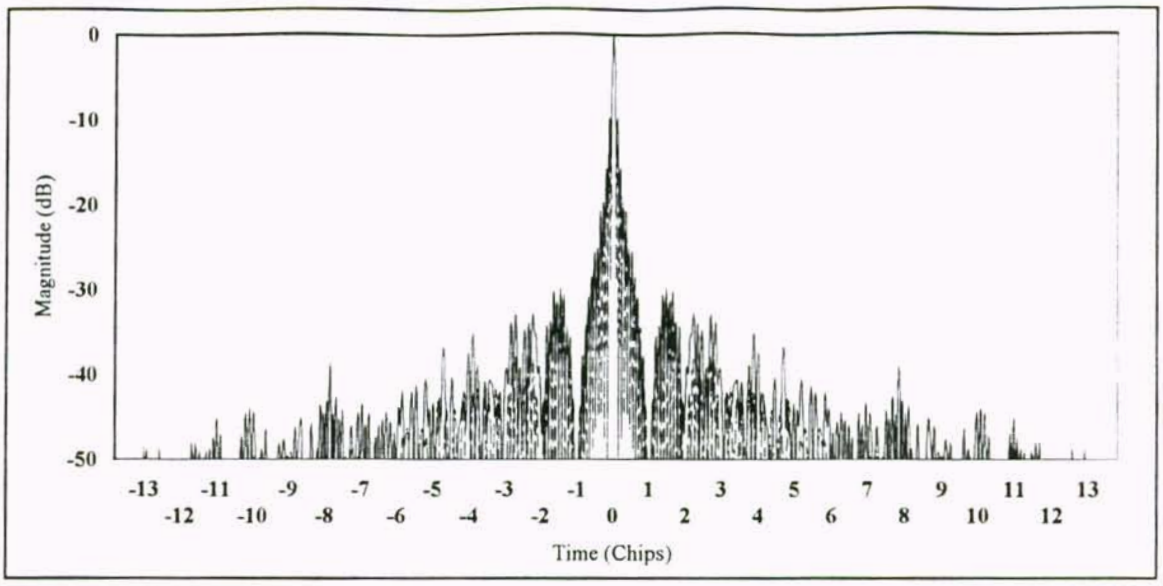

Figure 46. Normalized experimental SAW device (solid line) and theoretical (dashed line) correlation functions for a $4f_o$ sampled 13 chip uniformly weighted stepped chirp code signal where f_o = 85.79 MHz and T_c = 0.507 usec.

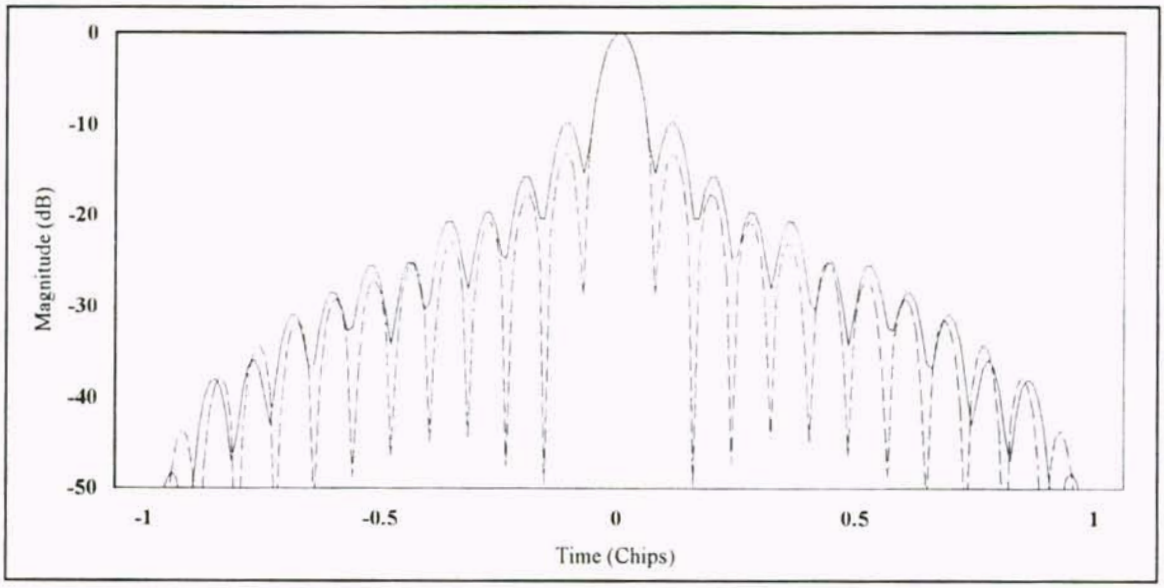

Figure 47. Normalized experimental SAW device (solid line) and theoretical (dashed line) peak correlation regions for a $4f_o$ sampled 13 chip uniformly weighted stepped chirp code signal where f_o = 85.79 MHz and T_c = 0.507 usec.

8.122 Hamming Weighted

Figure 48 compares the experimental SAW device (solid line) and theoretical (dashed line) PSD function for the $4f_o$ sampled 13 chip Hamming weighted stepped chirp code signal. Again the experimental PSD function can be seen to have a lift in its response at the edges when compared to the theoretical PSD function due to weighting errors. These errors will be seen to dramatically degrade the correlation performance of the experimental SAW devices.

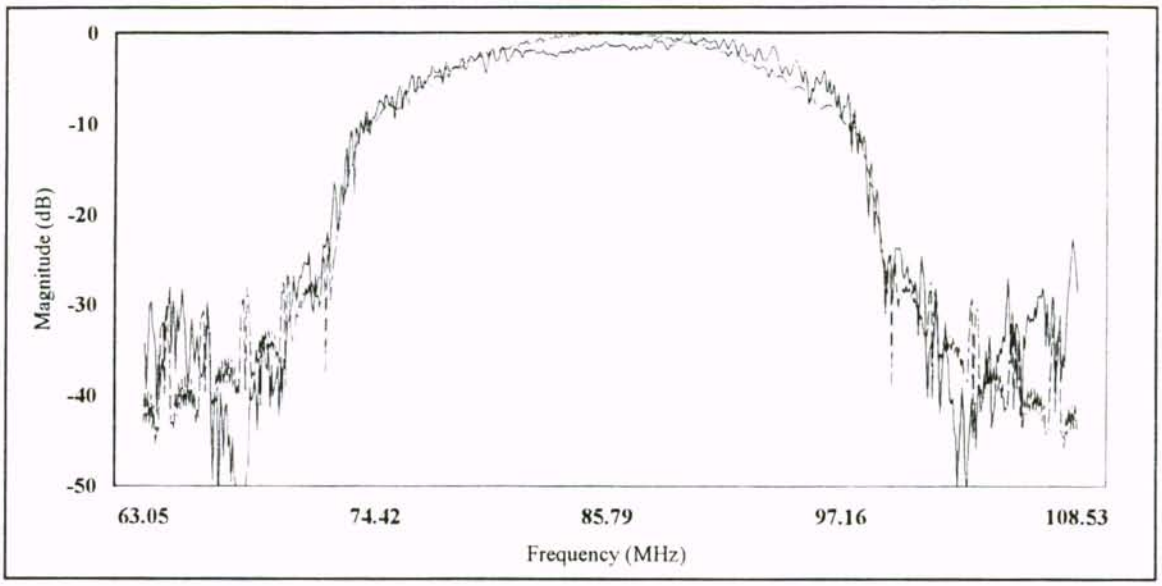

Figure 48. Normalized experimental SAW device (solid line) and theoretical (dashed line) PSD functions for a $4f_o$ sampled 13 chip Hamming weighted stepped chirp code signal where f_o = 85.79 MHz and T_c = 0.507 usec.

Figures 49 and 50 show the experimental SAW device (solid line) and theoretical (dashed line) correlation functions for the $4f_o$ sampled 13 chip Hamming weighted stepped chirp code signal. The experimental correlation function has a CR = 126, a PSL in the

peak correlation region of -18.4 dB, a PSL in the cross-correlation region of -33.2 dB, and an ISL = -39.9 dB. The theoretical correlation function has a CR = 115, a PSL in the peak correlation region of -42.8 dB, a PSL in the cross-correlation region of -39.4 dB, and an ISL = -49.7 dB. The experimental correlation function shows good agreement to the theoretical correlation function in CR but a much degraded sidelobe response due to the inaccuracies in the weighting of the code signal transducers. As discussed earlier, the small weights on the chips at the end of the code signal are greatly impacted by the weighting errors.

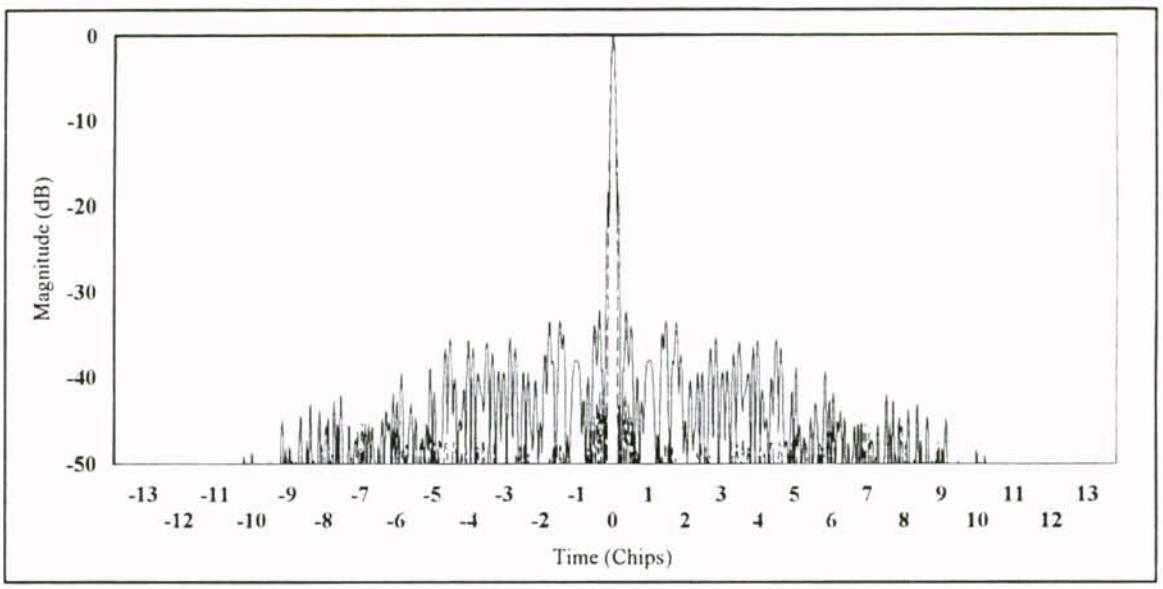

Figure 49. Normalized experimental SAW device (solid line) and theoretical (dashed line) correlation functions for a $4f_o$ sampled 13 chip Hamming weighted stepped chirp code signal where f_o = 85.79 MHz and T_c = 0.507 usec.

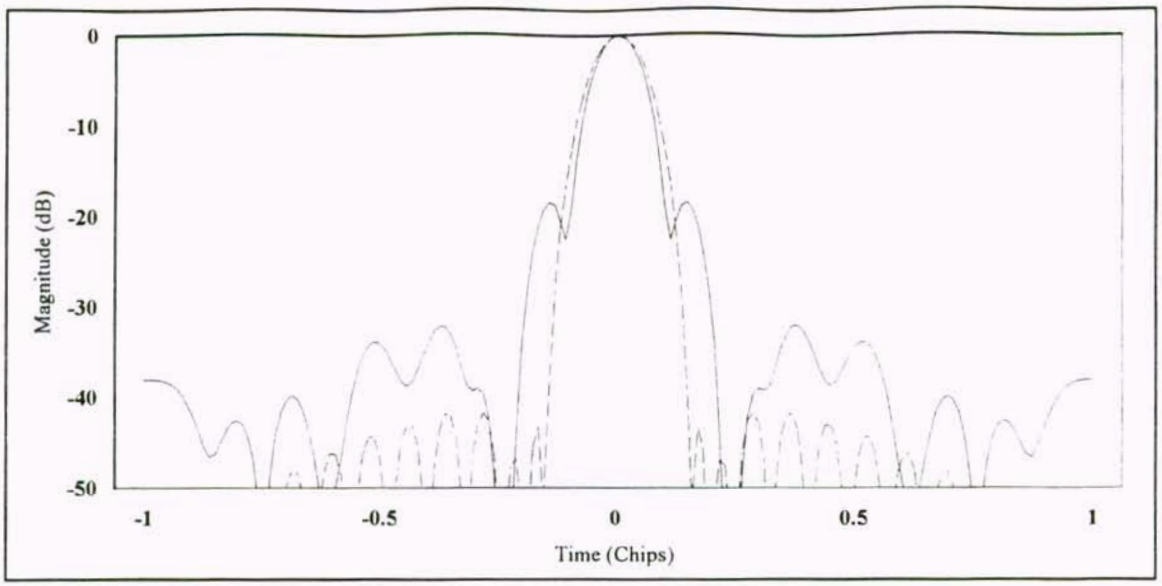

Figure 50. Normalized experimental SAW device (solid line) and theoretical (dashed line) peak correlation regions for a $4f_o$ sampled 13 chip Hamming weighted stepped chirp code signal where $f_o = 85.79$ MHz and $T_c = 0.507$ usec.

8.2 Compensating for the Weighting Errors

The weighting errors between the experimental SAW device and theoretical PSD functions in Section 8.1 were determined to be systemic. Figure 51 shows the error curve between the PSD functions of the experimental SAW devices and the theoretical results. The error curve was obtained by subtracting the theoretical PSD function from the experimental SAW device PSD function and using a polynomial regression to fit the error data to a 5th order polynomial. Comparing the error curve to Figure 31 in Chapter 7 it can be seen that the weighting in Table 5 of Chapter 7 over compensated for the second transducer's frequency response. This error curve was used to compensate the experimental SAW device PSD functions for the 13 chip uniformly and Hamming weighted stepped chirp code signal SAW devices from Section 8.1.

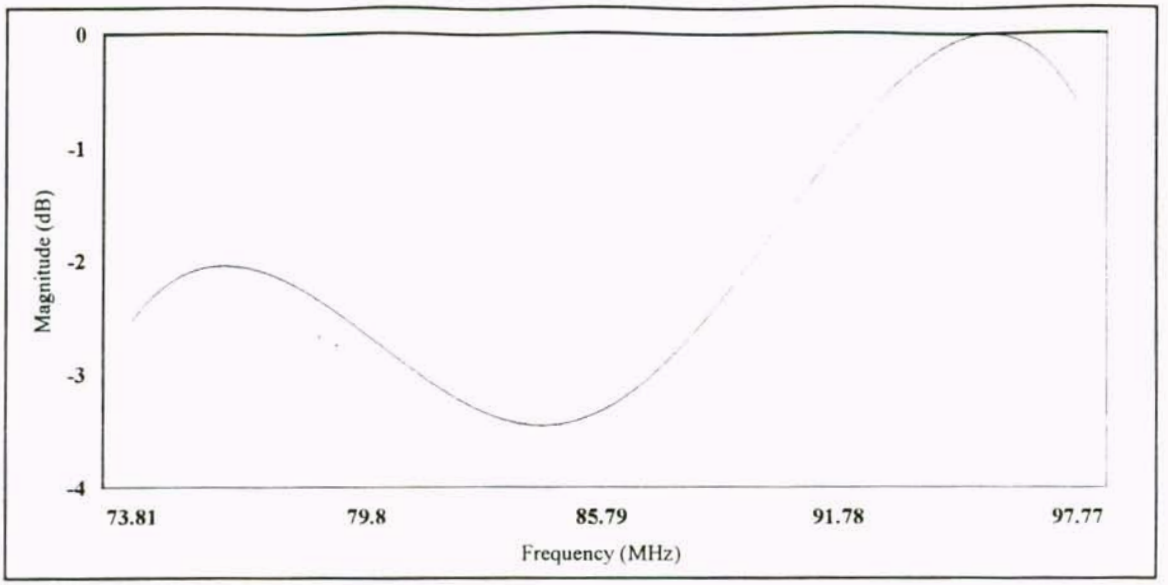

Figure 51. Normalized error between the experimental SAW device and theoretical weighted stepped chirp code signal PSD functions using a 5th order polynomial regression.

8.21 Uniformly Weighted

Figure 52 compares the compensated experimental SAW device (solid line) and theoretical (dashed line) PSD functions for the $4f_o$ sampled 13 chip uniformly weighted stepped chirp code signal. Compensating for the weighting error curve in Figure 51 has removed the bow in the PSD function of the uncompensated experimental SAW devices found in Figure 45. Figure 52 shows that the compensated experimental SAW device PSD function now closely matches the theoretical PSD function.

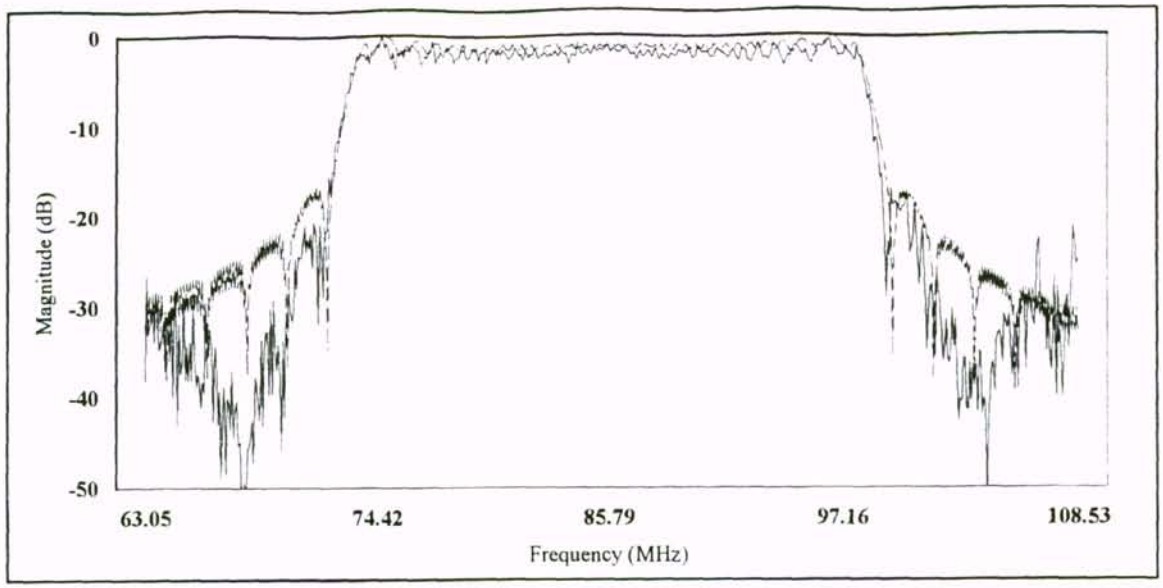

Figure 52. Normalized experimental SAW device compensated for the weighting errors (solid line) and theoretical (dashed line) PSD functions for a $4f_o$ sampled 13 chip uniformly weighted stepped chirp code signal where f_o = 85.79 MHz and T_c = 0.507 usec.

Figures 53 and 54 show the compensated experimental SAW device (solid line) and theoretical (dashed line) correlation functions for the $4f_o$ sampled 13 chip uniformly weighted stepped chirp code signal. The compensated experimental correlation function has a CR = 169, a PSL in the peak correlation region of -13.2 dB, a PSL in the cross-correlation region of -30.3 dB, and an ISL = -34.8 dB. The theoretical correlation function has a CR = 169, a PSL in the peak correlation region of -13.3 dB, a PSL in the cross-correlation region of -33.1 dB, and an ISL = -32.5 dB. The experimental results show good agreement with the theoretical results. The improvement due to compensating for the weighting errors can be seen by comparing Figure 53 and 54 to Figures 46 and 47.

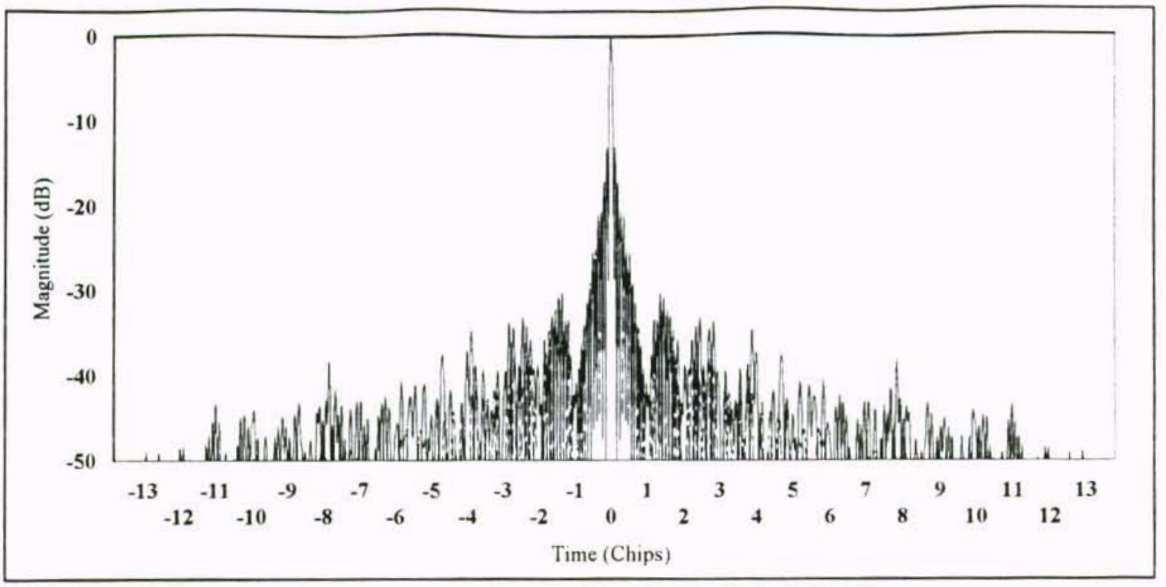

Figure 53. Normalized experimental SAW device compensated for the weighting errors (solid line) and theoretical (dashed line) correlation functions for a $4f_o$ sampled 13 chip uniformly weighted stepped chirp code signal where f_o = 85.79 MHz and T_c = 0.507 usec.

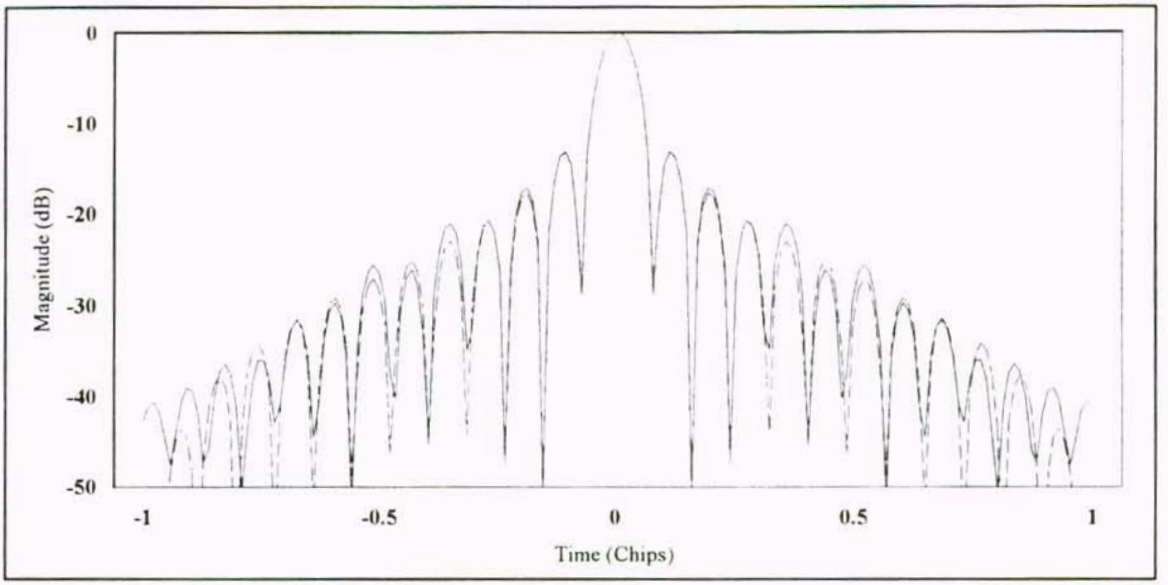

Figure 54. Normalized experimental SAW device compensated for the weighting errors (solid line) and theoretical (dashed line) peak correlation regions for a $4f_o$ sampled 13 chip uniformly weighted stepped chirp code signal where f_o = 85.79 MHz and T_c = 0.507 usec.

8.22 Hamming Weighted

Figure 55 compares the compensated experimental SAW device (solid line) and theoretical (dashed line) PSD functions for the $4f_o$ sampled 13 chip Hamming weighted stepped chirp code signal. Compensating for the weighting error curve in Figure 51 has removed the bow in the PSD function of the uncompensated experimental SAW devices found in Figure 48. Figure 55 shows that the compensated experimental SAW device PSD function now closely matches the theoretical PSD function.

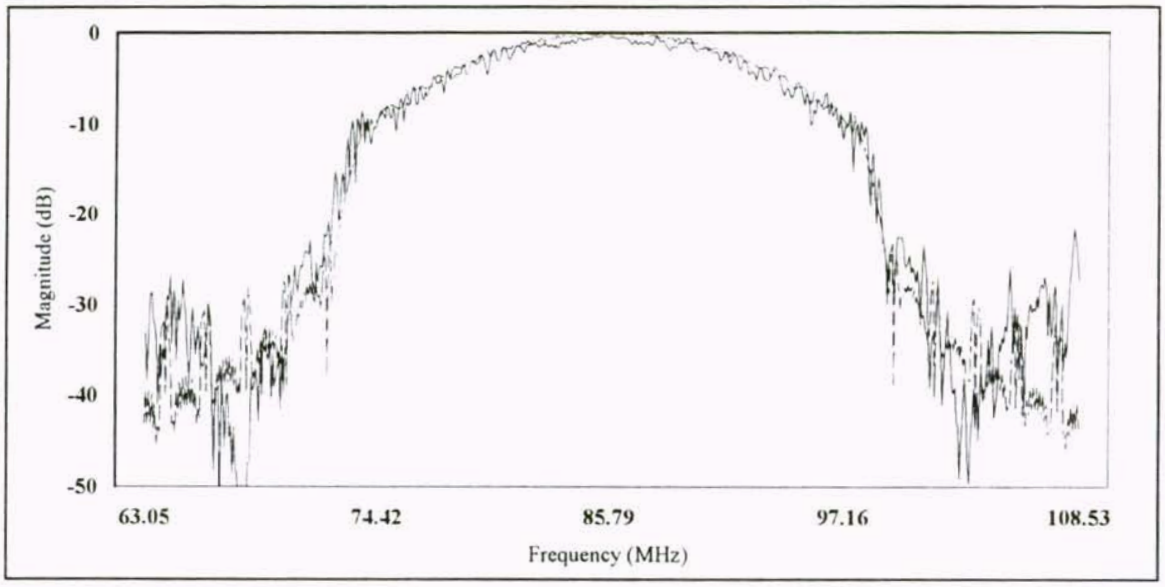

Figure 55. Normalized experimental SAW device compensated for the weighting errors (solid line) and theoretical (dashed line) PSD functions for a $4f_o$ sampled 13 chip Hamming weighted stepped chirp code signal where f_o = 85.79 MHz and T_c = 0.507 usec.

Figures 56 and 57 show the compensated experimental SAW device (solid line) and theoretical (dashed line) correlation functions for the $4f_o$ sampled 13 chip Hamming weighted stepped chirp code signal. The compensated experimental correlation function

has a CR = 115, a PSL in the peak correlation region of -36.9 dB, a PSL in the cross-correlation region of -40 dB, and an ISL = -49.1 dB. The theoretical correlation function has a CR = 115, a PSL in the peak correlation region of -42.8 dB, a PSL in the cross-correlation region of -39.4 dB, and an ISL = -49.7 dB. The experimental results show good agreement with the theoretical results. The improvement due to compensating for the weighting errors can be seen by comparing Figure 56 and 57 to Figures 49 and 50.

The excellent agreement between experimental and theoretical results when using the single error curve shows that the error is a design flaw and systemic; a second design iteration would produce the desired results.

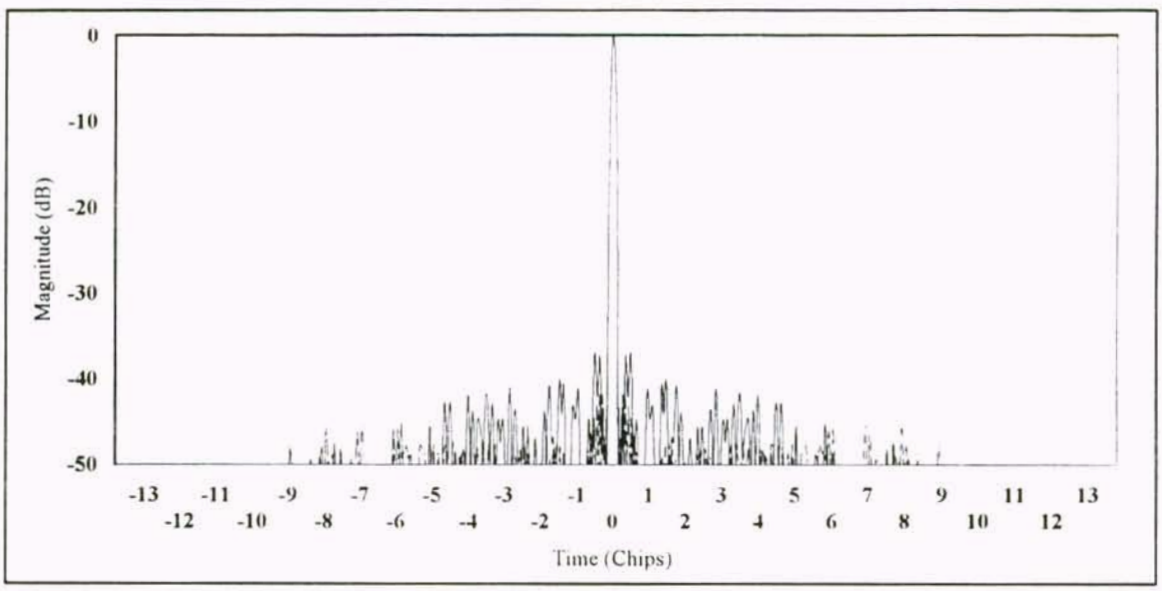

Figure 56. Normalized experimental SAW device compensated for the weighting errors (solid line) and theoretical (dashed line) correlation functions for a $4f_o$ sampled 13 chip Hamming weighted stepped chirp code signal where f_o = 85.79 MHz and T_c = 0.507 usec.

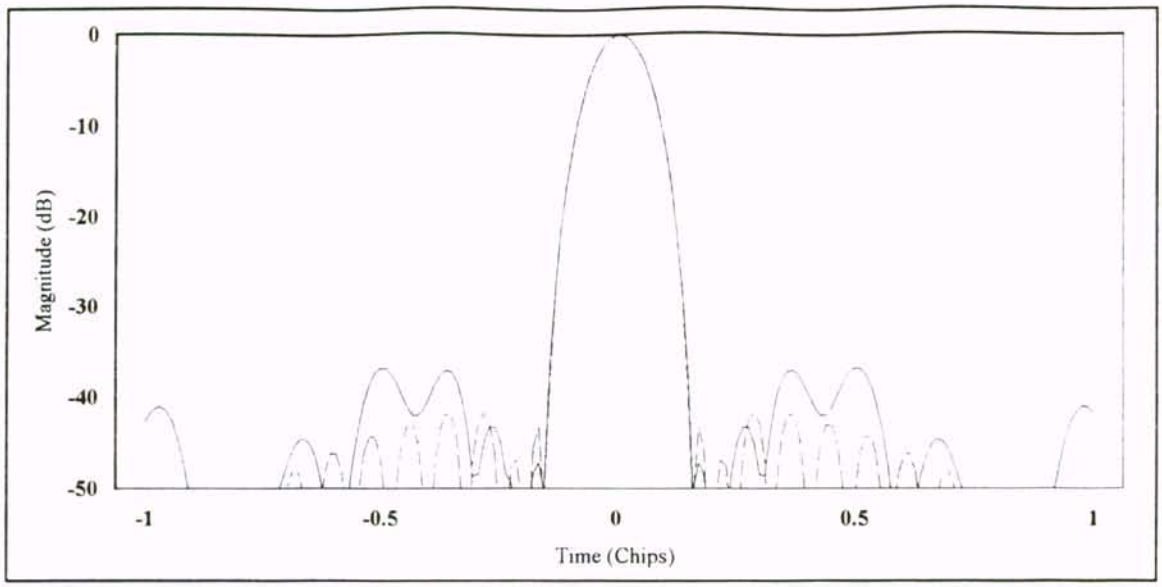

Figure 57. Normalized experimental SAW device compensated for the weighting errors (solid line) and theoretical (dashed line) peak correlation regions for a $4f_o$ sampled 13 chip Hamming weighted stepped chirp code signal where $f_o = 85.79$ MHz and $T_c = 0.507$ usec.

8.3 Sampling at $4f_n$

The PSD functions and correlation functions for the weighted stepped chirp code signal experimental SAW devices sampled at $4f_n$ for each chip n of the code signal are presented and compared to the theoretical results and also to the results when sampling at $4f_o$. Due to the line width accuracy restriction discussed in Chapter 7, the frequencies of the chips for $4f_n$ sampling found in Table 6 of Chapter 7 are offset from the desired frequencies found in Table 5 of Chapter 7. These frequency errors will result in a much less smooth PSD function than when using the ideal frequencies when $4f_o$ sampling.

8.31 The 9 Chip Weighted Stepped Chirp Code Signal

The 9 chip uniformly weighted stepped chirp code signal and the 9 chip cosine-squared weighted stepped chirp code signal experimental SAW device PSD functions and correlation functions are compared to the theoretical results when sampling at $4f_n$ and also to the results when sampling at $4f_o$.

8.311 Uniformly Weighted

Figure 58 compares the experimental SAW device (solid line) and theoretical (dashed line) PSD functions for the $4f_n$ sampled 9 chip uniformly weighted stepped chirp code signal. The PSD functions can be seen to a have a much more jagged frequency response than for the $4f_o$ sampled PSD functions found in Figure 39. Again the experimental PSD function can be seen to have a lift in its response at the edges when compared to the theoretical PSD function. The frequency errors will be shown to have a significantly negative impact on the correlation function. Also, the weighting errors from the theoretical PSD function will be seen to slightly degrade the correlation performance of the experimental SAW devices when compared to the theoretical.

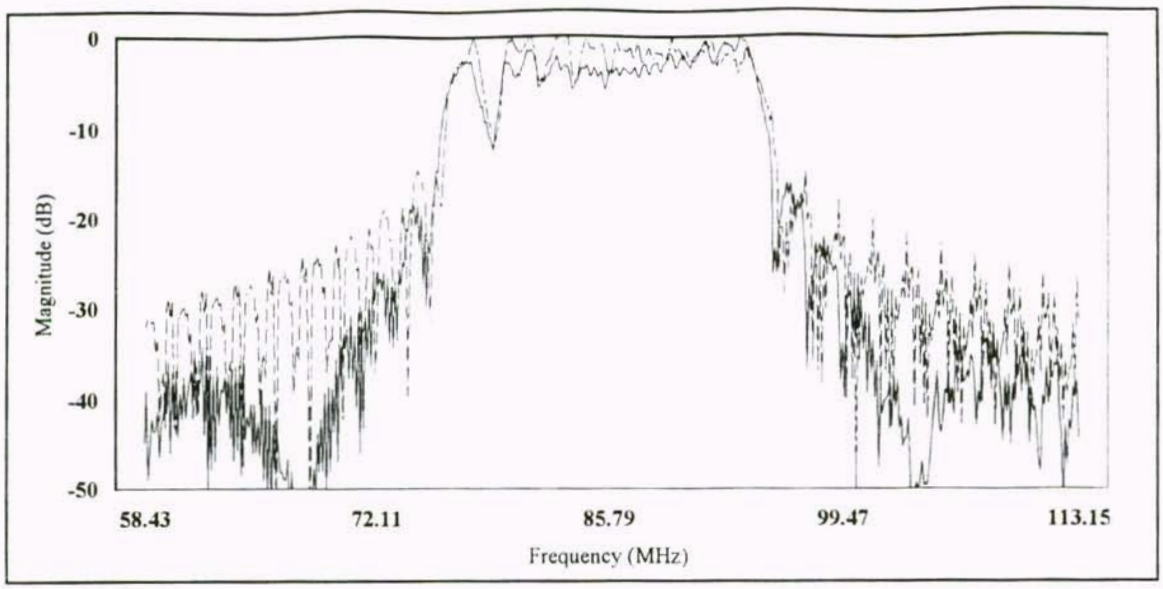

Figure 58. Normalized experimental SAW device (solid line) and theoretical (dashed line) PSD functions for a $4f_n$ sampled 9 chip uniformly weighted stepped chirp code signal where f_o = 85.79 MHz and T_c = 0.507 usec.

Figures 59 and 60 show the experimental SAW device (solid line) and theoretical (dashed line) correlation functions for the $4f_n$ sampled 9 chip uniformly weighted stepped chirp code signal. The experimental correlation function has a CR = 83, a PSL in the peak correlation region of -15.7 dB, a PSL in the cross-correlation region of -25 dB, and an ISL = -28.5 dB. The theoretical correlation function has a CR = 78, a PSL in the peak correlation region of -15.7 dB, a PSL in the cross-correlation region of -22.3 dB, and an ISL = -30.6 dB. The experimental correlation function shows good agreement to the theoretical correlation function. Comparing Figures 59 and 60 to the $4f_o$ sampled correlation functions in Figures 40 and 41 shows the degradation in the sidelobes due to the frequency errors.

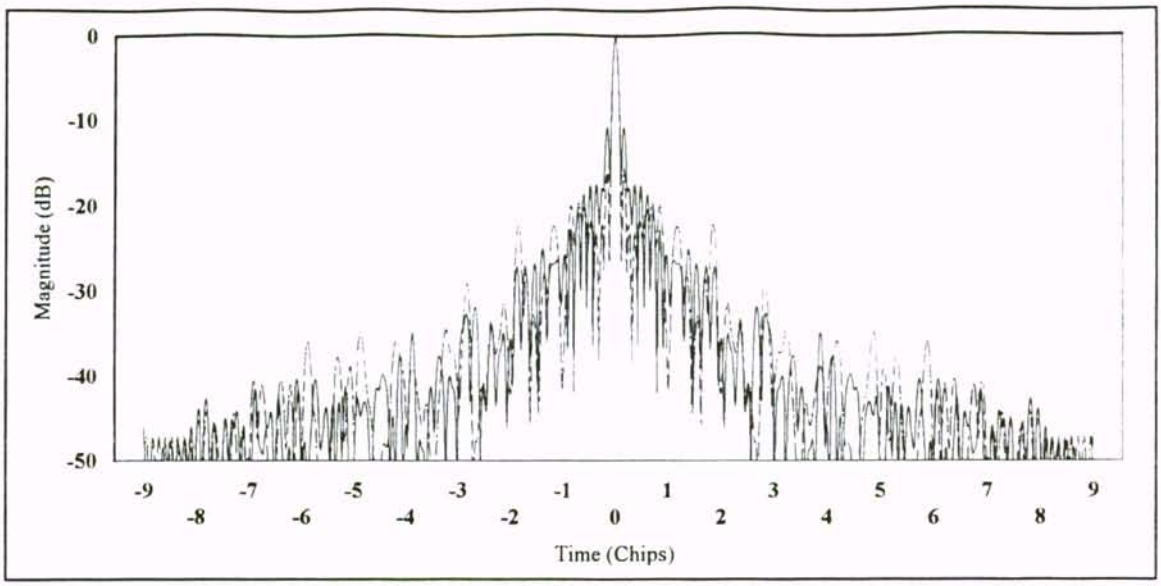

Figure 59. Normalized experimental SAW device (solid line) and theoretical (dashed line) correlation functions for a $4f_n$ sampled 9 chip uniformly weighted stepped chirp code signal where $f_o = 85.79$ MHz and $T_c = 0.507$ usec.

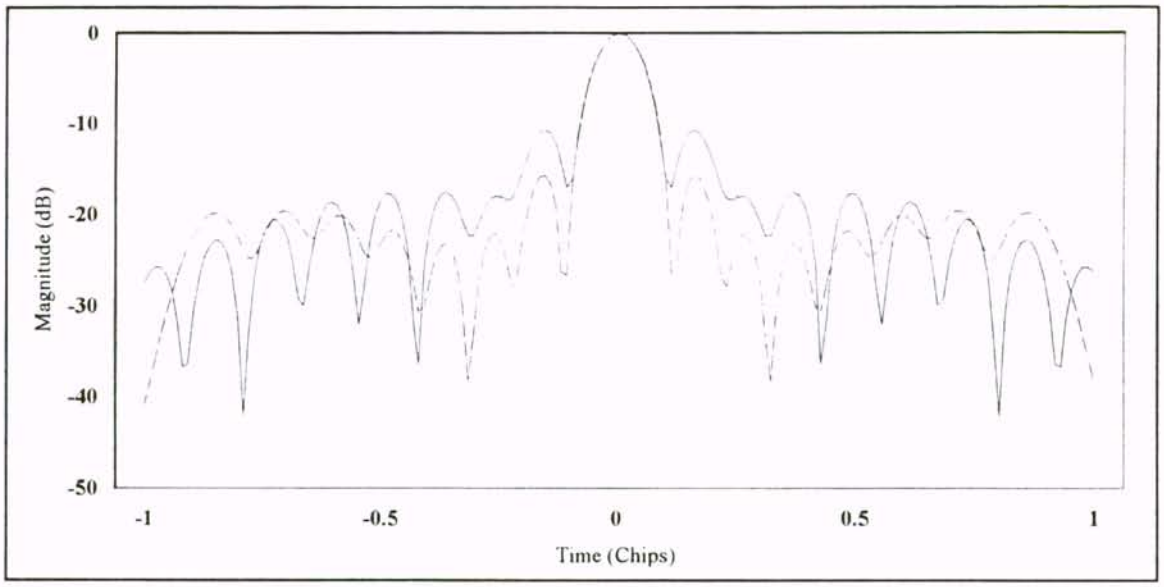

Figure 60. Normalized experimental SAW device (solid line) and theoretical (dashed line) peak correlation regions for a $4f_n$ sampled 9 chip uniformly weighted stepped chirp code signal where $f_o = 85.79$ MHz and $T_c = 0.507$ usec.

8.312 Cosine-squared Weighted

Figure 61 compares the experimental SAW device (solid line) and theoretical (dashed line) PSD functions for the $4f_n$ sampled 9 chip cosine-squared weighted stepped chirp code signal. Again, the PSD functions can be seen to a have a much more jagged frequency response than for the $4f_o$ sampled PSD functions found in Figure 42. Again the experimental PSD function can be seen to have a lift in its response at the edges when compared to the theoretical PSD function. The frequency errors will be shown to have a significantly negative impact on the correlation function.

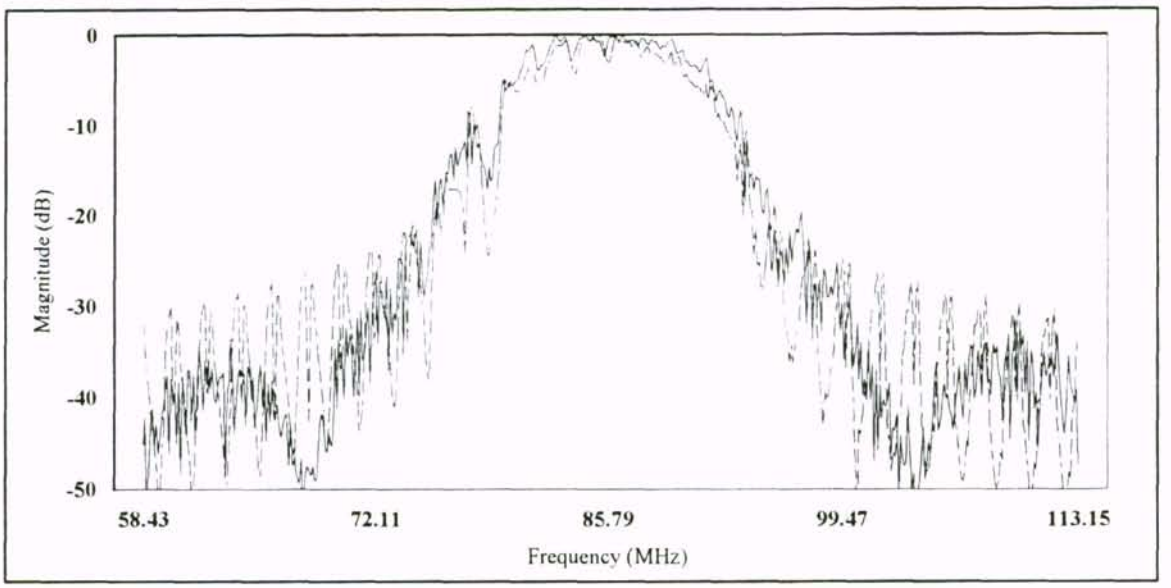

Figure 61. Normalized experimental SAW device (solid line) and theoretical (dashed line) PSD functions for a $4f_n$ sampled 9 chip cosine-squared weighted stepped chirp code signal where f_o = 85.79 MHz and T_c = 0.507 usec.

Figures 62 and 63 show the experimental SAW device (solid line) and theoretical (dashed line) correlation functions for the $4f_n$ sampled 9 chip cosine-squared weighted

stepped chirp code signal. The experimental correlation function has a CR = 56, a PSL in the peak correlation region of -21.5 dB, a PSL in the cross-correlation region of -22.4 dB, and an ISL = -35.3 dB. The theoretical correlation function has a CR = 51, a PSL in the peak correlation region of -21.4 dB, a PSL in the cross-correlation region of -21.5 dB, and an ISL = -33.8 dB. The experimental correlation function shows good agreement to the theoretical correlation function. The fact that the sidelobe responses show good agreement shows that the effects of the weighting errors are less critical than the effects of the frequency errors. Comparing Figures 62 and 63 to the $4f_o$ sampled correlation functions in Figures 43 and 44 shows the degradation in the sidelobes due to the frequency errors.

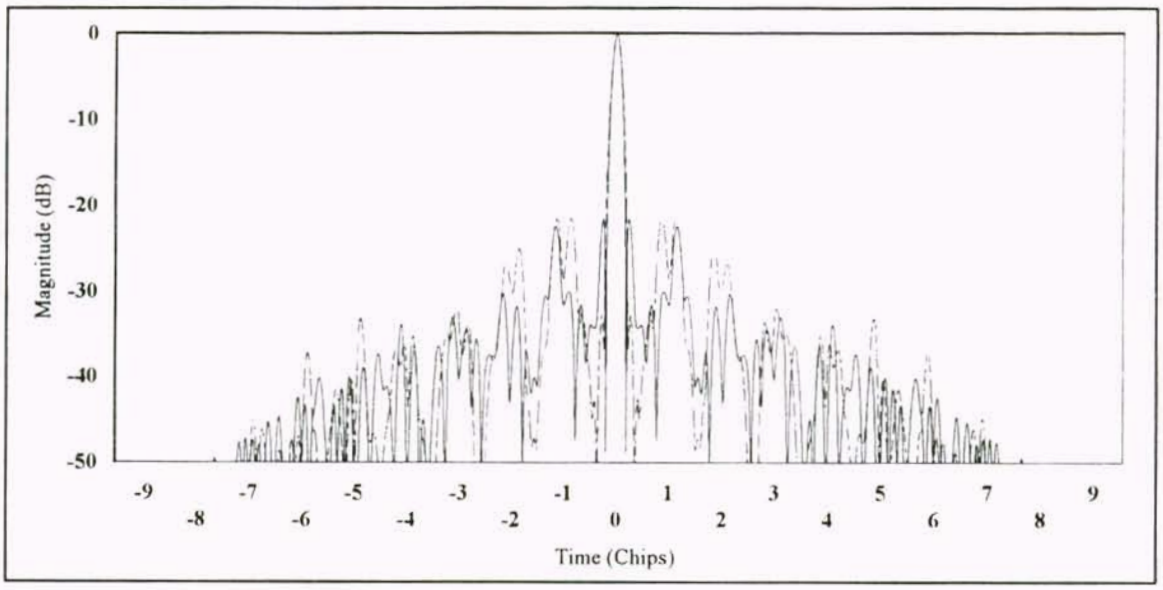

Figure 62. Normalized experimental SAW device (solid line) and theoretical (dashed line) correlation functions for a $4f_n$ sampled 9 chip cosine-squared weighted stepped chirp code signal where f_o = 85.79 MHz and T_c = 0.507 usec.

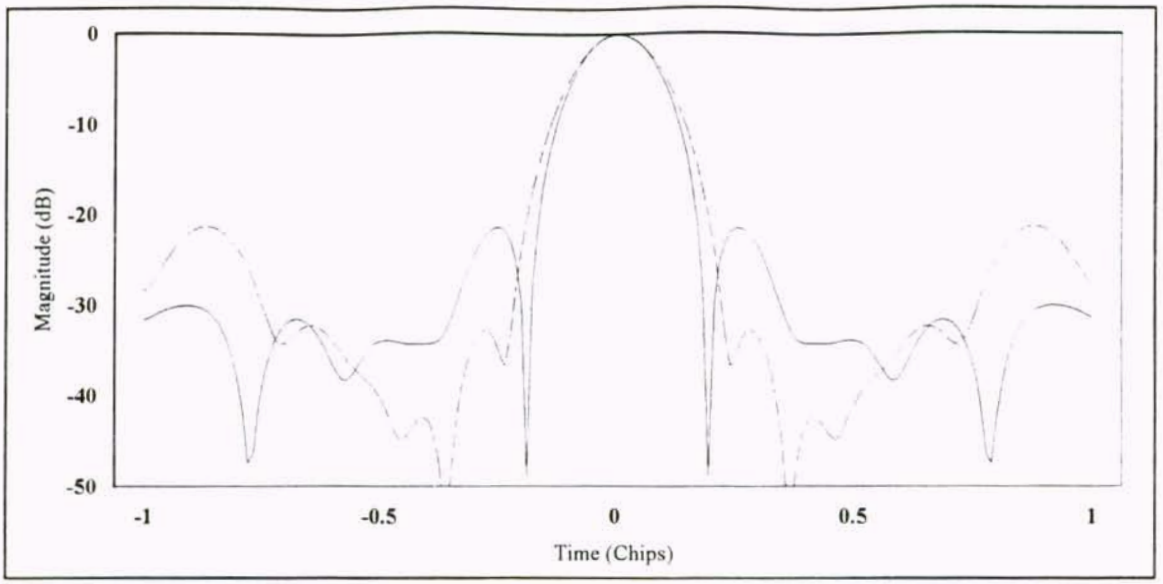

Figure 63. Normalized experimental SAW device (solid line) and theoretical (dashed line) peak correlation regions for a $4f_n$ sampled 9 chip cosine-squared weighted stepped chirp code signal where $f_o = 85.79$ MHz and $T_c = 0.507$ usec.

8.32 The 13 Chip Weighted Stepped Chirp Code Signal

The 13 chip uniformly weighted stepped chirp code signal and the 13 chip Hamming weighted stepped chirp code signal experimental SAW device PSD and correlation functions are compared to the theoretical results when sampling at $4f_n$ and also to the results when sampling at $4f_o$.

8.321 Uniformly Weighted

Figure 64 compares the experimental SAW device (solid line) and theoretical (dashed line) PSD functions for the $4f_n$ sampled 13 chip uniformly weighted stepped chirp code signal. Again, the PSD functions can be seen to a have a much more jagged frequency response than for the $4f_o$ sampled PSD functions found in Figure 45. Again the

experimental PSD function can be seen to have a lift in its response at the edges when compared to the theoretical PSD function. The frequency errors will be shown to have a significantly negative impact on the correlation function. Also, the weighting errors will be seen to slightly degrade the correlation performance of the experimental SAW devices versus the theoretical.

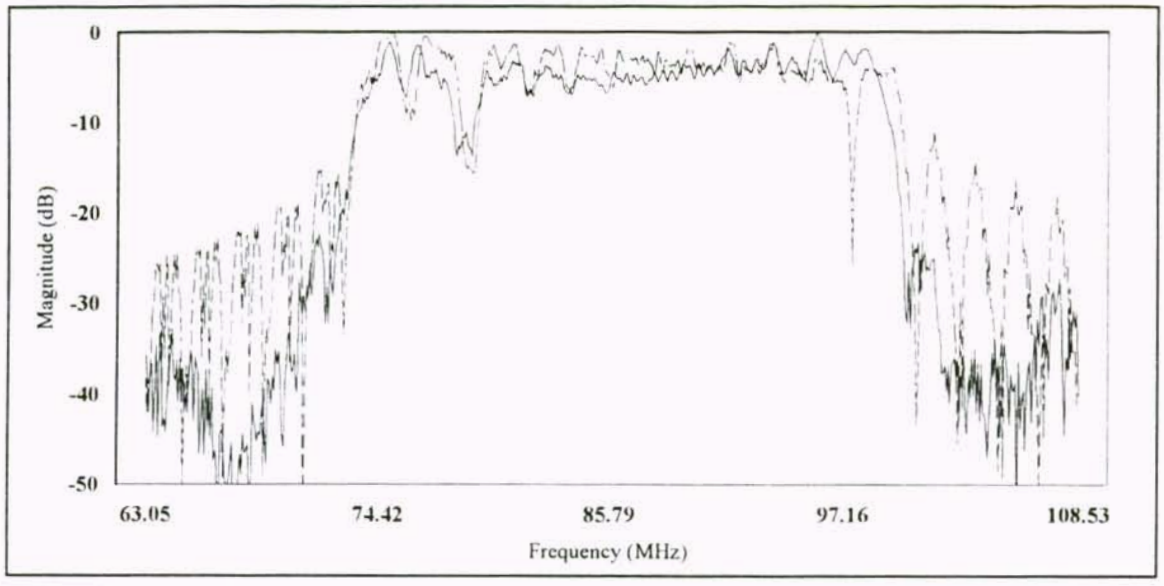

Figure 64. Normalized experimental SAW device (solid line) and theoretical (dashed line) PSD functions for a $4f_n$ sampled 13 chip uniformly weighted stepped chirp code signal where f_o = 85.79 MHz and T_c = 0.507 usec.

Figures 65 and 66 show the experimental SAW device (solid line) and theoretical (dashed line) correlation functions for the $4f_n$ sampled 13 chip uniformly weighted stepped chirp code signal. The experimental correlation function has a CR = 174, a PSL in the peak correlation region of -10.3 dB, a PSL in the cross-correlation region of -21.9 dB, and an ISL = -30.7 dB. The theoretical correlation function has a CR = 174, a PSL in the

peak correlation region of -15.3 dB, a PSL in the cross-correlation region of -28.2 dB, and an ISL = -31.5 dB. The experimental correlation function shows good agreement to the theoretical correlation function. The frequency errors have masked the weighting errors. Comparing Figures 65 and 66 to the $4f_o$ sampled correlation functions in Figures 46 and 47 shows the degradation in the sidelobes due to the frequency errors.

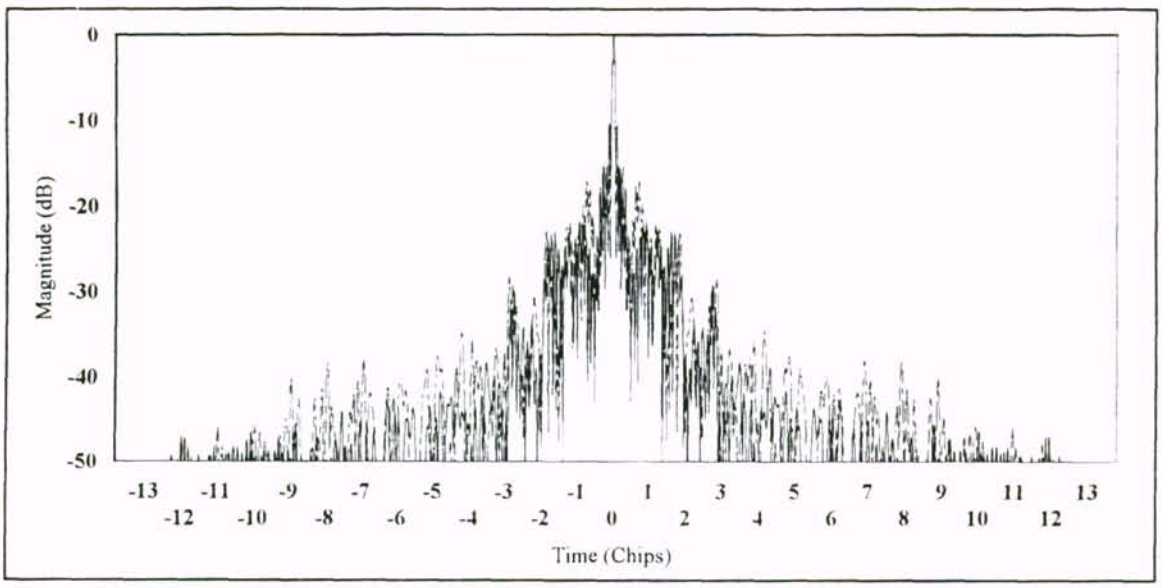

Figure 65. Normalized experimental SAW device (solid line) and theoretical (dashed line) correlation functions for a $4f_n$ sampled 13 chip uniformly weighted stepped chirp code signal where f_o = 85.79 MHz and T_c = 0.507 usec.

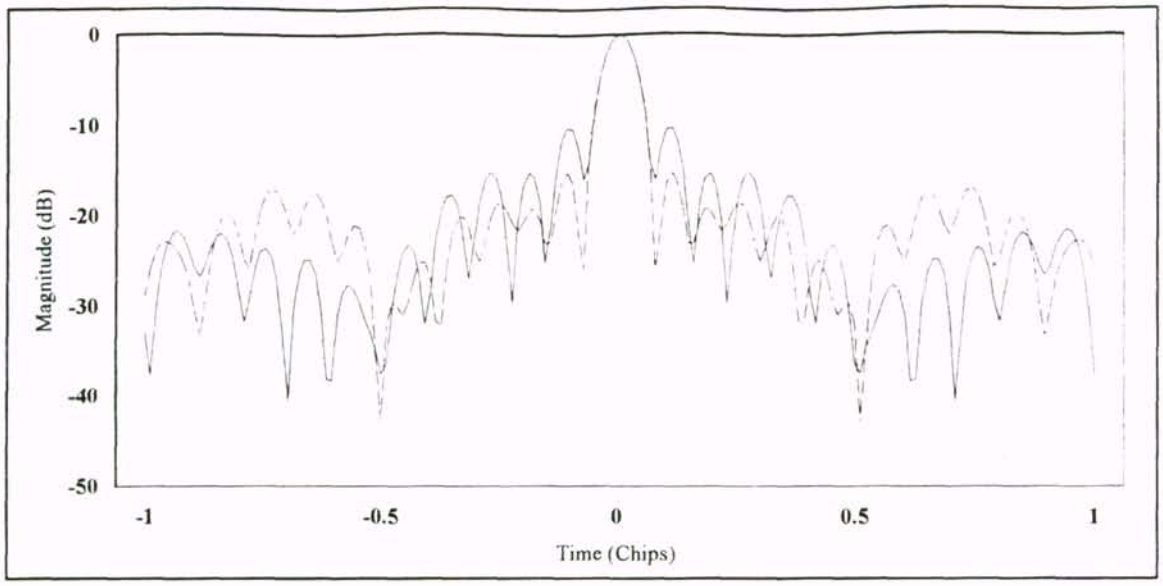

Figure 66. Normalized experimental SAW device (solid line) and theoretical (dashed line) peak correlation regions for a $4f_n$ sampled 13 chip uniformly weighted stepped chirp code signal where f_o = 85.79 MHz and T_c = 0.507 usec.

8.322 Hamming Weighted

Figure 67 compares the experimental SAW device (solid line) and theoretical (dashed line) PSD functions for the $4f_n$ sampled 13 chip Hamming weighted stepped chirp code signal. Again, the PSD functions can be seen to a have a much more jagged frequency response than for the $4f_o$ sampled PSD functions found in Figure 48. Again the experimental PSD function can be seen to have a lift in its response at the edges when compared to the theoretical PSD function. Again the frequency errors will be shown to have a significantly negative impact on the correlation function.

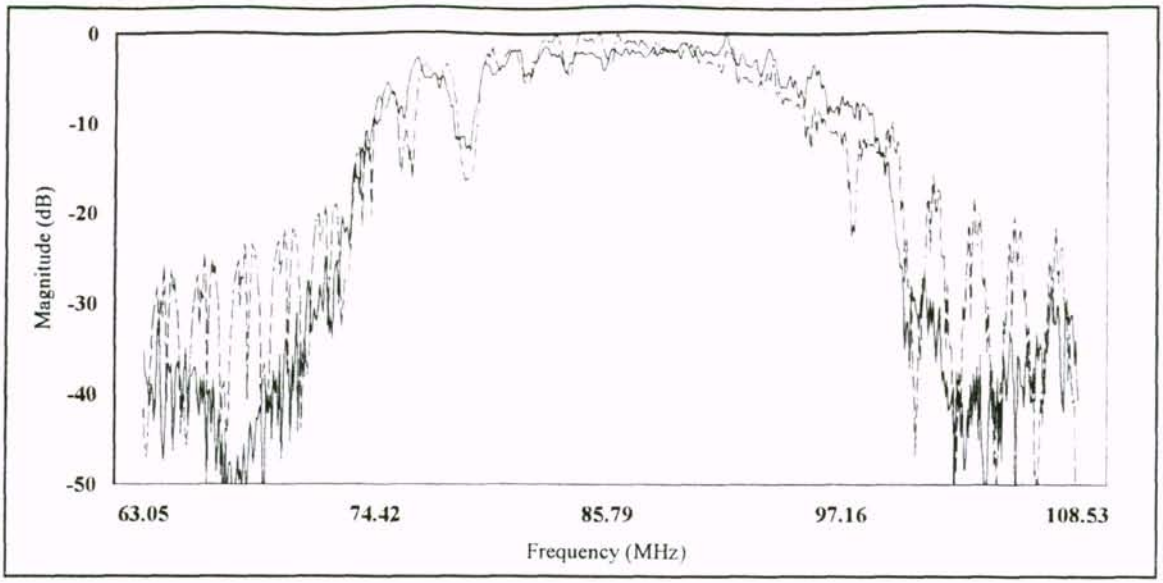

Figure 67. Normalized experimental SAW device (solid line) and theoretical (dashed line) PSD functions for a $4f_n$ sampled 13 chip Hamming weighted stepped chirp code signal where f_o = 85.79 MHz and T_c = 0.507 usec.

Figures 68 and 69 show the experimental SAW device (solid line) and theoretical (dashed line) correlation functions for the $4f_n$ sampled 13 chip Hamming weighted stepped chirp code signal. The experimental correlation function has a CR = 126, a PSL in the peak correlation region of -21.1 dB, a PSL in the cross-correlation region of -25.4 dB, and an ISL = -35.9 dB. The theoretical correlation function has a CR = 113, a PSL in the peak correlation region of -22 dB, a PSL in the cross-correlation region of -22.8 dB, and an ISL = -34.6 dB. The experimental correlation function shows good agreement to the theoretical correlation function. Again the frequency errors have masked the weighting errors. Comparing Figures 68 and 69 to the $4f_o$ sampled correlation functions in Figures 49 and 50 shows the degradation in the sidelobes due to the frequency errors.

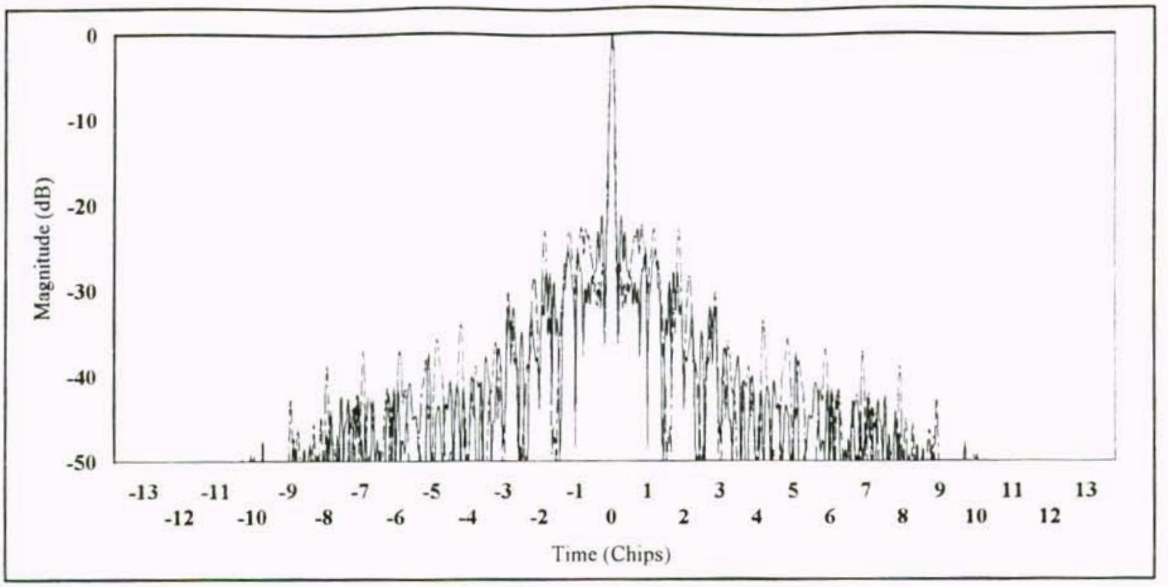

Figure 68. Normalized experimental SAW device (solid line) and theoretical (dashed line) correlation functions for a $4f_n$ sampled 13 chip Hamming weighted stepped chirp code signal where f_o = 85.79 MHz and T_c = 0.507 usec.

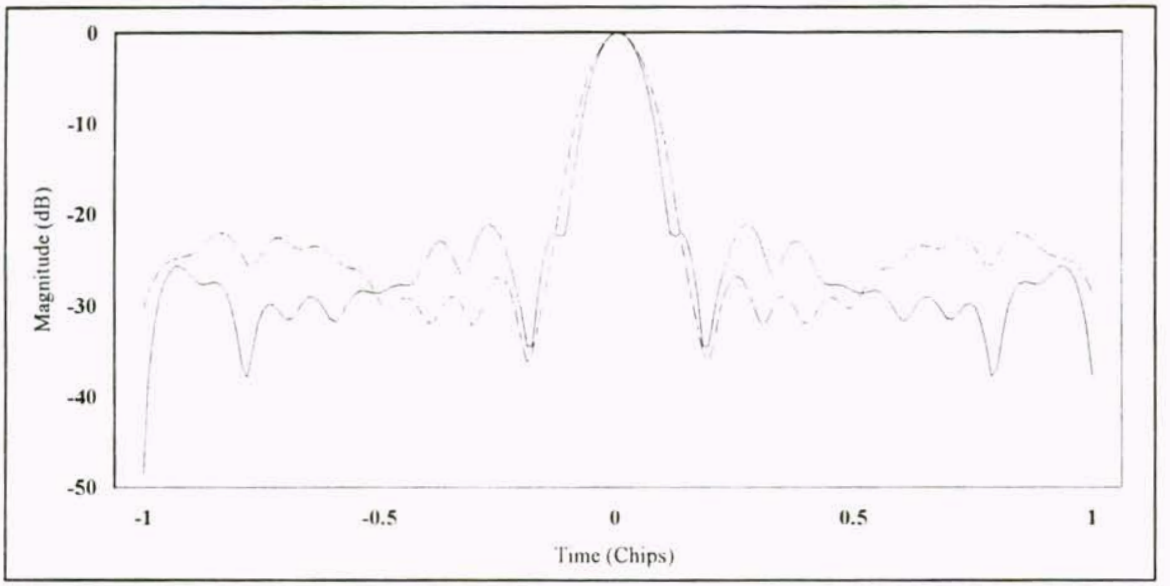

Figure 69. Normalized experimental SAW device (solid line) and theoretical (dashed line) peak correlation regions for a $4f_n$ sampled 13 chip Hamming weighted stepped chirp code signal where f_o = 85.79 MHz and T_c = 0.507 usec.

8.4 Sampling at $4f_o$ Versus Sampling at $4f_n$

It has already been shown that the frequency errors due to the line width accuracies result in extreme degradation of the correlation functions for the weighted stepped chirp code signal. The use of $4f_n$ sampling was evaluated in order to realize a 3 dB reduction in insertion loss over $4f_o$ sampling. Table 9 shows the differences in insertion loss for the experimental SAW devices.

Experimental SAW Device	$4f_o$ Insertion Loss dB	$4f_n$ Insertion Loss dB
9 Chip Uniformly Weighted	67.15	64.45
9 Chip Cosine-squared Weighted	63.08	60.85
13 Chip Uniformly Weighted	69.65	66.72
13 Chip Hamming Weighted	65.10	62.33

Table 9. Comparison of insertion losses in experimental SAW devices when sampling at $4f_o$ versus sampling at $4f_n$.

These results show that the $4f_n$ sampled experimental SAW devices resulted in a 2 to 3 dB reduction in the insertion loss compared to the $4f_o$ sampled experimental SAW devices.

CHAPTER 9

EXPERIMENTAL SAW DEVICE PROBABILITY OF ERROR

Using the correlation results from Chapter 8 and Equations 32-35 from Chapter 5, the probability of error curves can be plotted for the experimental SAW devices. Figure 70 compares the BER for the theoretical and experimental SAW device 9 chip uniformly weighted stepped chirp code signal to that of a 9 chip PN code. As shown in Chapter 5, the uniformly weighted stepped chirp code signal can operate at much lower SJR's. This figure also shows that the experimental SAW device BER is virtually identical to the theoretical BER for the 9 chip uniformly weighted stepped chirp code signal. Figure 71 compares the BER for the theoretical and experimental SAW device 13 chip uniformly weighted stepped chirp code signal to that of a 13 chip PN code. Again the uniformly weighted stepped chirp code signal can operate at much lower SJR's than the PN code. The experimental SAW device BER matches the BER for the theoretical 13 chip uniformly weighted stepped chirp code signal.

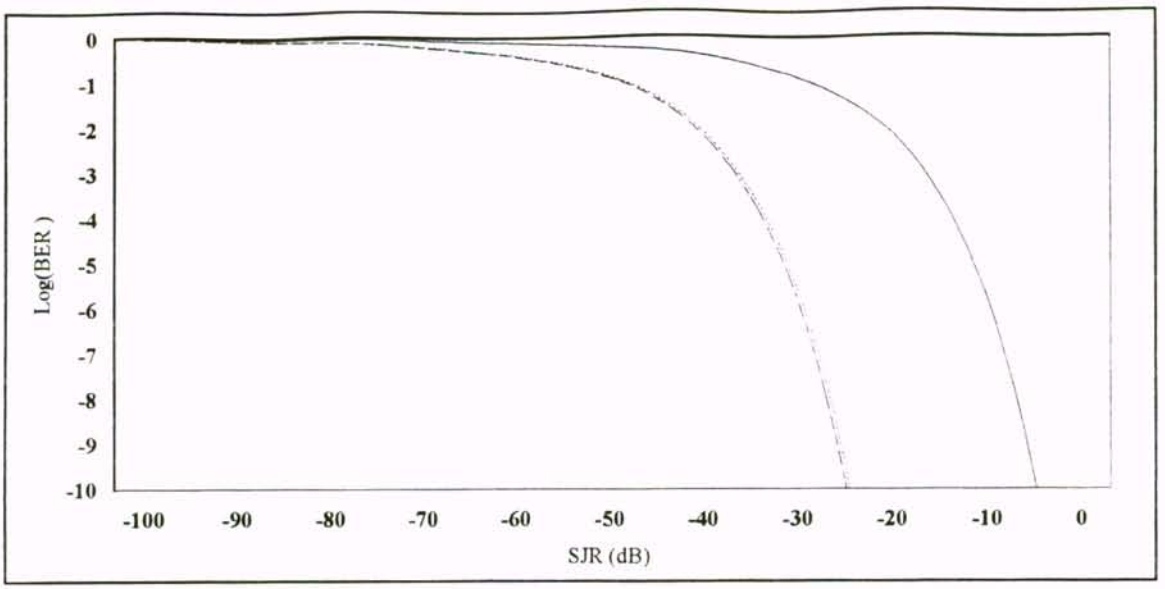

Figure 70. BER for a BPSK data stream as a function of SJR for the theoretical (dashed line) and experimental SAW device (dotted line) 9 chip uniformly weighted stepped chirp code signals, and a 9 chip PN code (solid line).

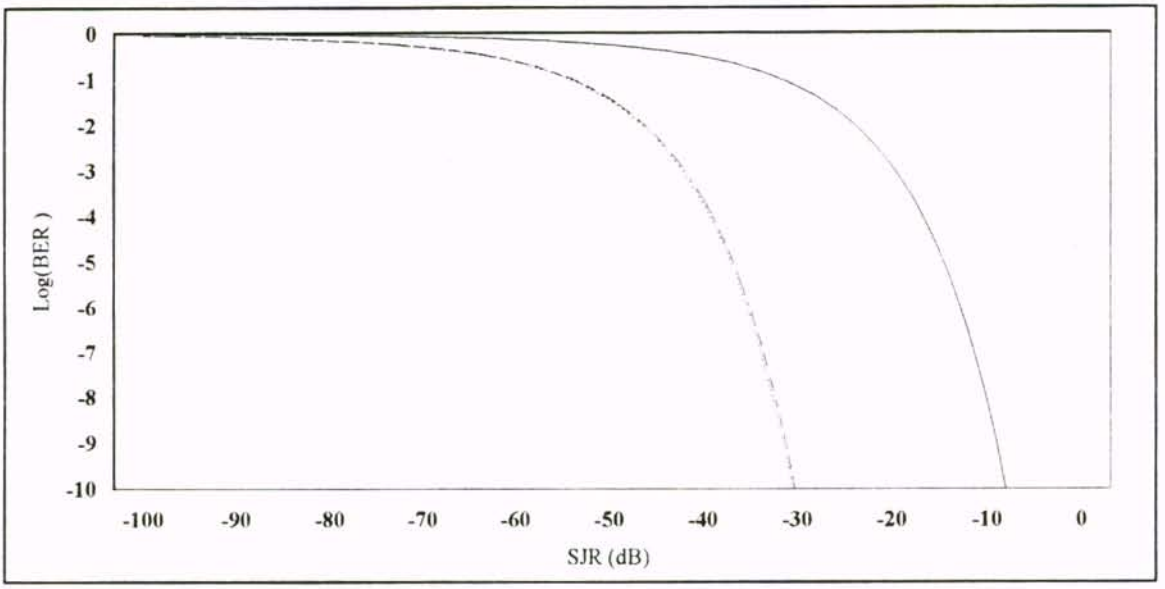

Figure 71. BER for a BPSK data stream as a function of SJR for the theoretical (dashed line) and experimental SAW device (dotted line) 13 chip uniformly weighted stepped chirp code signals, and a 13 chip PN code (solid line).

CHAPTER 10

CONCLUSION

The weighted stepped chirp code signal has been introduced for use in DS/SS communications systems. The center frequency and chip length requirements for optimal correlation function response were presented. The theoretical PSD and correlation functions showed that the weighted stepped chirp code signal behaves similarly to a CW chirp. The 9 chip cosine-squared and 13 chip Hamming weighted stepped chirp code signals were shown to achieve performance in CR, PSL, and ISL equal to or better than a 40 chip and 93 chip PN code respectively. The BER for the weighted stepped chirp code signal was also shown to be superior to that of a PN code of equal length.

The use of SAW devices in DS/SS communications systems was discussed. The advantages in cost, size, and speed of acquisition were presented. The need to compensate the weighted stepped chirp code signal for the frequency response of the impulse generator was discussed.

The design requirements for the implementation of the weighted stepped chirp code signal in a SAW device were presented. The impact of ISI from the output transducer was illustrated. The compensation of the weighted stepped chirp code signal for the output transducer's frequency response was shown. The possibility of

waveguiding in long code signal transducers was discussed with techniques for avoiding it. The sources and design techniques for avoiding RF feed-through were presented. The fabrication and packaging of the experimental weighted stepped chirp code signal SAW devices were shown.

The experimental SAW device correlation results were compared to the theoretical correlation results. It was shown that when properly compensated, the experimental SAW devices produced correlation functions and BER's which closely resembled the theoretical results. It also showed that the cosine-squared and Hamming weighted stepped chirp code signals were sensitive to weighting errors due to the small chip weights at the edges of the code signals. The frequency errors due to the line width accuracy restrictions were shown to be extremely detrimental to the correlation function results. However, the $4f_n$ sampled experimental SAW devices were shown to result in a 2 to 3 dB improvement in insertion loss.

Appendix A

Sample Computation of the Theoretical Correlation Function in MathCAD

Chip length in usec $Tc := 1$

Carrier frequency in MHz $f0 := 100.5$

Radian frequency $\omega 0 := 2 \cdot \pi \cdot f0$

Number of chips in the code $chips := 9$

Number of bits in the simulation $bits := 5$

Solution to the chip to chip correlation for n not equal to m

$$R1A(\tau, n, m) := \sin\left(\frac{2 \cdot \pi \cdot n \cdot \tau + \omega 0 \cdot \tau \cdot Tc + \omega 0 \cdot Tc^2 + \pi \cdot m \cdot Tc + \pi \cdot n \cdot Tc}{Tc}\right)$$

$$R1B(\tau, n, m) := \sin\left(\frac{2 \cdot \pi \cdot m \cdot \tau + \omega 0 \cdot \tau \cdot Tc + \omega 0 \cdot Tc^2 + \pi \cdot m \cdot Tc + \pi \cdot n \cdot Tc}{Tc}\right)$$

$$R1AB(\tau, n, m) := R1A(\tau, n, m) + R1B(\tau, n, m)$$

$$R1C(\tau, n, m) := \sin\left(\frac{2 \cdot \pi \cdot n \cdot \tau + \omega 0 \cdot \tau \cdot Tc - \pi \cdot m \cdot Tc + \pi \cdot n \cdot Tc}{Tc}\right)$$

$$R1D(\tau, n, m) := \sin\left(\frac{2 \cdot \pi \cdot m \cdot \tau + \omega 0 \cdot \tau \cdot Tc + \pi \cdot m \cdot Tc - \pi \cdot n \cdot Tc}{Tc}\right)$$

$$R1CD(\tau, n, m) := R1C(\tau, n, m) - R1D(\tau, n, m)$$

$$R1E(\tau, n, m) := \sin\left(\frac{-2 \cdot \pi \cdot m \cdot \tau - \omega 0 \cdot \tau \cdot Tc + \omega 0 \cdot Tc^2 + \pi \cdot m \cdot Tc + \pi \cdot n \cdot Tc}{Tc}\right)$$

$$R1F(\tau, n, m) := \sin\left(\frac{-2 \cdot \pi \cdot n \cdot \tau - \omega 0 \cdot \tau \cdot Tc + \omega 0 \cdot Tc^2 + \pi \cdot m \cdot Tc + \pi \cdot n \cdot Tc}{Tc}\right)$$

$$R1EF(\tau, n, m) := R1E(\tau, n, m) + R1F(\tau, n, m)$$

$$R1G(\tau, n, m) := \sin\left(\frac{2 \cdot \pi \cdot m \cdot \tau + \omega 0 \cdot \tau \cdot Tc - \pi \cdot m \cdot Tc + \pi \cdot n \cdot Tc}{Tc}\right)$$

$$R1H(\tau, n, m) := \sin\left(\frac{2 \cdot \pi \cdot n \cdot \tau + \omega 0 \cdot \tau \cdot Tc + \pi \cdot m \cdot Tc - \pi \cdot n \cdot Tc}{Tc}\right)$$

$$R1GH(\tau, n, m) := R1G(\tau, n, m) - R1H(\tau, n, m)$$

$$R\_chip1(\tau,n,m) := \begin{cases} Tc\cdot\left[\dfrac{R1AB(\tau,n,m)}{4\cdot(\omega0\cdot Tc+\pi\cdot m+\pi\cdot n)}+\dfrac{R1CD(\tau,n,m)}{4\cdot\pi\cdot(n-m)}\right] & \text{if } -Tc\le\tau\le 0 \\ Tc\cdot\left[\dfrac{R1EF(\tau,n,m)}{4\cdot(\omega0\cdot Tc+\pi\cdot m+\pi\cdot n)}+\dfrac{R1GH(\tau,n,m)}{4\cdot\pi\cdot(n-m)}\right] & \text{if } 0<\tau\le Tc \\ 0 \quad \text{otherwise} \end{cases}$$

Solution to the chip to chip correlation for n equal to m

$$R2A(\tau,n,m) := \left(\omega0+\frac{2\cdot\pi\cdot n}{Tc}\right)\cdot(Tc+\tau)\cdot\cos\left[\left(\omega0+\frac{2\cdot\pi\cdot n}{Tc}\right)\cdot\tau\right]$$

$$R2B(\tau,n,m) := \sin\left[\left(\omega0+\frac{2\cdot\pi\cdot n}{Tc}\right)\cdot(Tc+\tau)\right]$$

$$R2C(\tau,n,m) := \left(\omega0+\frac{2\cdot\pi\cdot n}{Tc}\right)\cdot(Tc-\tau)\cdot\cos\left[\left(\omega0+\frac{2\cdot\pi\cdot n}{Tc}\right)\cdot\tau\right]$$

$$R2D(\tau,n,m) := \sin\left[\left(\omega0+\frac{2\cdot\pi\cdot n}{Tc}\right)\cdot(Tc-\tau)\right]$$

$$R\_chip2(\tau,n,m) := \begin{cases} \dfrac{R2A(\tau,n,m)+R2B(\tau,n,m)}{2\cdot\left(\omega0+\dfrac{2\cdot\pi\cdot n}{Tc}\right)} & \text{if } -Tc\le\tau\le 0 \\ \dfrac{R2C(\tau,n,m)+R2D(\tau,n,m)}{2\cdot\left(\omega0+\dfrac{2\cdot\pi\cdot n}{Tc}\right)} & \text{if } 0<\tau\le Tc \\ 0 \quad \text{otherwise} \end{cases}$$

Chip to chip correlation for all values of n and m

$$R\_chip(\tau,n,m) := \begin{cases} R\_chip1(\tau,n,m) & \text{if } n\neq m \\ R\_chip2(\tau,n,m) & \text{otherwise} \end{cases}$$

$i := 0 .. chips - 1 \quad j := 0 .. (bits + 2) \cdot chips - 1 \quad ii := 0 .. 2 \cdot chips - 1$

Input two +1 bits followed by two -1 bits followed by a +1 bit

$$input_j := \begin{cases} 0 & \text{if } 0 \le j \le chips - 1 \\ 1 & \text{if } chips \le j \le 2 \cdot chips - 1 \\ 1 & \text{if } 2 \cdot chips \le j \le 3 \cdot chips - 1 \\ -1 & \text{if } 3 \cdot chips \le j \le 4 \cdot chips - 1 \\ -1 & \text{if } 4 \cdot chips \le j \le 5 \cdot chips - 1 \\ 1 & \text{if } 5 \cdot chips \le j \le 6 \cdot chips - 1 \\ 0 & \text{otherwise} \end{cases}$$

Weights of the input chips

$a\_input_{ii} := 1$

Weights of the correlator chips

$$a\_filter_{ii} := \begin{cases} \cos\left[\dfrac{\pi \cdot \left[ii - \left(\dfrac{chips - 1}{2}\right)\right]}{chips}\right]^2 & \text{if } ii < chips \\ \cos\left[\dfrac{\pi \cdot \left[ii - chips - \left(\dfrac{chips - 1}{2}\right)\right]}{chips}\right]^2 & \text{otherwise} \end{cases}$$

$j := 0 .. chips - 1$

$k := 0 .. bits$

n index of the chip functions

$$n_{ii} := \begin{cases} ii - \dfrac{(chips - 1)}{2} & \text{if } ii < chips \\ ii - chips - \dfrac{(chips - 1)}{2} & \text{otherwise} \end{cases}$$

Correlation of the input with the correlator

$$Rsum(\tau) := \sum_k \sum_i \sum_j input_{chips\cdot(k+1)-1-j+i} \cdot R\_chip\left[\tau - (chips\cdot k + i)\cdot Tc, n_{chips-i+j}, n_j\right] \cdot a\_input_{chips-i+j} \cdot a\_filter_j$$

$$Rmax := Rsum(chips\cdot Tc)$$

$$Rmax = 2.25$$

$$R(\tau) := \begin{cases} 20\cdot\log\left(\left|\frac{Rsum(\tau)}{Rmax}\right|\right) & \text{if } \left|\frac{Rsum(\tau)}{Rmax}\right| \geq 0.00001 \\ -100 & \text{otherwise} \end{cases}$$

$$\tau := (chips-1)\cdot Tc, (chips-1)\cdot Tc + \frac{1}{2\cdot f0} .. (3\cdot chips+1)\cdot Tc$$

Correlation over the +1,+1,-1 bits

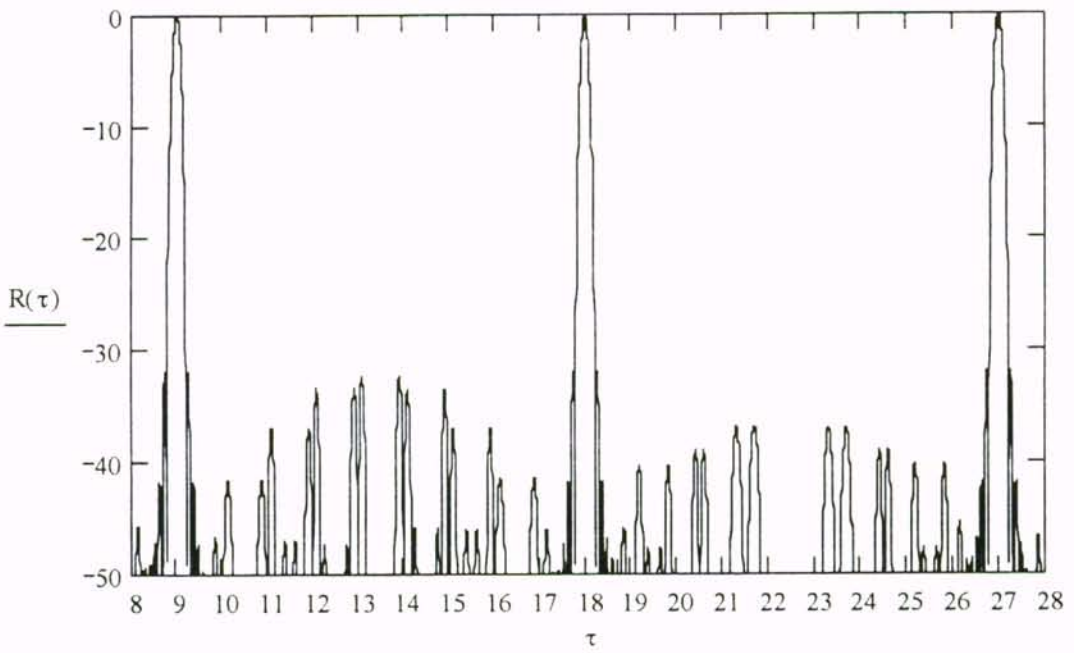

$$\tau := (2\cdot chips - 1)\cdot Tc, (2\cdot chips - 1)\cdot Tc + \frac{1}{2\cdot f0} .. (2\cdot chips + 1)\cdot Tc$$

Correlation at the second +1 bit peak correlation region

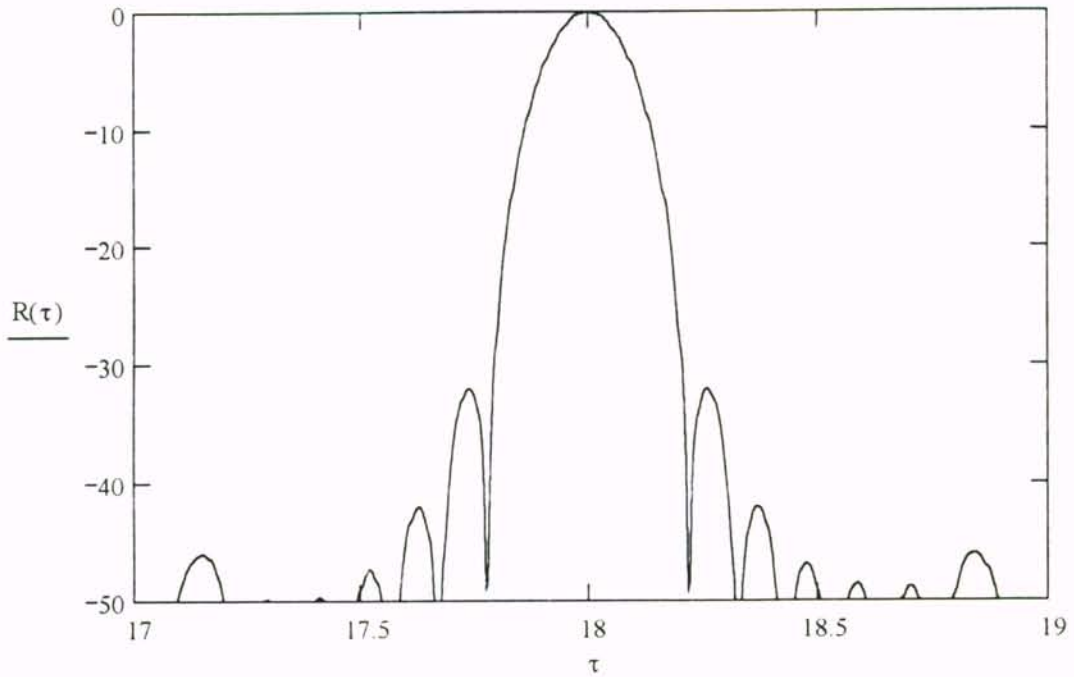

Index output correlation data over the +1,+1,-1 bits

$$N := 2\cdot f0\cdot\left(2 + \frac{2}{chips}\right)\cdot chips\cdot Tc + 1$$

$$N = 4.021\cdot 10^{3}$$

$$index := 0 .. N - 1$$

$$R_{index} := \frac{Rsum\left(chips - 1 + \frac{index}{2\cdot f0}\right)}{Rmax}$$

$$Time_{index} := chips - 1 + \frac{index}{2\cdot f0}$$

C:\..\R.dat

R

C:\..\time

Time

LIST OF REFERENCES

[1] August W. Rihaczek, *Principles of High-resolution Radar*, Mark Resources, Inc., 1977.

[2] T. H. Einstein, "Generation of High Resolution Radar Range Profiles and Range Profile Auto-Correlation Functions Using Stepped-Frequency Pulse Trains," Lexington, MA: Lincoln Laboratory, MIT, October 1984.

[3] Bernard Sklar, *Digital Communications Fundamentals and Applications*, Englewood Cliffs, NJ: Prentice-Hall, Inc., 1988.

[4] Andrew J. Viterbi, *CDMA Principles of Spread Spectrum Communication*, Reading, MA: Addison-Wesley Publishing Company, 1995.

[5] Marvin K. Simon, Jim K. Omura, Robert A. Scholtz, and Barry K. Levitt, *Spread Spectrum Communications Handbook*, New York, NY: McGraw-Hill, Inc., 1994.

[6] Raymond L. Pickholtz, Donald L. Schilling, and Laurence B. Milstein, "Theory of Spread-Spectrum Communications-A Tutorial,"IEEE Transactions on Communications, Vol. COM-30, No. 5, pp.855-884, May 1982.

[7] Viktor G. Nebabin, *Methods and Techniques of Radar Recognition*, Norwood, MA: Artech House, Inc., 1995.

[8] James C. Walker, The Design and Implementation of Surface Acoustic Wave Devices for Linear FM and a New Non-Linear FM Pulse Compression Technique for Radar Applications, Master's Thesis, University of Central Florida, 1986.

[9] Guy V. Morris, *Airborne Pulsed Doppler Radar*, Norwood, MA: Artech House, Inc., 1988.

[10] Carl W. Helstrom, *Elements of Signal Detection & Estimation*, Englewood Cliffs, NJ: Prentice-Hall, Inc., 1995.

[11] Marvin K. Simon, Jim K. Omura, Robert A. Scholtz, and Barry K. Levitt, *Spread Spectrum Communications*, Vol. 2, Computer Science Press, Inc., Rockville, MD, 1982.

[12] Scott E. Carter and Donald C. Malocha, "Finite Impulse Response Utilizing the Principle of Superposition," IEEE Transactions on Ultrasonics, Ferroelectrics, and Frequency Control, Vol. 44, No. 2, pp. 386-398, March 1997.

[13] Madjid A. Belkerdid, citation for bit error rate equation in BPSK direct sequence spread spectrum communications systems, University of Central Florida, June, 1998.

[14] A. Biran, "Low-sidelobe SAW Barker 13 Correlator," IEEE 1985 Ultrasonics Symposium Proceedings, pp. 149-152, 1985.

[15] Clemens C. W. Ruppel and Leonhard Reindl, "SAW Devices for Spread Spectrum Applications," IEEE ISSSTA '96 Proceedings, pp. 713-719, 1996.

[16] Takashi Shiba, Akitsuna Yuhara, Minoru Moteki, Yasuhiro Ota, Kouji Oda, and Kazuo Tsubouchi, "Low Loss SAW Matched Filters with Low Sidelobe Sequences and Spread Spectrum Applications," IEEE ISSSTA '96 Proceedings, pp. 740-745, 1996.